THESIS APPROVAL
GRADUATE SCHOOL, KASETSART UNIVERSITY

DEGREE: Master of Engineering (Irrigation Engineering)
MAJOR FIELD: Irrigation Engineering
DEPARTMENT: Irrigation Engineering

TITLE: Water Accounting Plus (WA+) for the Tonle Sap Lake Basin using Satellite-Derived Data and WEAP Model

NAME: MR. PHANIT MAB

THIS THESIS HAS BEEN ACCEPTED BY

-- **THESIS ADVISOR**
(Associate Professor Ekasit Kositsakulchai, Ph.D.)

-- **THESIS CO-ADVISOR**
(Mr. Chuphan Chompuchan, Ph.D.)

-- **DEPARTMENT HEAD**
(Assistant Professor Nimit Cherdchanpipat, M.Eng)

APPROVED BY THE GRADUATE SCHOOL ON --

-- **DEAN**
(Associate Professor Somwang Khantayanuwong, Ph.D.)

THESIS

WATER ACCOUNTING PLUS (WA+) FOR THE TONLE SAP LAKE BASIN USING SATELLITE-DERIVED DATA AND WEAP MODEL

PHANIT MAB

A Thesis Submitted in Partial Fulfillment of
the Requirements for the Degree of
Master of Engineering (Irrigation Engineering)
Graduate School, Kasetsart University
Academic Year 2018

PHANIT MAB : Water Accounting Plus (WA+) for the Tonle Sap Lake Basin using Satellite-Derived Data and WEAP Model. Master of Engineering (Irrigation Engineering), Major Field: Irrigation Engineering, Department of Irrigation Engineering. Thesis Advisor: Associate Professor Ekasit Kositsakulchai, Ph.D. Academic Year 2018

In this study, water balance analysis in term of water accounting plus was assessed by satellite-derived data. The main objectives of this study were to evaluate the satellite-derived data for estimating the components of water accounting plus (WA+), to analyze water balance in the Tonle Sap Lake basin by WEAP model, and to conduct the WA+ under the current situation. Water balance analysis showed that the Mekong River is the key water source of the Tonle Sap Lake. It represented more than half of total inflow, while the watershed streamflow contributed about one-third of total inflow. According to the resource base sheet of annual WA+, inflow from rainfall represented around 78% of the net inflow. Surface inflow from the Mekong River also showed significant component of around 22%. The depleted water from evapotranspiration was more than half, while the surface outflow was only 35%. For the seasonal WA+, the highest depleted water occurred during the wet season around 76%. Only 24% was released to downstream. Moreover, the storage of the Tonle Sap Lake showed also an important role in the available water during the dry season. The evapotranspiration sheet provided the water depletion from different land-use categories. The highest water depletion was in Utilized Land Use class, it takes place more than half. However, this land use type, most of the water depletion occurred from wetlands. Modified Land Use also demonstrated a high one around 29% which happened in the agricultural land. To maintain this amount of water, it should pay attention to agricultural water use by improving land and water productivity. These would be a help to decrease water consumption and increase crop production. The main sources for reducing water depletion is to reduce soil evaporation.

____________________ ____________________________________ _____ / _____ / _____

Student's signature | Thesis Advisor's signature

ACKNOWLEDGEMENTS

This thesis was supported by the Kasetsart University Scholarships for ASEAN for Commemoration of the 60th Birthday Anniversary of Professor Dr. Her Royal Highness Princess Chulabhorn Mahidol. Moreover, I would also like to show my gratitude to the WEAP model and Google Earth Engine (GEE) developers for providing a license during this research.

Firstly, I would like to express my sincere gratitude to my advisor Dr. Ekasit Kositsakulchai, for the continuous support of my study and related courses, for his patience, motivation, and immense knowledge. His guidance helped me in all the time of research and writing of this thesis.

Secondly, my sincere thanks also go to my co-advisor Dr. Chuphan Chompuchan, GIS and remote sensing courses who provided me many documents to learn, and taught and guided me through the concepts of GIS and remote sensing. Without his precious support, it would not be possible to conduct this thesis.

Many thanks to professors, Department of Irrigation Engineering, Faculty of Engineering, Kasetsart University at Kamphaeng Saen Campus, who provided me an opportunity to join their classes as a master's degree student. I am very grateful to whom that always concern.

I would like to thank Dr. Ketvara Sittichok and Dr. Areeya Rittima for all guidance through the final examination, their discussion, ideas, and feedbacks have been absolutely invaluable for me.

Besides my advisor, co-advisor and professors, I would like to thank my family, friends, who supported me for their insightful comments and encouragement.

PHANIT MAB

TABLE OF CONTENTS

Page

LIST OF TABLES

Page

LIST OF FIGURES

Page

WATER ACCOUNTING PLUS (WA+) FOR THE TONLE SAP LAKE BASIN USING SATELLITE-DERIVED DATA AND WEAP MODEL

INTRODUCTION

The Mekong River flows through to six countries namely Cambodia, China, Lao PDR, Myanmar, Thailand and Vietnam (Goh, 2017). The river originates in the Tangelo mountain range in Qinghai province of China (Phua, 2011). The part of the Mekong River Basin within China and the eastern end of Myanmar is known as the Upper Mekong River Basin (UMRB) (Wassmann *et al.*, 2004) and lower part is known as the Lower Mekong River Basin (LMRB) within Cambodia, Lao, Myanmar, Thailand and Vietnam (Pink, 2016). The LMRB covers about 70% of the basin and is the most significant region both economically and environmentally (Promkotra, 2014), including the Tonle Sap Lake basin. Out of total catchment area of 795,000 km^2, around 25% lies in the Lao PDR, 23% in Thailand, 21% in Yunnan (China), 20% in Cambodia, 8% in Vietnam and only 3% is part of the Myanmar (Eastham *et al.*, 2008)

The Tonle Sap ecosystem in Cambodia is a major component of the Mekong basin, consisting of the Tonle Sap Lake, the Tonle Sap River and their surrounding floodplains. The Tonle Sap Lake is linked to the Mekong River through the 100 km long Tonle Sap River tributary (Welcomme, 1985). When water levels in the Mekong rise above a threshold level, usually in late May - early June, flow in the Tonle Sap River is reversed and Mekong water is pushed into the Tonle Sap River and Lake. During the wet season, the volume of the lake increases from about 1.3 km^3 to 50-80 km^3 depending on the flood intensity, and its surface area increases from 2,500 km^2 to 10,000-15,000 km^2 (Kummu, 2003).

The lake is the largest freshwater body in Southeast Asia. The lake is reported to be very productive (MRC, 2002; Rainboth, 1996). The lake functions as a natural flood retention for the Mekong system during the dry season (November–April), when approximately half of the discharge to the Mekong Delta in Vietnam originates from the lake (Fujii *et al.*, 2003). The ecosystem is driven by a flood pulse regime, supporting a fishery and aquaculture that provides approximately up to 80% of the protein consumption of Cambodia (Ahmed *et al.*, 1998). Due to its extraordinary role the Tonle Sap Lake can be regarded as the 'Heart of the Mekong'; without it the Mekong River and its aquatic life would not flourish as it does today. The role of the Tonle Sap for Cambodia is even greater. It has been approximated that as many as half of the country's population benefits directly or indirectly from the lake's resources (Bonheur, 2001). Over 3.6 million Cambodian people depend on this lake in living and derive their livelihoods directly from its natural resources (ADB, 2005).

Over the last 50 years, the world situation has changed from an abundance of water to a situation of water scarcity. Over 1.2 billion people live in basins where water demand is reaching, or has exceeded limits of sustainable use (Gleick, 2000). Population growth, changing diets, and economic growth, are some of the main causes of increased water use, which has resulted in competition for water, closed basins (a basin where all available water is depleted), overexploited groundwater resources, degraded land, reduced ecosystem services and anthropologically induced droughts(Karimi *et al.*, 2013). Water resources have been less effective in managing water in this relatively new era of scarcity (Alcamo *et al.*, 2007).

Water accounting integrates the fields of hydrology, water and environmental management, water allocations, reporting and communication. It facilitates identification of central problems in river basins, constraints and opportunities for improved climate resilience. It assists with decisions regarding carbon sequestration and safeguarding sufficient water resources for a good quality life, also during periods of prolonged drought(Karimi *et al.*, 2013). Water accounting is described in this context below.

Water balance is a key determinant for the distribution and productivity (Churkina *et al.*, 1999) of terrestrial vegetation around the globe. In turn, the composition and distribution of plant communities are of fundamental importance for evapotranspiration and runoff generation (Dunn and Mackay, 1995). Water balance analysis can be used to: identify and quantify water inflows and outflows. It also identifies changes in stocks of water; quantifies components of the water balance. (Batchelor *et al.*, 2017).

Water resource management models are effective tools for addressing water shortages. This is because water supply and demand simulations can support decision processes for regional water resource planning (Andreu *et al.*, 1996). Techniques for estimating water balance range from very simple methods, such as lumped models and field-experiment techniques, to highly complex computer-based models that can calculate water balance at various temporal (e.g., hourly, daily, monthly, and yearly) and spatial scales(Xu and Singh, 1998; Zhang *et al.*, 2002). Selection of an appropriate technique depends on the objectives of the study and availability of data.

In this case, water accounting and water resources modelling system can be more effective tools to identify the water resources management. It can use the spatial information from the satellite-derived data.

In developing country likes Cambodia, the available data from the monitoring stations is the critical problem in order to study the water balance analysis. Rainfall, evapotranspiration (ET), are absence for the whole study areas. Even where data available, the quality and temporal data are not good enough. It causes too difficult to evaluate the components of hydrological cycle of the basin. However, all these datasets must be assessed for the water balance analysis components. The lack of meteorological stations forces the researcher to retrieve datasets from other sources. Remote sensing is the appropriate method to obtain the free online datasets. Additionally, the Google Earth Engine (GEE) could allow us to get datasets quickly and easily with the reliable outputs. In this study, the GEE is a main platform application to request all input data.

OBJECTIVES

In this study, it focused on the question: "How to conduct the assessment of water resources in an area with a limited data availability on Cambodia using satellite-derived data?" The main objectives of this study were:

1. To evaluate the satellite-derived data for estimating the components of Water Accounting Plus (WA+).

2. To analyze water balance in Tonle Sap Lake basin by a water resource system model.

3. To conduct the WA+ analysis of Tonle Sap Basin under the current situation.

SCOPE AND LIMITATION

In this work, the Water Accounting Plus (WA+) framework was selected in order to address the water resources situation in the Tonle Sap Lake watershed. The analysis was based on current surface water of the basin and selected annual and monthly time series data from 2000 to 2014. The Water Evaluation And Planning (WEAP) was used to calculate of the inter-connected water balance components in the basin.

LITERATURE REVIEWS

1. Water Accounting

The journals and reporting on water accounting has been reviewed many times by various researchers who worked on this sector. Water accounting changed framework many time following as the weakness points of each tools. Several international organizations had developed new generation of water accounting frameworks such as, the United Nation (UN), the International Water Management Institute (IWMI) and the Australian government.

The United Nations Statistics Division has proposed a water accounting framework called System of Environmental Economic Accounting for Water (SEEAW). SEEAW describes hydrological and economic information through a set of standard tables and has also some supplementary tables to cover social aspects (UN, 2007). The SEEAW accounting components have precipitation, soil water, and evapotranspiration. This tool presents water from precipitation and the total amount of ET, excluding rainfall partitioning by different land use class. It does not show the beneficial of non-beneficial of depletion in term of ET.

The International Water Management Institute (IWMI) established a water accounting too. It demonstrated the water depletion instead of withdrawals. The water depletion is neglected recycling water and included evapotranspiration. The output per unit is provided in a means to simulation (Molden, 1997; Molden and Sakthivadivel, 1999). Water depletion are separated into two different types, beneficial and non-beneficial. The IWMI WA tool was designed for irrigation structures within a basin. However, it was later used for basin analysis. Some of the components of the IWMI WA are too generic for basin level studies. As the result, water depletion at irrigation service scale represents only crop evapotranspiration (Karimi *et al.*, 2013).

The Australian organisation accounting is originally designed on SEEA-Water with runoff. Comparison of rainfall and ET, stream flows and rivers illustrate with a small fraction of the total water movement (Sivapalan *et al.*, 2003). This tool accounting is to be withdraw water rather than water consumption. It is neglected the water being sink in water cycle. The Australian method studies irrigated agriculture, industrial and domestics water use. It presents the total water resources, economic, social, and benefit from the environment.

A common water accounting framework has so far been missing from the emerging debate on global water governance. The standard flow accounting method is heavily dependent on gauge data, thus while the development of water accounts is being prioritized in many parts of the world, it has been mostly limited to the well-gauged basins of Europe, Australia, the USA and Canada (Karimi, 2014; Molden and Sakthivadivel, 1999). However, the standard flow accounting method is heavily dependent on data. Application to relatively ungauged basins, such as the Niger, is therefore problematic at best. Additionally, most methods exclude natural landscapes, ET and rain-fed agriculture, which are important variables in the most basins (Karimi, 2014; Mainuddin *et al.*, 2010), including the Tonle Sap Lake.

Water accounting is presented in Figure 1. It involves classifying water balance components into water-use categories that reflect the consequences of human interventions in the hydrologic cycle. Water accounting integrates water balance information with uses of water. Inflows into the domain are classified into various use categories as defined below.

Gross inflow is the total amount of water flowing into the water balance domain from precipitation, and surface and subsurface sources.

Net inflow is the gross inflow plus any changes in storage. If water is removed from storage over the time period of interest, net inflow is greater than gross inflow; if water is added to storage, net inflow is less than gross inflow. Net inflow is either depleted or flows out of the water balance domain. Sustainability may be in question when net inflow differs from gross inflow over a long period of time.

Water depletion is a use or removal of water from a water basin that renders it unavailable or unsuitable for further use. Water depletion is a key concept for water accounting, as it is often the productivity and the derived benefits per unit of water depleted that are of primary interest. It is extremely important to distinguish water depletion from water diverted to a service or use, because not all water diverted to a use is necessarily depleted (Keller and Keller, 1995; Molden, 1997).

Beneficial depletion occurs when water is depleted in providing an input to produce a good such as an agricultural output, or providing a need such as drinking or bathing water, or in any other manner deemed beneficial such as supplying water for environmental uses (Molden and Sakthivadivel, 1999).

Committed water is that part of outflow that is allocated to other uses. For example, downstream water rights or needs may require that a certain amount of outflow be realized from an irrigated area. Or water may be allocated to environmental uses such as minimum stream flows, or outflows to sea to maintain fisheries.

Uncommitted outflow is water that is neither depleted nor committed, is available for a use within a basin or for export to other basins, but flows out due to lack of storage or operational measures.

Available water is the net inflow less the amount of water set aside for committed uses and less non-utilizable uncommitted outflow. It represents the amount of water available for use at the basin, service or use levels.

Non-depletive uses of water are uses where benefits are derived from an intended use without depleting water.

Depleted fraction (DF) is that part of the inflow that is depleted by intended process uses. Defined in terms of gross inflow, depleted fraction is:

$$\text{DFnet}=\frac{\text{Depletion}}{\text{Grow inflow}} \qquad \text{Eq. 1}$$

Beneficial utilization (BU) indicates the percentage of water beneficially depleted. In terms of available water, it is:

$$\text{BUavailable}=\frac{\text{Beneficially depleted}}{\text{Available water}} \qquad \text{Eq. 2}$$

Productivity of water (PW), expressed in terms of available water, is:

$$\text{PWavailable}=\frac{\text{Productivity}}{\text{Available water}} \qquad \text{Eq. 3}$$

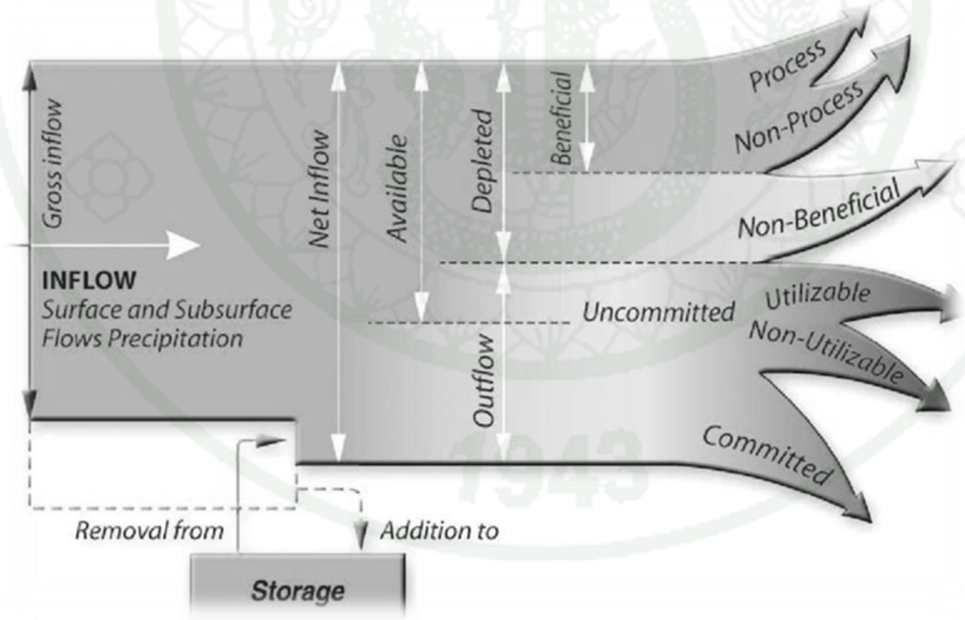

Figure 1 Water accounting framework

Source: (Molden *et al.*, 2003)

2. Water Accounting Plus

Water Accounting Plus (WA+) is a new framework that uses the IWMI WA principles of tracking water depletions rather than withdrawals. WA+ adopts the same definition for water depletion as the IWMI WA. It is often associated with withdrawals (Karimi *et al.*, 2013). This new framework was considered on this study.

Water accounting involved classifying water balance components into water-use categories that reflected the consequences of human interventions in the hydrologic cycle. Water accounting integrates water balance information with uses of water as visualized conceptually (Molden and Sakthivadivel, 1999).

Inflows into the domain are classified into various use categories as defined below: There are four sheets for accounting, namely: (1) Resources base sheet, (2) Evapotranspiration sheet, (3) Productivity sheet and (4) Withdrawal sheet. In this study, we conducted for the first (1) and second (2) sheets.

2.1 Resource based sheet

The **WA+ Resource based shee**t is presented in Figure 2. It provides information on water volumes. Inflows are shown on the left of the resource base sheet diagram, the middle part provides information on how and through what processes the water is depleted within a domain, and information on exploitable water and reports on outflows are summarized on the right (Karimi *et al.*, 2013).

Precipitation plus any surface or groundwater that flows to the domain from outside its boundaries is *Gross inflow*. *Net inflow* includes water storage changes over the period of accounting. The fresh water storage changes is surface water. The net inflow is partitioned into *landscape ET* and *exploitable water* present in streams, soils and aquifers. The *landscape ET* is a consequence of a certain rainfall distribution across a composite terrain with mixed land use, geological formations, soil types, slopes, elevations and natural drainage to streams. The net inflow minus landscape ET can be referred to as *exploitable water*. It represents the portion of the net inflow that is not evaporated and is available for downstream use and withdrawals. The landscape ET is further divided into the four land use categories “conserved land use (CLU)”, “utilized land use (ULU)”, “modified land use (MLU)”, and “managed water use (MWU)”.

Not all of the exploitable water is available for use as part of it has to be reserved to meet downstream water right requirements (committed outflow, navigational flow and environmental flow). Guidelines for environmental flow are provided by for instance (Smakhtin, 2004). This water is called reserved outflow and is equal to the maximum of committed outflows, navigational flow and environmental flow. Exploitable water less reserved outflows is available water. It is the available water that can be allocated to various water use sectors. Part of the available water is depleted. This depleted water is called utilised flow and mainly takes place through incremental ET. The available water less the utilised water is utilisable water representing the amount of additional water that could be utilised. It represents the water that is not depleted, nor reserved, and is, thus, available for use within the basin or for export and intra basin water transfers. Depleted water is total ET. Outflows refer to the amount of water that physically leaves the basin through surface water system.

The resource based sheet in WA+ has a set of minimum performance indicators that are presented as fractions. These indicators are to help basin planners to understand the key information on water management in a basin, or any domain that water accounts are provided for. Time series of these indicators reveal trends. The impact of water policy interventions on water scarcity and benefits from water can be quantified. Exploitable water fraction is that part of the net inflow that is not lost to the landscape ET processes. The fraction relates to total run-off generated in a river basin and also exploited water from fresh water storage.

$$\text{Exploitable water fraction} = \frac{\text{Exploitable water}}{\text{Net inflow}} \qquad \text{Eq. 4}$$

Storage change fraction defines the degree of dependency on fresh storage change (ΔSfw). The fresh water resources are surface water storage, groundwater storage and total water storage. The negative values indicate storage depletion while positive values indicate that in the accounting period water storage has been increased in the domain.

$$\text{Storage change fraction} = \frac{\Delta \text{sfw}}{\text{Exploitable water}} \qquad \text{Eq. 5}$$

Available water fraction relates available water to exploitable water. It describes the portion of exploitable water that is actually available for withdrawals within a basin.

$$\text{Available water fraction} = \frac{\text{available water}}{\text{Exploitable water}} \qquad \text{Eq. 6}$$

Basin closure fraction describes to what extent available water is already depleted in a basin or domain. A closed basin is one where all available water is depleted. According to this definition a closed basin can still have substantial discharge in case all outflow is reserved.

$$\text{Basin closure fraction} = \frac{\text{Utilised flow}}{\text{Available water}} \qquad \text{Eq. 7}$$

Reserved outflows fraction relates the reserved outflows to outflow via streams and aquifers. It indicates whether the committed outflows are being met. The reserved outflows are intended to surface.

$$\text{Reserved outflow fraction} = \frac{\text{Reverved outflow}}{\text{Qout,surface water}} \qquad \text{Eq. 8}$$

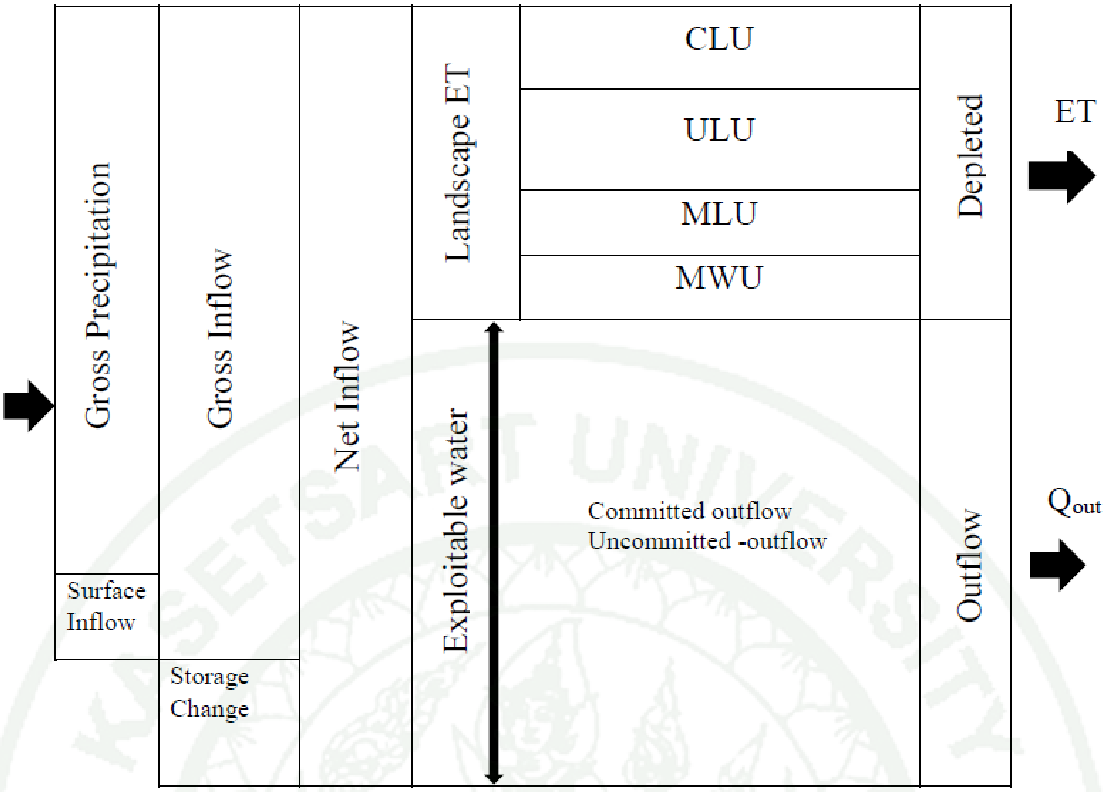

Figure 2 Resource based sheet of the Tonle Sap Lake

2.2 Evapotranspiration sheet

The **WA+ Evapotranspiration sheet** (Figure 3) shows the processing of ET manageable or non-manageable that requires a value to specify beneficial and non-beneficial ET occurs through certain physical processes: evaporation (from soil, water), and interception evaporation from wet leaves and canopies (Rutter *et al.*, 1971) and wet surfaces (e.g., buildings, roads). However, in some cases, interception evaporation is important for temperature regulation of plants and, hence, is beneficial. Transpiration (T) is the transfer of water by the plant to the atmosphere through stomata in the leaves. Water vapour transfer via transpiration and CO_2 inhalation are biophysically linked (Monteith, 1988). While T is generally considered as beneficial, it can be considered non-beneficial in some cases such as weed infestations in cropland or in degraded landscapes, or when there are non-desirable plants. E is usually considered as non-beneficial as the vast majority of E originates from wet soils (Choudhury and DiGirolamo, 1998). However, E from natural surface water is often beneficial.

Performance indicators for the WA+ evapotranspiration sheet provide key information on the magnitude of beneficial ET in a basin. Water use by key water users in a basin is expressed in term of fractions. Transpiration fraction is the part of ET that is transpired by plants and its reflects an impact on bio-physical process in water scare basin.

$$\text{Tfraction} = \frac{T}{ET} \qquad \text{Eq. 9}$$

Beneficial ET fraction relates E and T to the total ET in a basin.

$$\text{Beneficial fraction} = \frac{Ebeneficial + Tbeneficial}{ET} \qquad \text{Eq. 10}$$

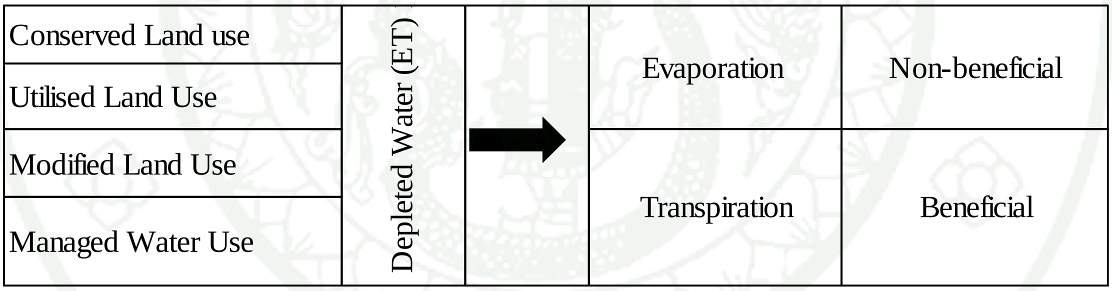

Figure 3 Evapotranspiration sheet of the Tonle Sap Lake

3. Previous Studied on Water Accounting and WA+

The IWMI WA has been applied to assess productivity of water use in several basins across the globe at various scales. Example of applications include Egypt's Nile (Molden *et al.*, 1998). China's Yellow River basin, India's Krishna basin, Nepal's Indrawati basin, Indonesia's Singkarak-Ombilin River basin and Zhang IIe Irrigation District in China and the Karkheh River basin (Karimi *et al.*, 2012b).

Molden and Sakthivadivel (1999) applied Water Accounting to different levels of analysis ranging from a micro level such as a household, to a macro level such as a complete water basin. Indicators are defined to give information on the productivity of the water resource. Examples from Egypt's Nile River and a cascade of tanks in Sri Lanka are presented to demonstrate the methodology.

Peter *et al.* (2010) applied WA+ on the Okavango River Basin which remained one of the watersheds least affected by human impacts on the African continent based on remote sensing and will therefore be easily applicable worldwide without the need of extensive field monitoring and data collection. Water Accounting, lack of data, has overcome in the proposed WA+ by relying heavily on satellite data.

Droogers *et al.* (2010) was applied WA+ in the Okavango River Basin using remote sensing data that collected from satellite images. Shilpakar *et al.* (2011) used remote sensing-based approach for water accounting in the East Rapti River Basin, Nepal. This study successfully demonstrated that the key inputs required for evaluating and monitoring the overall water resources conditions in a mountainous river basin can be computed from satellite data with a minimal support from ground information.

Karimi *et al.* (2012a) had presented Water Accounting for Indus Basin. Total area is 1,160,000 km^2 which is shared by Pakistan, India, China, and Afghanistan, each respectively occupying 53, 33, 8, and 6 % of the basin area. With a population of about 250 million, the basin is among three major highly populated river basins in South Asia alongside Ganges and Brahmaputra Basins.

MATERIALS AND METHODS

1. Study Area

The Tonle Sap Lake is the largest permanent freshwater lake, locating in Cambodia at the Lower Mekong River basin (Campbell *et al.*, 2009). During the dry season, the lake is about 120 km long and 35 km wide with an area of about 2,500 km^2. During the flood period, the lake expands to 250 km long and 100 km wide with an area of about 17,500 km^2, and the depth reaches 8-10 m. The Tonle Sap basin is 85,796 km^2 in total, extends over 44% of Cambodia's total area. It is shared by Cambodia 95 % and Thailand 5% of the total basin area (Campbell *et al.*, 2006; Junk *et al.*, 2006). There are five provinces bordering Tonle Sap Lake namely: Siem Reap, Battambang, Pusat, Kampong Cham, and Kampong Thom. The Tonle Sap Basin consists of 11 river basins namely (ST1) Stung Baribor, (ST2) Stung Chikreng, (ST3) Stung Chinit, (ST4) Stung Dauntri, (ST5) Stung Mongkol Borei, (ST6) Stung Pursat, (ST7) Stung Sangker, (ST8) Stung Sen, (ST9) Stung Siem Reap, (ST10) Stung Sreng and (ST11) Stung Staung. The Tonle Sap Lake location is presented in Figure 4. Area of each basin is summarized in Table 1.

Table 1 Subtotal area of each basins

Basin code	Basin name	Area (km^2)
ST1	Boribor	7,152
ST2	Chikreng	2,713
ST3	Chinit	8,235
ST4	Dauntri	3,695
ST5	Mongkolborey	15,020
ST6	Pursat	5,963
ST7	Sangke	6,051
ST8	Sen	16,340
ST9	Sieamreap	3,618
ST10	Sreng	9,930
ST11	Staung	4,356
	Tonle Sap Lake	2,723
Total		**85,796**

The Tonle Sap Lake basin is located in the tropical region with wet and dry season. Average daily temperatures vary between about 20 °C and 36 °C (Figure 5) with lowest temperatures in January and highest in April (Campbell *et al.*, 2006).

The Tonle Sap River, which flows from the south-eastern end of Tonle Sap Lake, joins the Mekong River at the Chaktomuk confluence, in the vicinity of Phnom Penh. After the confluence, the river immediately splits into the smaller Bassac River and the larger Mekong River. In the wet season, from May to September, flooding and the associated water level increase in the Mekong River causes the Tonle Sap River to change flow direction and flow towards the northwest (upstream) into Tonle Sap Lake (Kummu *et al.*, 2014).

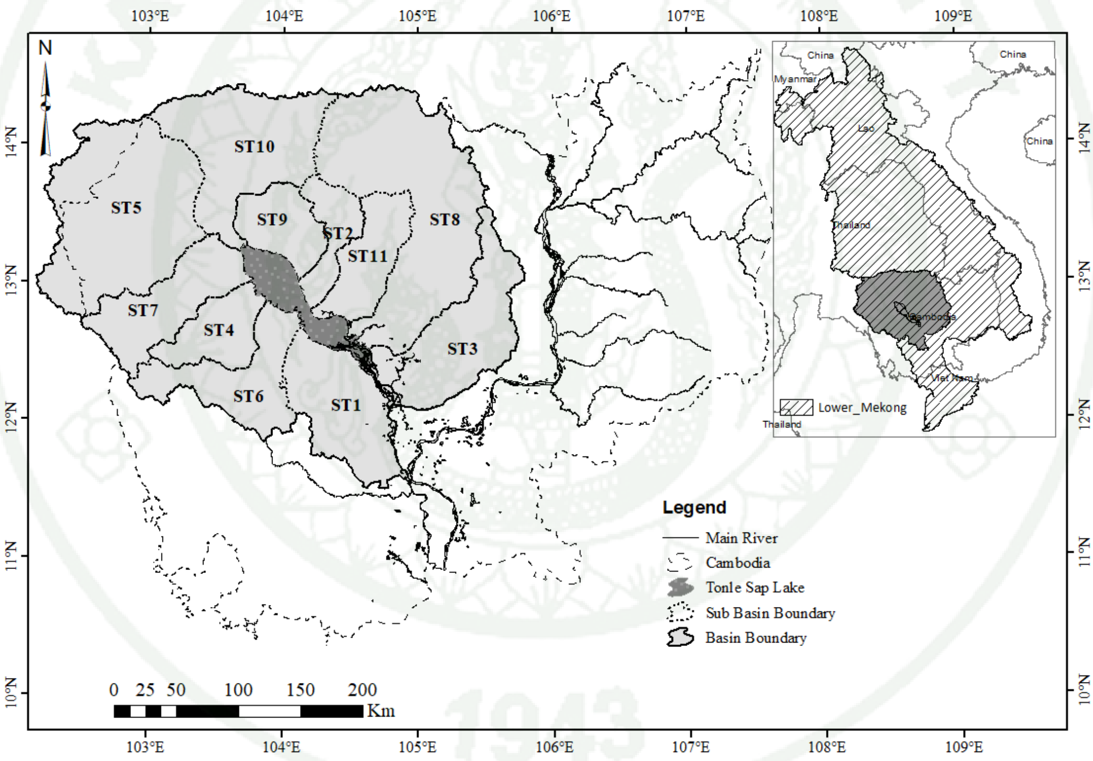

Figure 4 The Tonle Sap Lake and its catchments

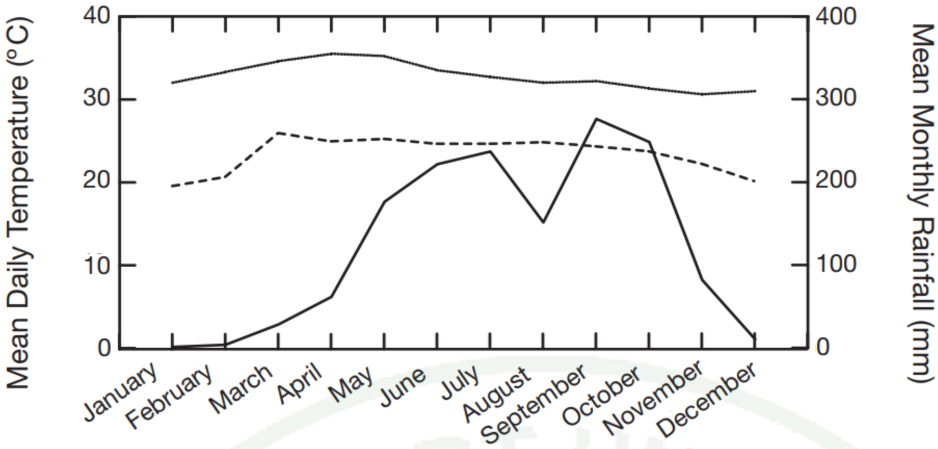

Figure 5 Mean monthly temperature (short dashed) and rainfall (long dashed)

Source: Campbell *et al.* (2006)

2. Water Accounting Plus Method

Water Accounting Plus (WA+) in Tonle Sap Lake is a method to access with satellite images, which help to understand and interpret satellite images information. Moreover, evapotranspiration, rainfall, and land-use has been taken into account in this study.

Depletion water accounting frameworks, such as WA+, have been trialled in recent years to focus on the consumptive use of water including water consumption for natural processes (green water consumption) as well as human uses (blue water consumption) (Falkenmark and Rockström, 2006; Karimi, 2014). Water accounting methods is following as:

$$Q = P - ET \pm \Delta S \qquad \text{Eq. 11}$$

Where Q is discharge (mm/yr), P is precipitation (mm/yr), ET is the sum of actual evaporation and transpiration (mm/yr) and ΔS is changes in storage.

2.1 Land-use classes in water accounting plus

Land use classification is most basic work to research land use, it direct affected the research and practice of land use (Mingzhou, 1997). Land use/land-cover is one of the most important factors affecting runoff and evapotranspiration in the watershed (Setegn *et al.*, 2010).

WA+ explicitly recognizes the influence of land use on the water cycle. To provide the link between water balance, land use and water use, it groups land use classes with common management characteristics including “Conserved Land Use” (CLU), “Utilized Land Use” (ULU), “Modified Land Use” (MLU), and “Managed Water Use” (MWU). CLU includes National Parks and other protected areas, ULU is land use with intensive ecosystems services, MLU is land with human influences such as the cultivation of rainfed crops, plantations and soil treatment. Withdrawals in the MWU class is by means of man-made infrastructures (diversion dam, canals, ditches, pumping stations, gates, weirs, pipes etc.) (Karimi *et al.*, 2012a). The more detailed description of land use type for water accounting is presented in Table 2. Categories of land use classed form in water accounting plus is presented in Table 3.

Table 2 Definition of landuse classes on WA+

Conserved land use (CLU)	**Utilized land use (ULU)**	**Modified land use (MLU)**	**Managed water use (MWU)**
Area no changes in land water are possible or advisable.	Human influences is limited, vegetation is not managed on a regular basis.	Area where vegetation/ soils are managed.	All sectors that withdraw water from surface water and or groundwater.
Examples: wetlands, tropical rainforests, mountainous vegetation, national parks.	Examples: forests, natural pastures, savannas, deserts.	Examples: rain-fed agriculture, built up and urban area.	Examples: irrigated agriculture urban water supply and industrial extraction.

Table 3 General landuse classes of WA+

Conserved land use	**Utilized land use**	**Modified land use**	**Managed water use**
Reserves or national park	Closed natural forest	Plantation trees	Irrigated pastures
Areas set aside for conservation	Tropical rain forest	Rainfed pastures	Irrigated crops
Glaciers	Open natural forest	Rainfed crop	Reservoir
Coastal protection	Woody savanna	Rainfed fruit	Greenhouses
	Open savanna	Rainfed biofuels	Aquaculture
	Natural pastures	Parks	Residential area
	Deserts	Fallow Land	Industrial area
	Mountains	Urban	Parks
	Rocks		Managed wetland
	Flood plains		Inundation areas
	Bare land		Mining
	Waste land		Evaporation ponds
	Wetland		Waste water treatment
	swamps		Power plants

Source: Karimi *et al.* (2013)

3. Water Balance Analysis on the Tonle Sap Lake by WEAP Model

The Water Evaluation and Planning (WEAP) model was developed by the Stockholm Environment Institute (SEI). It operates at a monthly step on the basic principle of water balance accounting. The user represents the system in terms of its various sources of supply (e.g. rivers, groundwater, and reservoirs), withdrawals, water demands, and ecosystem requirements (Lévite *et al.*, 2003). The water balance schematic of all sub-basins is presented in Figure 10.

Model elements can fall into two main categories: nodes, where water is demanded or made available for supply, and links, which transfer water between the nodes. The water management model is driven by user-defined demand priorities, supply preferences and environmental requirements for the various nodes. The water allocation problem is solved using linear programming on a daily or monthly basis (Psomas *et al.*, 2016).

Maliehe and Mulungu (2017) presented as WEAP operates on a monthly time step water balance accounting: total inflows equal total outflows, net of any change in storage (in reservoirs and aquifers). A linear programming is used to maximize the satisfaction of demand site and user-specified in stream flow requirements, subject to demand priorities, supply preferences, mass balance and other constraints.

4. Data Processing

In this study, rainfall and evapotranspiration datasets have been extracted from the satellite-derived data by the Google Earth Engine platform. It is a part of remote sensing concept.

4.1 Remote sensing

Remote Sensing is unique in that it can be used to collect data, unlike other techniques, such as thematic cartography, geographic information systems, or statistics that must rely on data that are already available. Remote sensing is defined, for purposes, as the measurement of object properties on the earth's surface using data acquired from aircraft and satellites (Schowengerdt, 2006). WA+ is based on remote sensing and will therefore be easily applicable worldwide without the need of extensive field monitoring and data collection and in ungauged and poorly gauged basins (Droogers *et al.*, 2010).

4.2 Google earth engine

Recently, the Google Earth Engine (GEE) leverages cloud computing services to provide analysis capabilities on over 40 years of Landsat data (Dong *et al.*, 2016). Google Earth Engine (GEE) platform facilitates a fast analysis by using Google's cloud-computing infrastructure (https://earthengine.google.org/). It is a cloud-based platform that makes it easy to access high-performance computing resources for processing very large geospatial datasets (Gorelick *et al.*, 2017). As a remote sensing platform, its ability to analyze global data rapidly lends itself to being an useful tool on data visualization (Patel *et al.*, 2015). Additionally, dataset is processing of geospatial on the online complex spatial analyses using the Javascript Application Programming Interface (API). This API can be developed a code in order to request datasets of publicly available remotely sensed imagery and other data.

The pre-processed daily data of Tropical Rainfall Measuring Mission, or TRMM 3B42V7, biomass and 8-day Potential evapotranspiration (PET) datasets are available datasets through GEE. It was used to assess data sources across the study area by GEE script from 2000 to 2014. All datasets have been summarized into yearly and monthly via JavaScript, excepted biomass in yearly. The example of code is presented in Figure 6. For more detail coding can assess via this link on the GEE (https://code.earthengine.google.com/ec0763b56fea94628615c48ee2acdac8). For further information is presented in Appendix B.

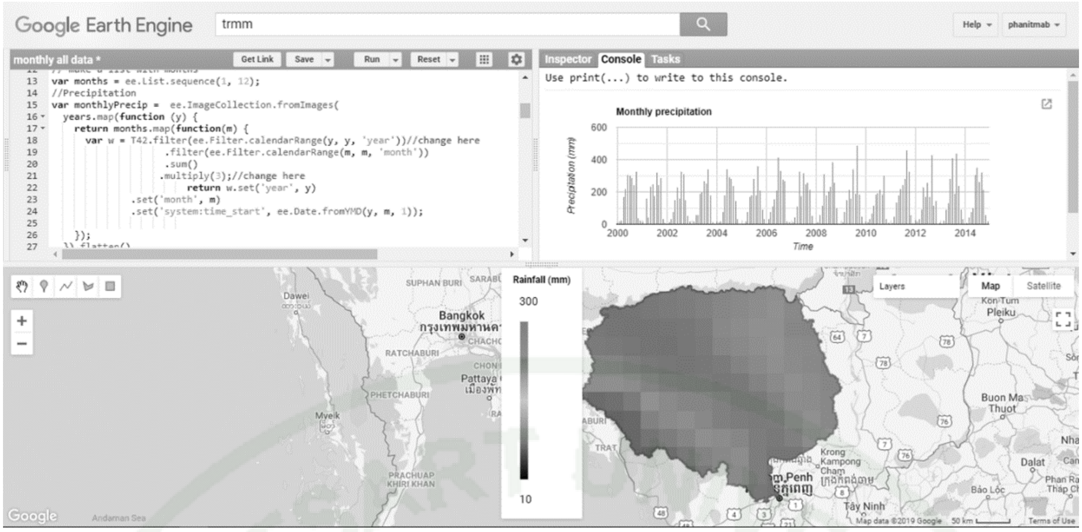

Figure 6 Google earth engine platform

5. Data Usage

5.1 Streamflow gauge of each sub-basins

The summation of streamflow gauge is presented in Table 4. Figure 7 is represented the location of water level stations and gauge stations. Data available with the observed area is also showed for different year on sub-basins (Appendix F).

Table 4 Streamflow gauge station

Basin Code	Station	Station name	Area (km^2)	WGS 1984 Zone48		Data availability
				X	Y	Monthly
ST1	590101	Boribo	869	444601	1368830	2000-2010
ST2	570101	Kampong Kdei	1920	428770	1450651	2000-2010
ST3	620101	Kampong Thmar	4130	513952	1381657	2000-2011
ST4	551101	Prek Chik	1640	325645	1396938	2000-2006
ST5	520101	Mongkul Borey	4170	282538	1498510	2000-2004
ST6	580103	Bac Trakoun	4480	364757	1365618	2000-2011
ST7	550102	Battambang	3230	305283	1447688	2000-2010
ST8	610101	Kampong Thom	14000	488257	1405285	2000-2011
ST9	560102	Prasat Keo	549	379128	1486491	2000-2010
ST10	540101	Kralanh	8175	328804	1504008	2000-2010
ST11	600101	Kampong Chen	1895	453526	1430818	2000-2011

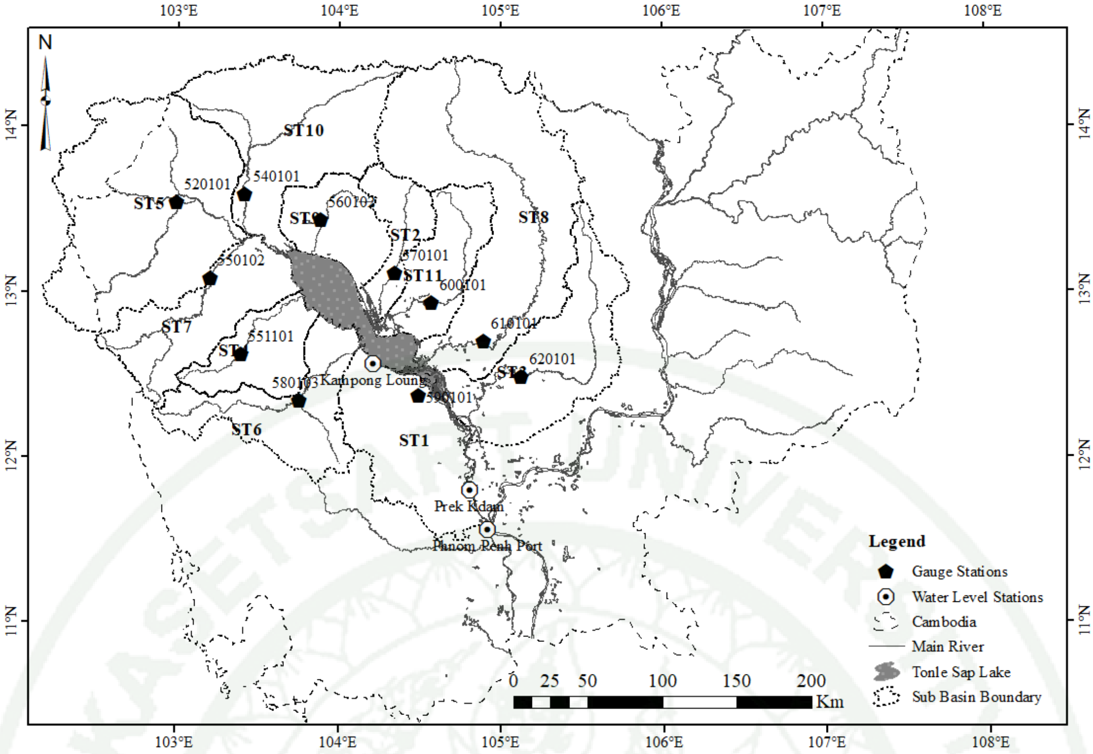

Figure 7 Gauge stations and water level stations

5.2 Rainfall and evapotranspiration

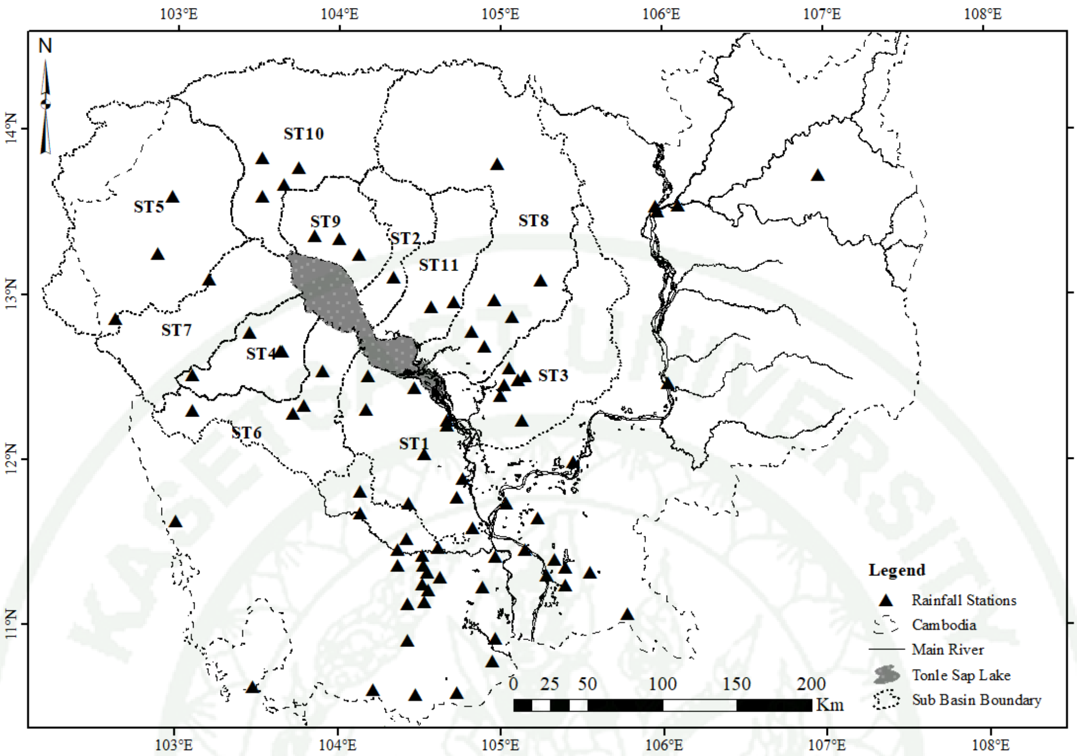

Figure 8 Rainfall stations of the Tonle Sap Lake basin

Precipitation is a critical variable in the global hydrologic cycle, and it influences our daily lives (drought, floods, agricultural, irrigation, outdoor activities, etc.). Precipitation is the primary input for WA+. A new technique is presented in which half-hourly global precipitation. It estimates derived-data from passive microwave satellite scans. The frequency passive microwave (PMW-derived precipitation estimates that are presently used in the Climate Prediction Center morphing method (CMORPH) are generated from observations obtained from the National Oceanic and Atmospheric Administration (NOAA) polar-orbiting operational meteorological satellites, the U.S. Defense Meteorological Satellite Program (DMSP) satellites, and from the Tropical Rainfall Measuring Mission satellite (Joyce *et al.*, 2004).

Since its launch in 1997, the Tropical Rainfall Measuring Mission (TRMM) has provided precipitation estimates that have been widely used in tropical cyclone (TC) rainfall studies (Lonfat *et al.*, 2004). The TRMM 3B42 (V7) three-hourly, $0.25° \times 0.25°$ product is used in this study. This product depends on input from two different types of sensors, namely microwave and IR. The three-hourly estimates are produced in four stages: (1) the microwave estimates are combined, (2) IR estimates are created with microwave calibration, (3) the microwave and IR are combined such that the microwave estimates are taken "as is" with the IR estimates used to fill the gaps, and (4) finally, gridded monthly rain gauge analyses are used to rescale the TRMM satellite precipitation estimates to remove bias where possible to create the final TRMM 3B42 product (Huffman *et al.*, 2007). It is available from 1998 to present at https://pmm.nasa.gov/data-access/downloads/trmm.

CHIRPS stands for Climate Hazards Group IR Precipitation Station and is a third generation precipitation procedure which is based on various interpolation schemes to create spatially continuous grids from raw point data. CHIRPS incorporates 0.05° resolution satellite imagery (Funk *et al.*, 2014). CHIRPS was created in collaboration with scientists at the U.S. Geological Survey (USGS) Earth Resources Observation and Science (EROS) Center in order to deliver reliable, up to date, and more complete datasets for a number of early warning objectives (such as trend analysis and seasonal drought monitoring) (Funk *et al.*, 2015). The available data is from 1981 to near present.

PERSIANN-CDR stands for Precipitation Estimation from Remotely Sensed Information Using Artificial Neural Networks-Climate Data Record. PERSIANN primarily uses infrared brightness temperature data from geostationary satellites to estimate rainfall rate, updating its parameters using PMW observations from low-orbital satellites. The PERSIANN half-hourly 0.25° rain-rate product is available for March 2000 to the present (Hsu *et al.*, 1997). The version 7 TMPA data product (Huffman *et al.*, 2007) has 3-hourly and 0.25° temporal and spatial resolution, respectively, starting from January 1998.

Evapotranspiration is one of the most important components of the hydrological cycle. Combined with rainfall and runoff, it controls the availability and distribution of water at the Earth's surface, and for this reason, is of significance to a number of water-related research and application areas. Quantifying the spatial variability in hydrological and land surface variables is important to water resource management, particularly in agricultural regions (McCabe and Wood, 2006).

The MOD16A2 V105 product provides information about 8-day global terrestrial potential evapotranspiration at 1km pixel resolution. Evapotranspiration (ET) is the sum of evaporation and plant transpiration from the Earth's surface to the atmosphere. With long-term ET data, the effects of changes in climate, land use, and ecosystems disturbances can be quantified data which is based on the Penman–Monteith method and calculates both canopy conductance and ET (Running *et al.*, 2017).

5.3 Landuse type of the Tonle Sap Lake basin

In this study, landuse type of the lake basin has been obtained from the Mekong River Committee on 2003 (Figure 9). The main landuse types in this study area are agricultural lands or rice fields, wetland, forest, open water or lake. The area of each landuse type has summarized in Table 5.

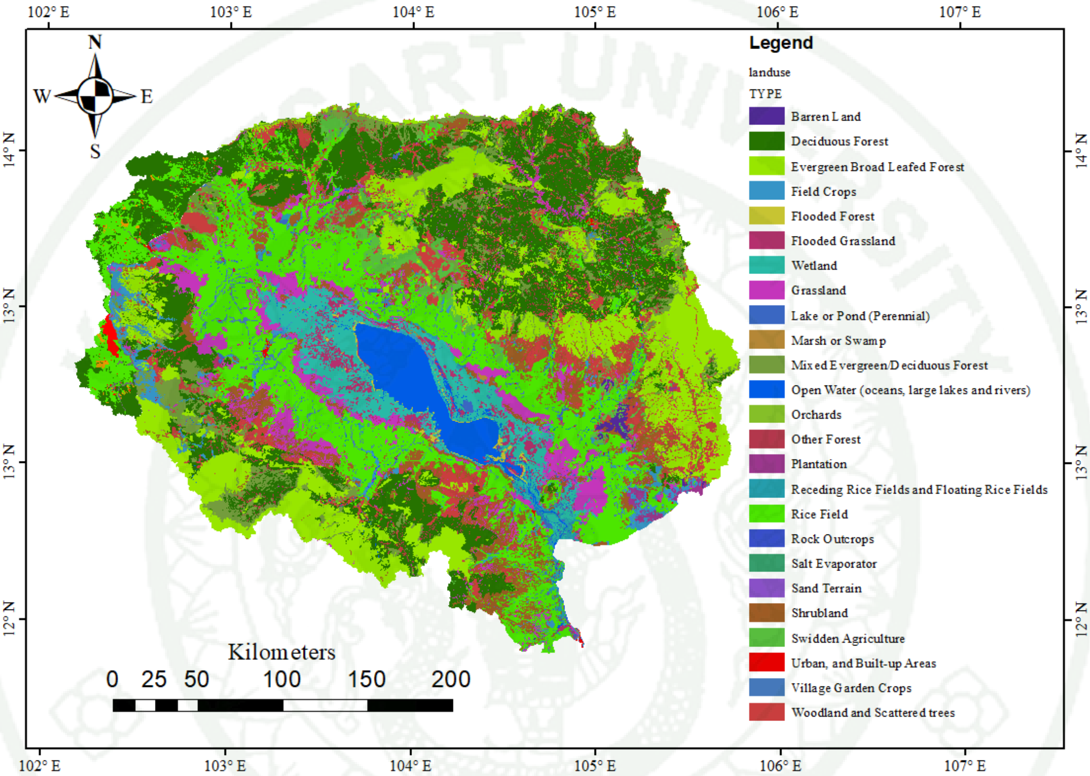

Figure 9 Landuse type of the Tonle Sap Lake basin

Table 5 Landuse classes of the Tonle Sap Lake basin

Land-use classes	**WA+ classes**	**Area (km^2)**	**%**
Woodland and Scattered trees	CLU	5,472.09	6.38
Forest	CLU	2,022.28	2.36
Miscellaneous land	CLU	91.29	0.11
Subtotal	**CLU**	**7,585.67**	**8.84**
Barren Land	ULU	217.80	0.25
Deciduous Forest	ULU	15,491.77	18.06
Evergreen Broad Leafed Forest	ULU	13,722.61	15.99
Flooded Forest	ULU	116.95	0.14
Flooded Grassland	ULU	1,103.05	1.29
Wetland	ULU	4,171.16	4.86
Grassland	ULU	4,946.15	5.77
Marsh or Swamp	ULU	129.65	0.15
Mixed Evergreen/Deciduous Forest	ULU	4,817.12	5.61
Plantation	ULU	218.44	0.25
Rock Outcrops	ULU	2.38	0.00
Sand Terrain	ULU	5.42	0.01
Shrubland	ULU	5,683.83	6.62
Other Forest	ULU	1,273.59	1.48
Subtotal	**ULU**	**51,899.92**	**60.49**
Field Crops	MLU	1,560.85	1.82
Orchards	MLU	4.21	0.00
Receding Rice Fields and Floating Rice Fields	MLU	428.63	0.50
Rice Field/Agrcultural land	MLU	17,790.99	20.74
Swidden Agriculture	MLU	1,796.60	2.09
Urban, and Built-up Areas	MLU	280.62	0.33
Village Garden Crops	MLU	997.49	1.16
Subtotal	**MLU**	**22,859.38**	**26.64**
Lake or Pond (Perennial)	MWU	365.67	0.43
Open Water (oceans, large lakes and rivers)	MWU	3,085.36	3.60
Subtotal	**MWU**	**3,451.03**	**4.02**
Total watershed area		**85,796.00**	

5.4 Reclassification of landuse classes of the Tonle Sap Lake basin

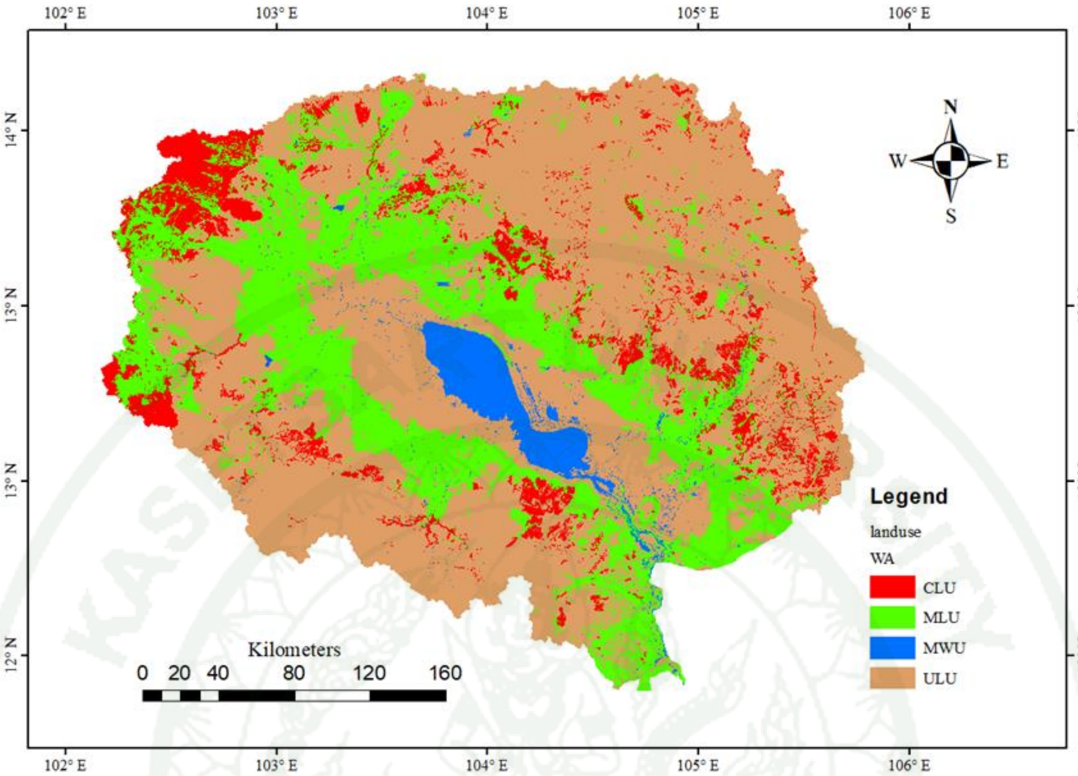

Figure 10 Landuse classification on the Tonle Sap Lake basin

Based on the landuse classes of Water Accounting Plus categories, there are four type of landuse type (Figure 10). Based on the Table 5, the highest one is Utilized Land Use around 51899 km^2, following by Modified Land Use (22859 km^2), Conserved Land Use (7585 km^2) and Managed Water Use (3451 km^2).

6. Methodology

6.1 Overall framework

The general framework is presented in Figure 11. The Google Earth Engine (GEE) was the main platform to retrieve satellite-derived data such as rainfall and ET during these study periods from 2000 to 2014. To reach these goals, a JavaScript has been coded on the GEE server platform in order to evaluate the datasets. Datasets availability depend on the temporal of satellite images which is available on the free open access.

The Water Evaluation and Planning (WEAP) model was the first priority to be used satellite-derived data (rainfall and ET). Both datasets were input into model to complete water balance components analysis of the Tonle Sap Lake Basin. In this model, schematic of the sub-basins were drawn based on study area shapefile as a background. Moreover, rainfall and potential evapotranspiration of each sub-basins were also used as input data. Storage of the lake and water level has been input. Water balance approach, in this case, landuse of the Tonle Sap Lake Basin has been reclassified to four different categories of water accounting plus by the Geographic Information System (GIS). Another thing to note is streamflow was calibrated using the Parameter Estimation Tool (PEST). Calibration depended on the data availability from the streamflow gauge stations during this study period. After this process, water balance components of the lake were conducted in term of water volume such as surface inflow from the Mekong River, rainfall, exchanged flow between the Tonle Sap Lake and the Mekong River, actual evapotranspiration (ETa) and others.

The last part of this objective, Water Accounting Plus (WA+) sheets (Resource based and Evapotranspiration sheets) have been considered in term of WA+ framework. Datasets were prepared using data from the water balance analysis. Hence, WA+ sheets has been conducted in term of four different land-use categories such as Conserved Land Use, Modified Land Use, Utilized Land Use and Managed

Water Use. All data were presented to gross inflow, storage change, depleted water and outflow of the lake.

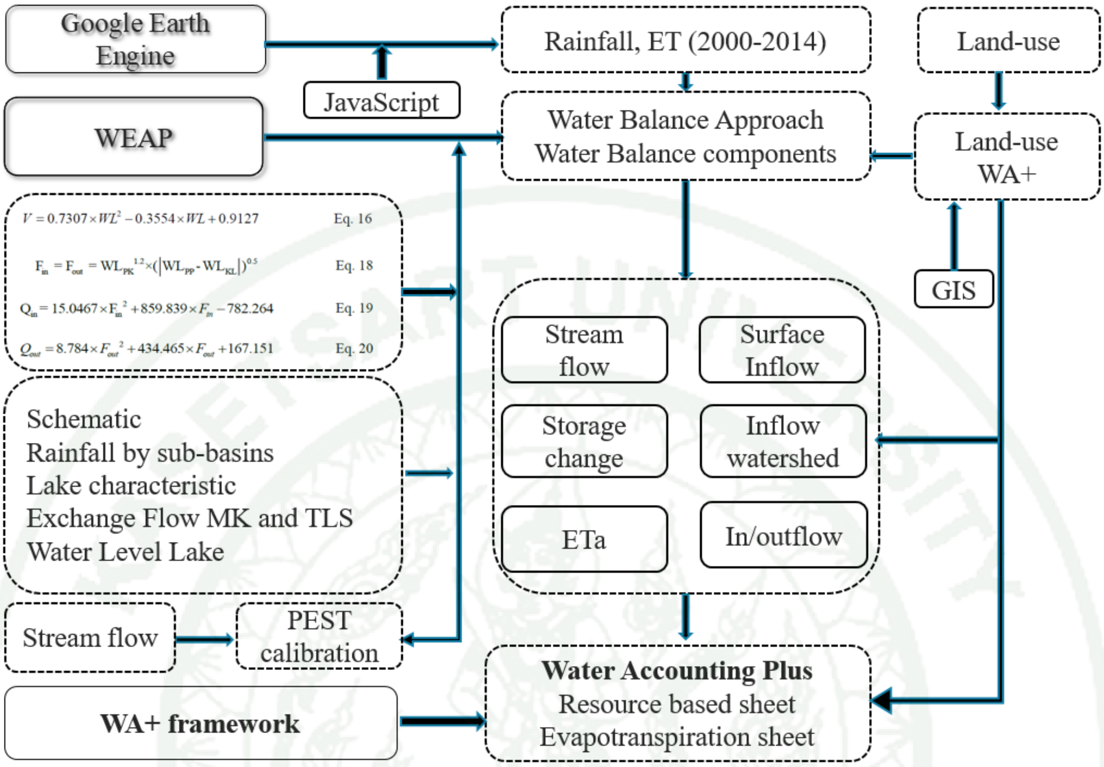

Figure 11 General framework

6.2 Water balance analysis of the Tonle Sap Lake

The water balance analysis relies on the Law of Conservation of Mass, which requires that, for a specified domain over a specified period of time, water inflows are equal to water outflows, plus or minus any change of storage (Batchelor *et al.*, 2017). The water balancing of Tonle Sap Lake was based on the equation:

$$S_i = S_{i-1} + I_i + I_{MK,i} - O_{MK.i} - NET_i \qquad \text{Eq. 12}$$

where S_{i-1} and S_i are the storage of the Tonle Sap Lake at the beginning and the end of each time step, I_i is the inflow from the Tonle Sap watershed, $I_{MK,\,i}$ is the inverse flow in Tonle Sap River from the Mekong River, O_i is the outflow to the Mekong River, and NET_i is the net evaporation which equals to the difference between the potential evapotranspiration and rainfall over the lake surface (PET_i-P_i). The lake surface-area and volume were estimated using the relationships proposed by Kummu *et al.* (2014):

$$V = 0.7307 \times WL^2 - 0.3554 \times WL + 0.9127 \quad \text{Eq. 13}$$

$$A = 5.5701 \times \mathrm{WL}^3 + 1.374 \times WL^2 + 470.29 \times WL + 1680.2 \quad \text{Eq. 14}$$

where, A is surface area of the lake (km^2), V is volume of the lake (km^3) and WL_{KL} represents the water level of Tonle Sape Lake measured at Kampong Loung (KL) station in meter above mean sea level (MSL). Water level of each stations is presented in Appendix G.

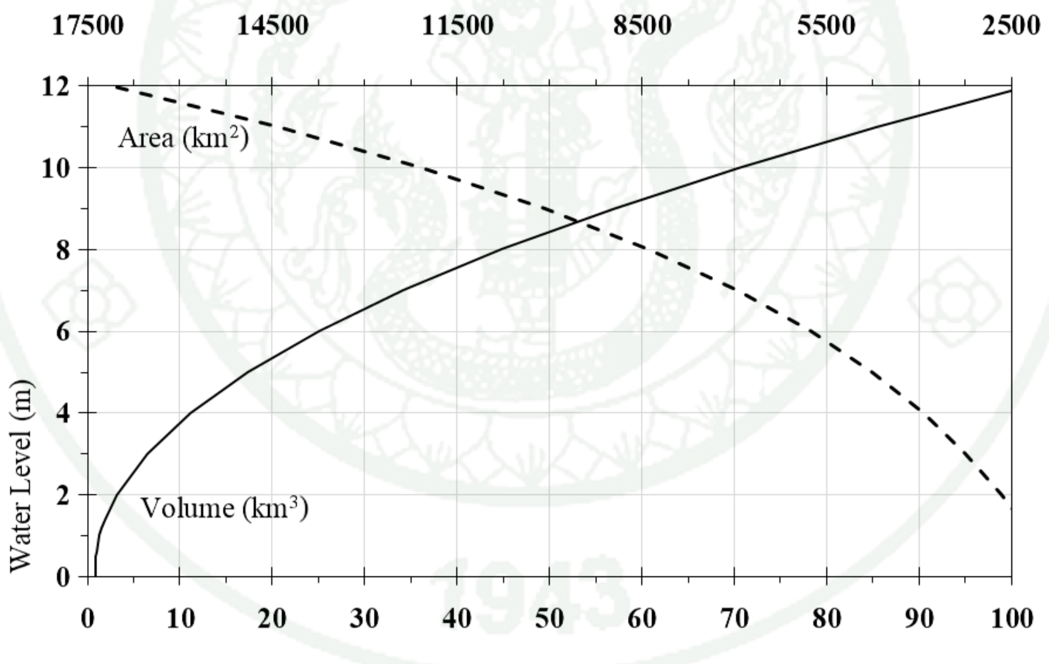

Figure 12 Tonle Sap Lake characteristic

The balancing of inflows and outflows was calculated by the Water Evaluation and Planning System or WEAP model. The WEAP model is developed by the Stockholm Environment Institute (SEI, 2016). The model fundamentally operates on monthly time-step. The watershed of Tonle Sap Lake was divided into 11 sub-basins and represented in the model as shown in Figure 13.

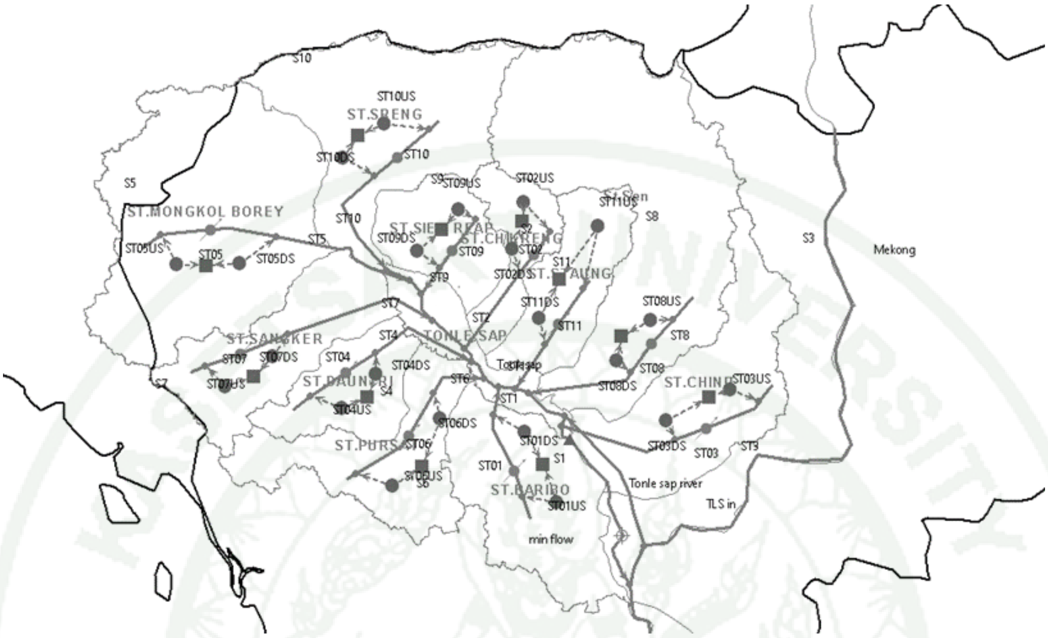

Figure 13 Schematic of the Tonle Sap Lake system represented in WEAP model

6.3 Estimation of exchanged flow between the Mekong and Tonle Sap Lake

The Mekong River and the Tonle Sap Lake have a great significance of exchanged flow. The water level of the river and the lake are related to seasonal pattern. The Tonle Sap River functions naturally as tributary of the Mekong River. Outflow from the Tonle Sap Lake takes place between mid-September and early May. Between early May and mid-September, the inversed flow in the Tonle Sap River occurs when the water levels in the Mekong River are higher than those in the lake. The estimations of exchanged flow between Tonle Sap Lake and Mekong river were followed the relationships proposed by Kummu *et al.* (2014):

$$F_{in} = F_{out} = WL_{PK}^{1.2} \times (\left|WL_{PP} - WL_{KL}\right|)^{0.5} \qquad \text{Eq. 15}$$

$$Q_{in} = -15.0467 \times F_{in}^{2} + 859.839 \times F_{in} - 782.264 \qquad \text{Eq. 16}$$

$$Q_{out} = 8.784 \times F_{out}^{2} + 434.465 \times F_{out} + 167.151 \qquad \text{Eq. 17}$$

where, WL is the water level (MSL), WL_{PK} at Prek Kdam, WL_{PP} at Phnom Penh Port, WL_{KL} at Kampong Loung, Q_{in} is inversed flow into the Lake, Q_{out} is outflow from the Lake.

6.4 Estimation of streamflow of Tonle Sap tributaries

The WEAP model implements several rainfall-runoff methods from simple coefficient, soil moisture, to complex plant-growth simulation. In this study, the MABIA method, which based on the FAO-56 dual crop-coefficient approach (FAO, 1998) was selected. Although the time-step for MABIA is daily, the time-step for the rest of your WEAP analysis does not need to be daily. For each WEAP time-step (e.g., monthly), MABIA would run for every day in that time-step and aggregate its results to that time-step. Groundwater-surface water interactions were also taken into an account. Groundwater flow to stream was estimated as the percentage of monthly streamflow, first derived by a built-in PEST calibration module in WEAP.

RESULTS AND DISCUSSION

1. Comparison of Satellite Rainfall Data to Observation

Based on the Table 6, Persian, Chirp and TRMM have been compared to the observation. The result showed that TRMM is high correlation (r=0.98) compared to observation during this study period on 2010. Chirp and Persian satellite-derived data were also provided a high correlation. Both r datasets were 0.96. Hence, TRMM was selected to simulate during this study periods from 2000 to 2014. For further detail on rainfall data during this study periods is presented in Appendix C.

Table 6 Statistical indicator of satellite rainfall of the Tonle Sap Lake basin

Indicator	Persian	Chirp	TRMM
r	0.96	0.96	0.98
Mean Error	-9.88	-8.58	1.38

Table 7 Satellite rainfall data on the Tonle Sap Lake basin

Month	Observation	Persian	Chirp	TRMM (GIS)	TRMM (GEE)
Jan	11.02	39.60	7.20	20.50	20.88
Feb	6.98	35.00	17.84	15.85	15.84
Mar	28.69	54.08	42.07	33.84	35.28
Apr	61.55	103.91	85.79	68.63	67.68
May	97.23	133.61	142.93	112.57	112.32
Jun	164.21	205.62	189.18	184.98	186.48
Jul	217.24	212.50	180.68	189.48	188.64
Aug	246.29	205.53	330.92	205.62	203.76
Sep	234.87	256.64	288.05	186.30	185.04
Oct	273.64	325.04	266.07	291.21	291.60
Nov	42.66	38.58	34.36	37.48	38.16
Dec	8.07	19.54	13.28	12.77	12.96
Total	**1,392.44**	**1,729.66**	**1,675.35**	**1,359.22**	**1,358.64**

2. Rainfall and Actual ET

The average of annual rainfall varied from 1,338 mm in dry year 2010 to 1,974 mm in wet year in 2011 during these study periods as shown in Figure 14. Mean annual rainfall was about 1,700 mm. The heavy rainfall is seasonal, mainly occurring between April and November, with a peak of 332 mm in September (Appendix C).

The mean actual ET (ETa) was 1463 mm. It varied from 1276 mm to 1709 mm. Monthly data presented in Figure 15. The average monthly actual evapotranspiration varies between 14 mm and 188 mm (Appendix D). January was a high ET in dry season. However, this occurred might be as the amount of water containing in high during the end of wet season. So, it affected to the beginning of dry season which was high ETa in this month. Other month to note is February was released less water in term of ETa. It might be contained less water in soil moisture during this month.

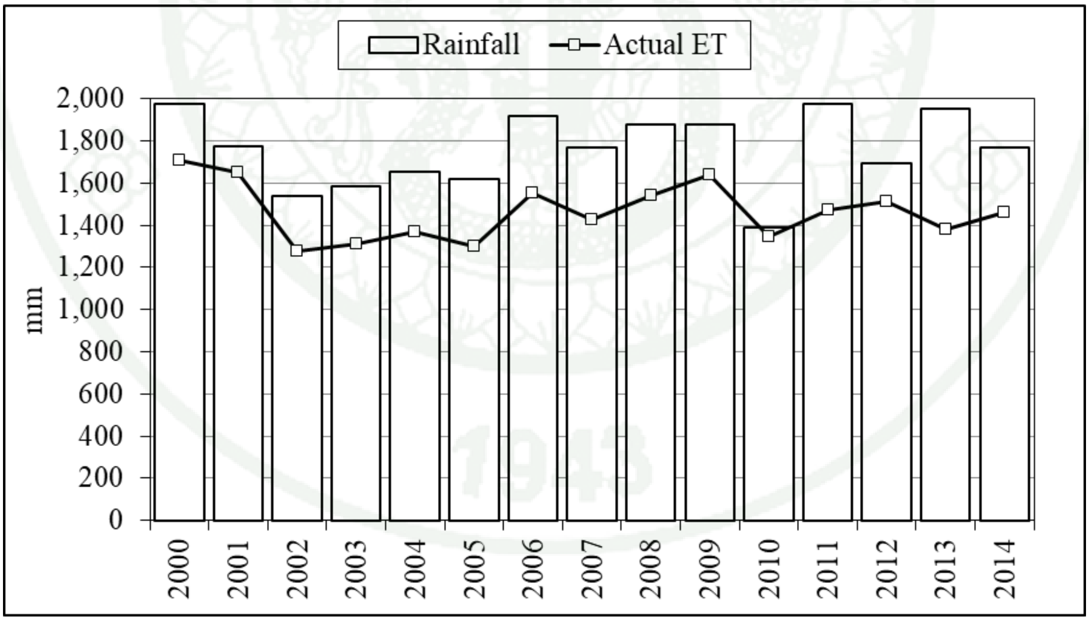

Figure 14 Yearly rainfall and actual ET of the lake

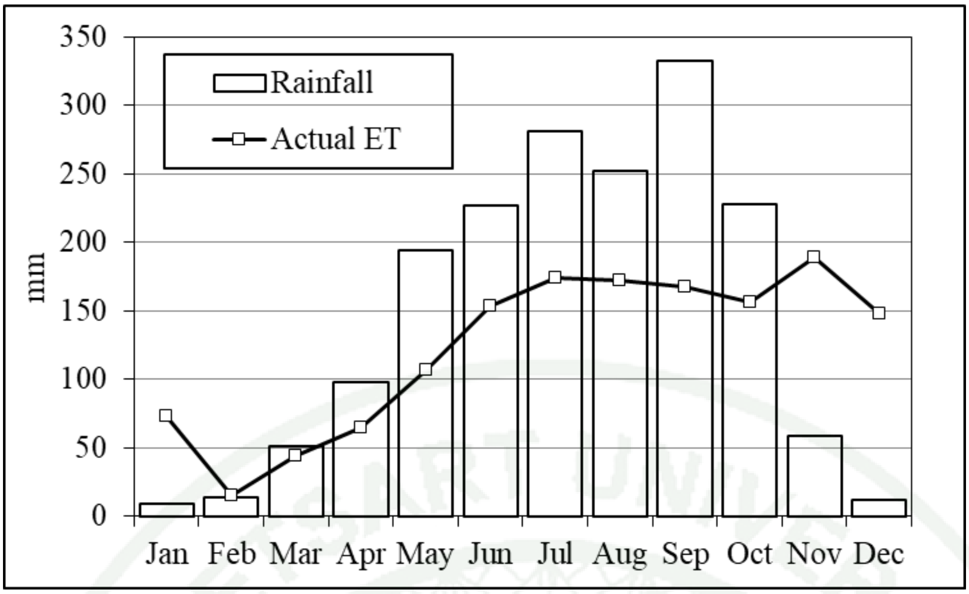

Figure 15 Monthly rainfall and actual ET of the lake

3. The Estimation of Streamflow of the Tonle Sap Lake Basin

Figure 16 to 26 showed the stream flow from sub basins of the Tonle Sap Lake. In Table 7, mean monthly rainfall in sub-basins are presented. In Table 8, mean monthly stream flow in sub-basins are also showed. ST7 received the highest rainfall during this study periods 2049 mm per year. The lowest rainfall is on the basin ST9 1510 mm per year.

Table 8 Average rainfall data of each sub-basins

Month	ST1	ST2	ST3	ST4	ST5	ST6	ST7	ST8	ST9	ST10	ST11
Jan	14.6	8.1	6.1	10.9	9.6	16.4	13.3	3.9	4.8	5.3	4.1
Feb	5.4	6.6	7.1	27.7	24.1	27.8	27.9	7.4	5.9	9.5	4.7
Mar	49.9	34.1	42.8	79.1	58.2	84.8	80.1	39.5	32.3	39.7	34.4
Apr	89.9	74.2	98.0	116.5	111.7	127.9	120.3	92.7	69.5	86.3	77.9
May	155.9	177.9	199.4	209.0	188.2	226.0	236.6	210.5	163.0	182.6	176.4
Jun	210.8	223.0	249.1	212.1	208.6	245.3	257.3	250.6	204.6	198.8	230.4
Jul	233.9	255.8	299.7	320.2	244.7	359.6	349.9	317.7	230.0	238.4	270.1
Aug	224.1	223.1	262.3	220.2	233.6	264.6	266.6	308.3	202.4	247.3	231.4
Sep	323.0	348.9	327.6	346.0	293.1	389.9	353.1	365.7	302.8	302.4	349.5
Oct	263.0	234.4	217.0	273.0	215.6	284.4	263.7	201.3	233.1	193.3	226.8
Nov	85.2	49.8	68.3	90.9	44.4	91.6	71.4	47.2	50.0	39.2	52.8
Dec	22.8	13.7	16.8	9.0	6.2	15.2	8.7	11.8	11.3	8.1	11.9
Total	**1,679**	**1,649**	**1,794**	**1,914**	**1,638**	**2,133**	**2,049**	**1,857**	**1,510**	**1,551**	**1,670**

Table 9 Average streamflow of each sub-basins

Month	ST1	ST2	ST3	ST4	ST5	ST6	ST7	ST8	ST9	ST10	ST11
Jan	0.56	0.18	0.67	0.30	1.11	0.52	0.52	1.33	0.24	0.37	0.32
Feb	0.33	0.10	0.39	0.17	0.64	0.31	0.31	0.77	0.13	0.22	0.17
Mar	0.37	0.12	0.44	0.20	0.72	0.34	0.34	0.87	0.14	0.24	0.20
Apr	0.96	0.29	1.17	0.52	1.92	0.91	0.91	2.20	0.35	0.65	0.52
May	1.69	0.48	2.19	0.95	2.93	1.72	1.71	3.84	0.59	1.22	0.92
Jun	2.58	0.61	3.94	1.59	4.33	3.08	3.07	5.09	0.95	2.20	1.14
Jul	4.25	0.92	7.65	3.71	6.59	7.75	7.53	14.17	1.42	4.03	2.17
Aug	5.51	1.52	12.03	4.89	11.31	11.53	10.56	25.12	2.54	6.15	3.17
Sep	8.27	3.26	19.24	7.61	17.65	19.64	16.98	50.30	3.85	8.11	5.31
Oct	7.95	4.22	14.30	7.47	19.85	19.16	14.66	32.11	4.18	8.78	5.84
Nov	3.36	1.28	3.85	1.99	6.67	3.37	3.40	8.30	1.68	2.14	2.12
Dec	1.15	0.42	1.38	0.61	2.26	1.07	1.07	2.84	0.53	0.76	0.69
Avg.	**3.08**	**1.12**	**5.60**	**2.50**	**6.33**	**5.78**	**5.09**	**12.24**	**1.38**	**2.91**	**1.88**

The high stream of each basin occurs during the wet period from May to October. ST8 received the highest stream flow compared to all sub-basins. It showed that streamflow is varied between 0.77 m^3s^{-1} during the dry period and 50 m^3s^{-1} during the raining season.

The estimation of streamflow of each sub-basin was used the amount of rainfall. It was translated to the streamflow of each sub basin. It showed clearly that during the raining season the streamflow is also high. Otherwise, streamflow is low during the dry season.

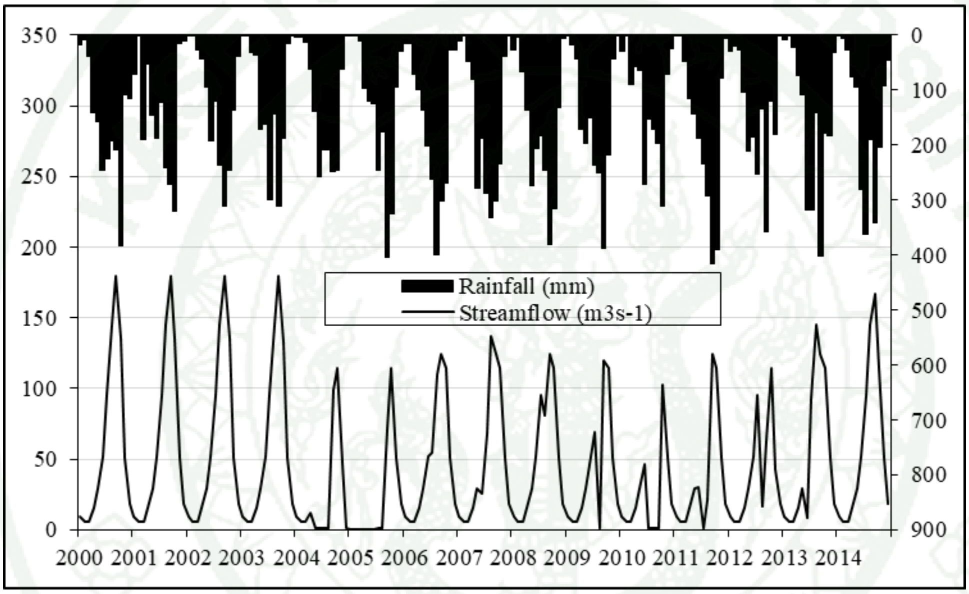

Figure 16 Estimation of streamflow on ST1

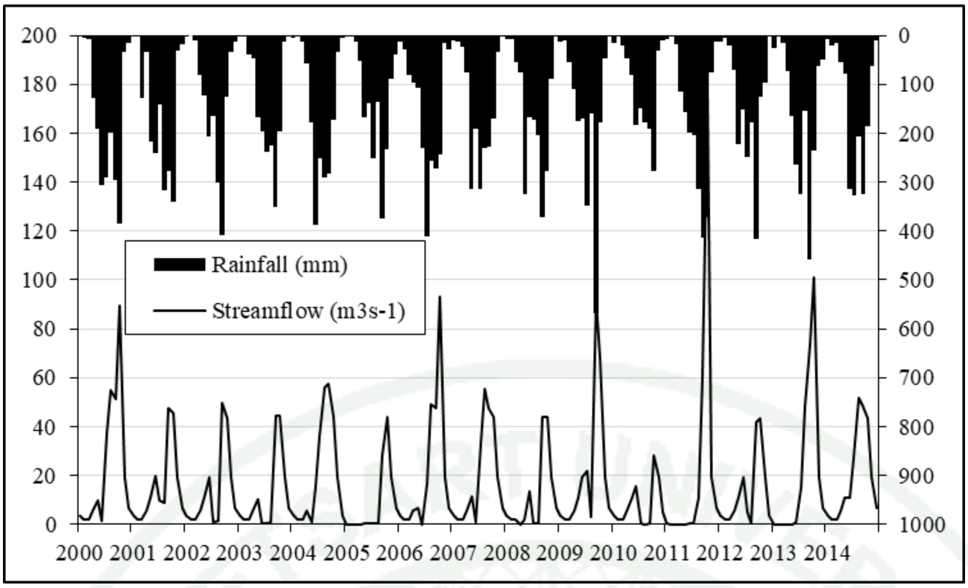

Figure 17 Estimation of streamflow on ST2

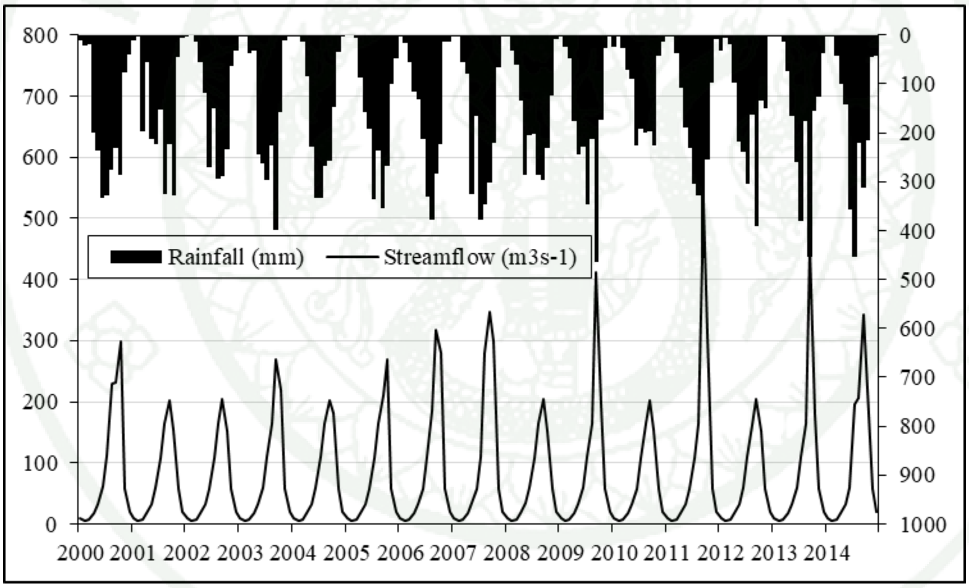

Figure 18 Estimation of streamflow on ST3

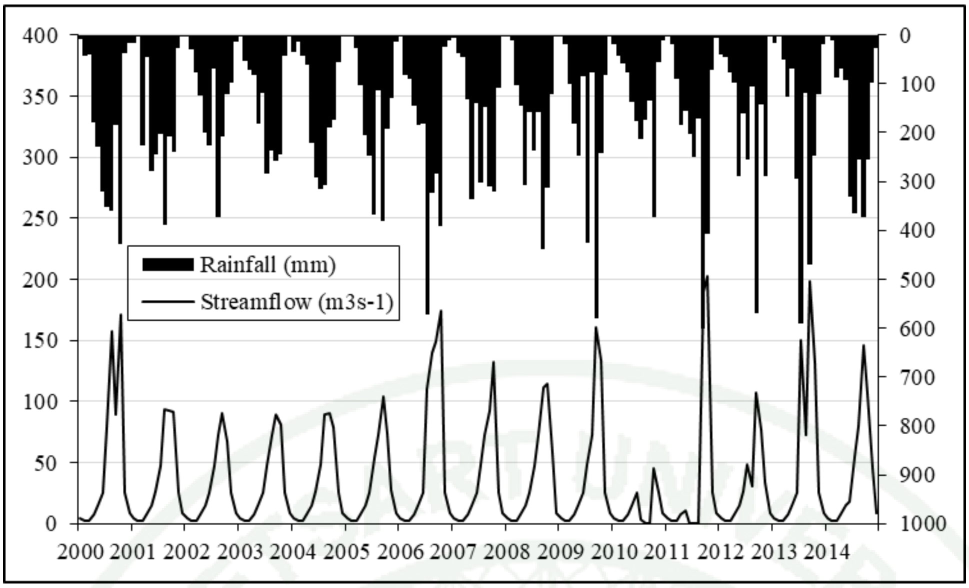

Figure 19 Estimation of streamflow on ST4

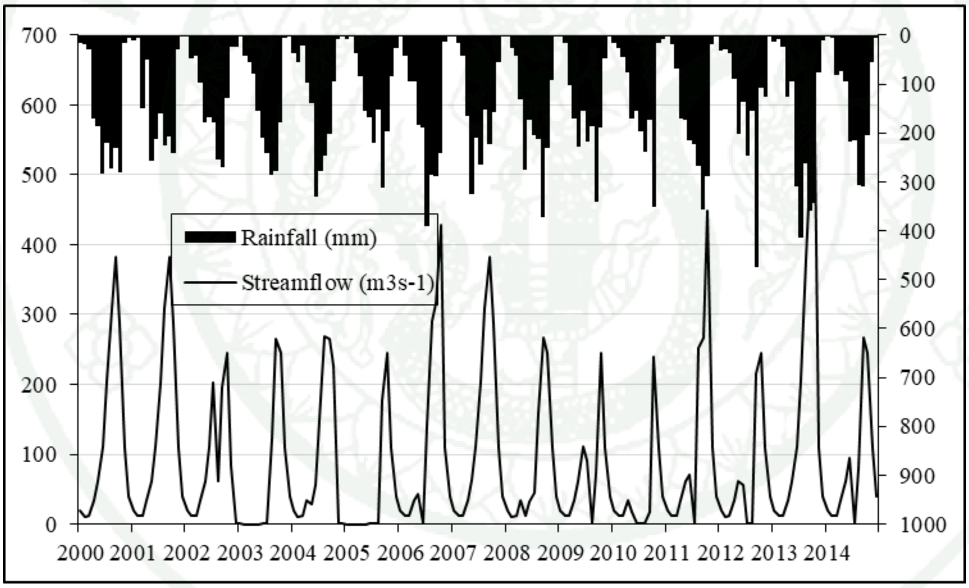

Figure 20 Estimation of streamflow on ST5

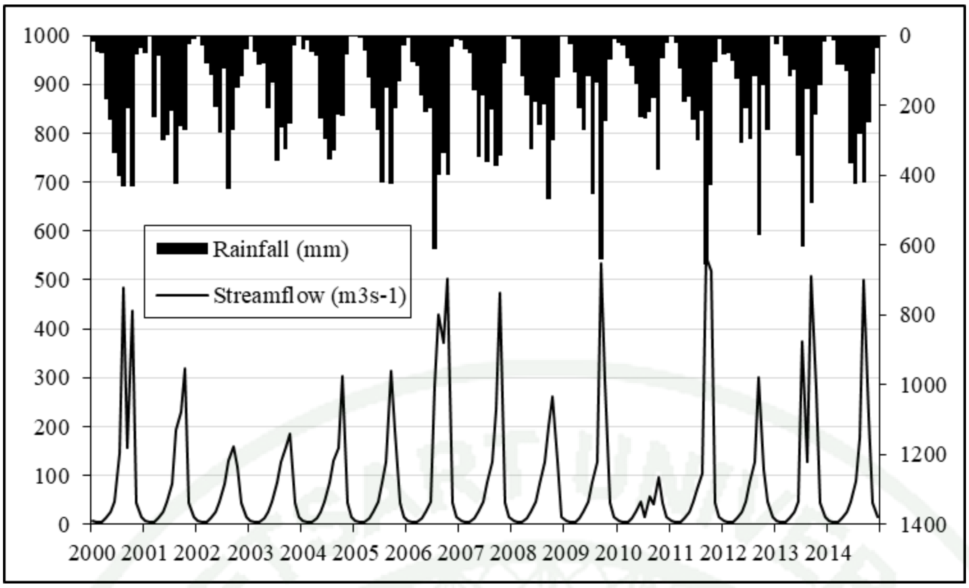

Figure 21 Estimation of streamflow on ST6

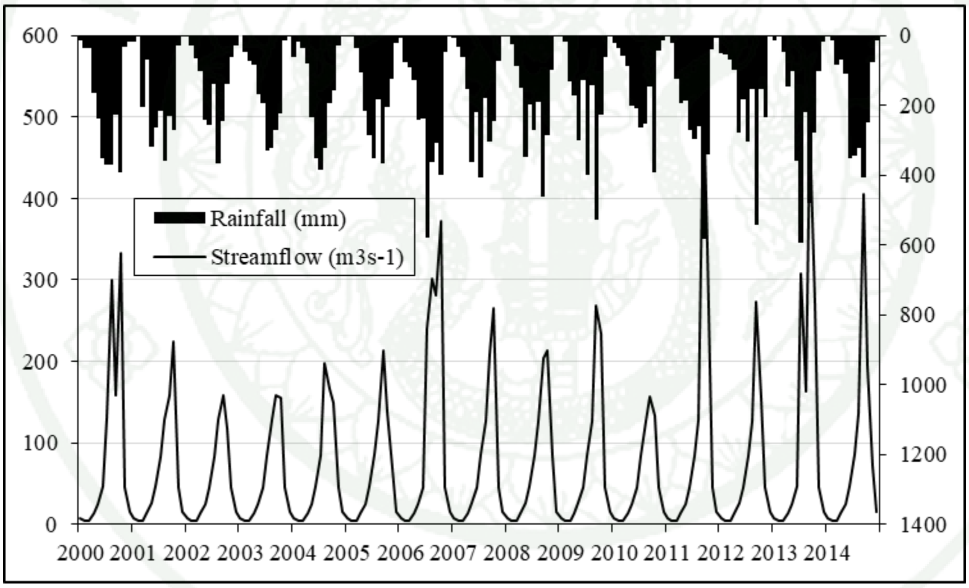

Figure 22 Estimation of streamflow on ST7

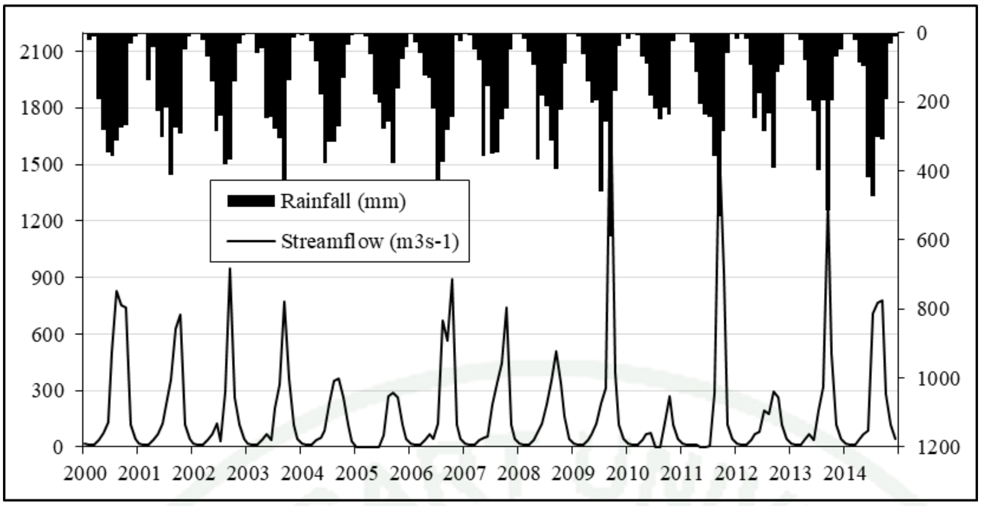

Figure 23 Estimation of streamflow on ST8

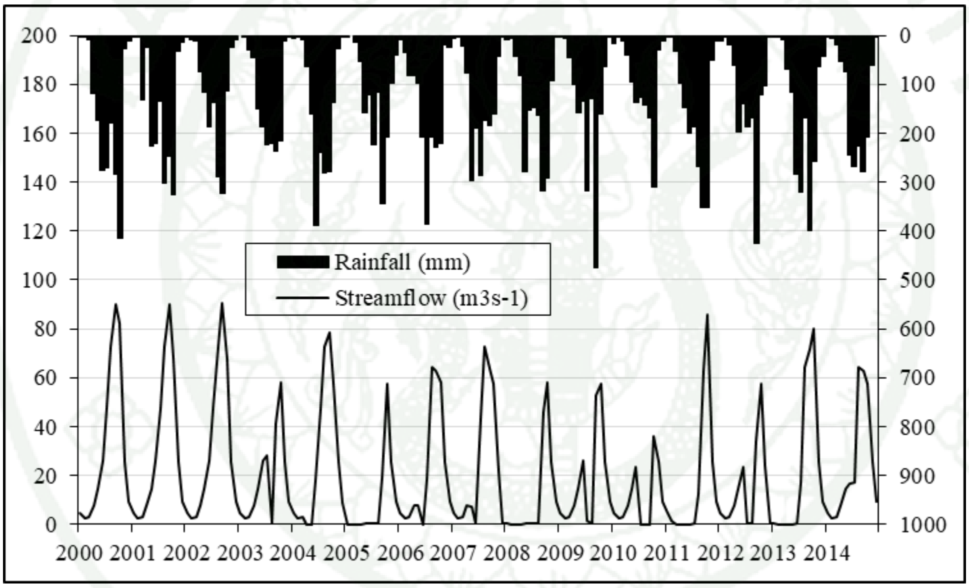

Figure 24 Estimation of streamflow on ST9

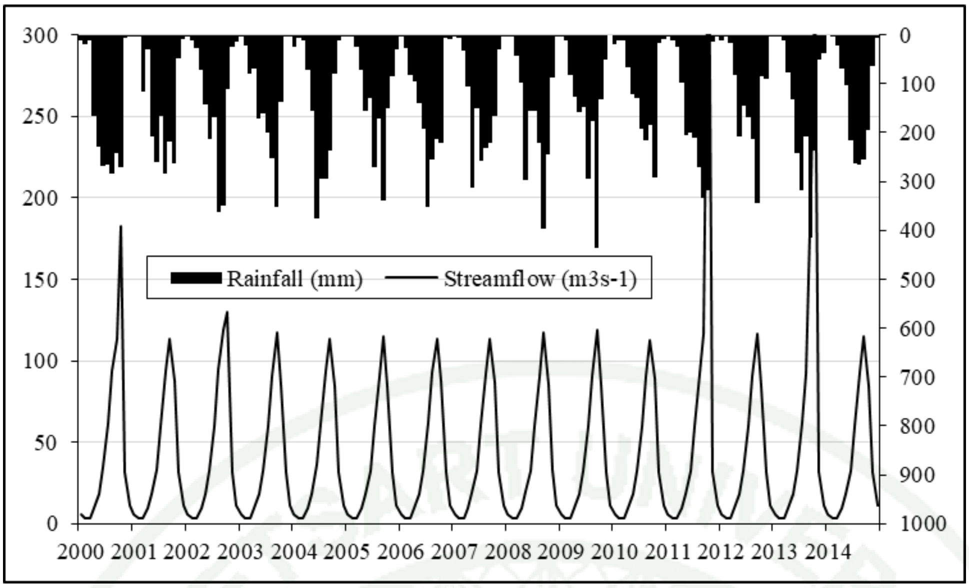

Figure 25 Estimation of streamflow on ST10

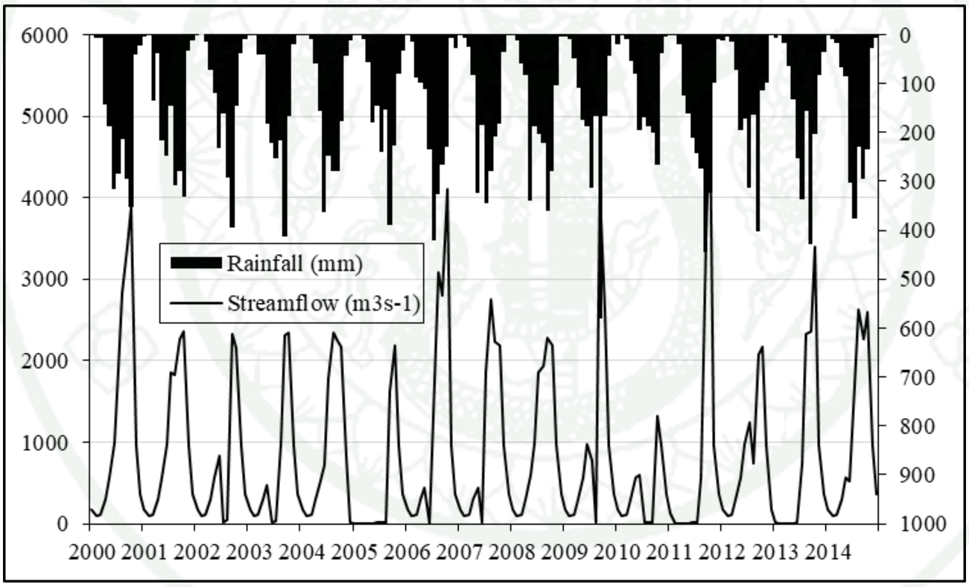

Figure 26 Estimation of streamflow on ST11

3.1 Streamflow calibration on ST8

In this study, sub-basin ST8 (Figure 27) has been calibrated using PEST tool which it is based on the streamflow gauge. It also had streamflow gauge stations from 2000 to 2011. ST8 is a biggest basin among the other sub-basins. So, it is high influence to the Tonle Sap Lake. The result showed that the model performed less well during the raining season. The simulation is over estimated during the wet period with R^2=0.6 (Figure 28).

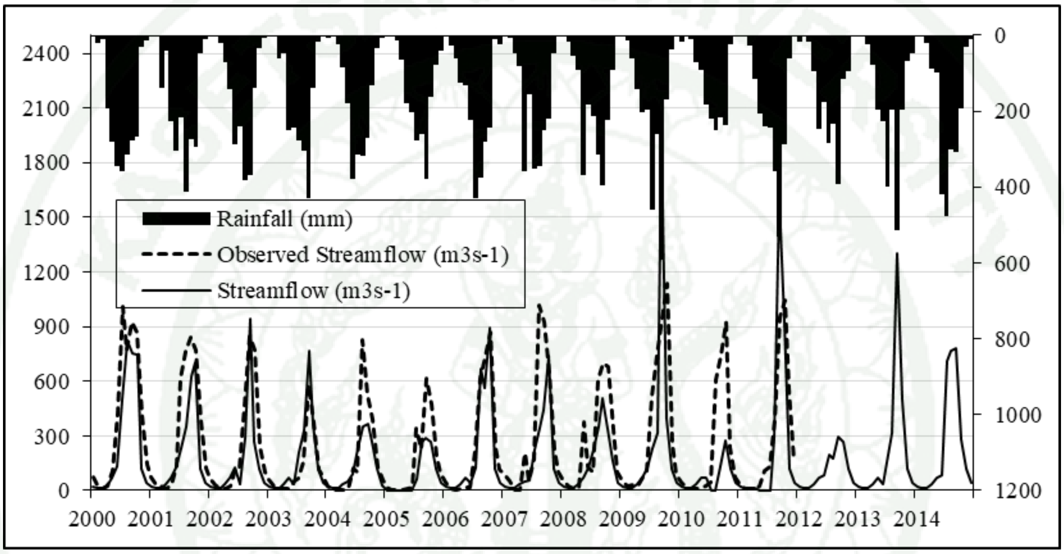

Figure 27 Observed vs. simulated streamflow of ST8

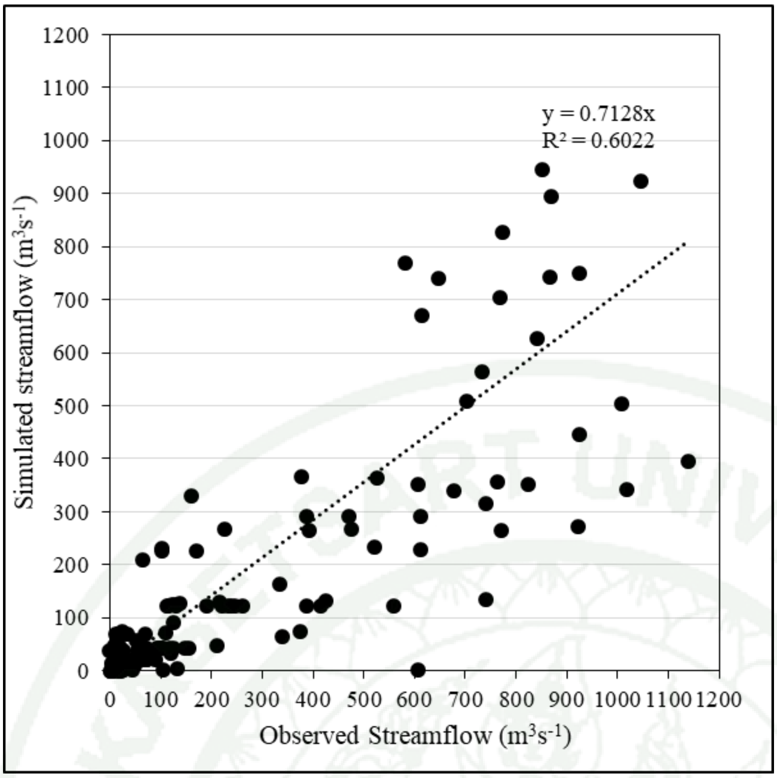

Figure 28 Scatter plot between observed and simulated streamflow of ST8

Table 10 Value of parameters calibration

Parameter	CLU	ULU	MLU	MWU
Surface Layer Thickness (m)	0.3	0.3	0.3	0.3
Total Soil Thickness (m)	1.5	1.5	1.5	1.5
Soil Water Capacity (%)	16	16	14	16
Max Percolation (mm/day)	1.5	1.5	0.7	1.5

Some parameters had high influence to the streamflow are presented in Table 10. The parameters of the basin has affected to the streamflow calibration was surface layer thickness around 0.3 m. Total soil thickness was around 1.5 m. Max percolation varied between 0.7 and 1.5 mm per day.

3.2 Observed and simulated volume

Over the fifteen-year simulated period from 2000 to 2014, the model indicated very well (R^2 = 0.94) with observed volume of the Lake compared to simulated volume. However, the model performed less well during the end of the dry and wet season, shown in Figure 29.

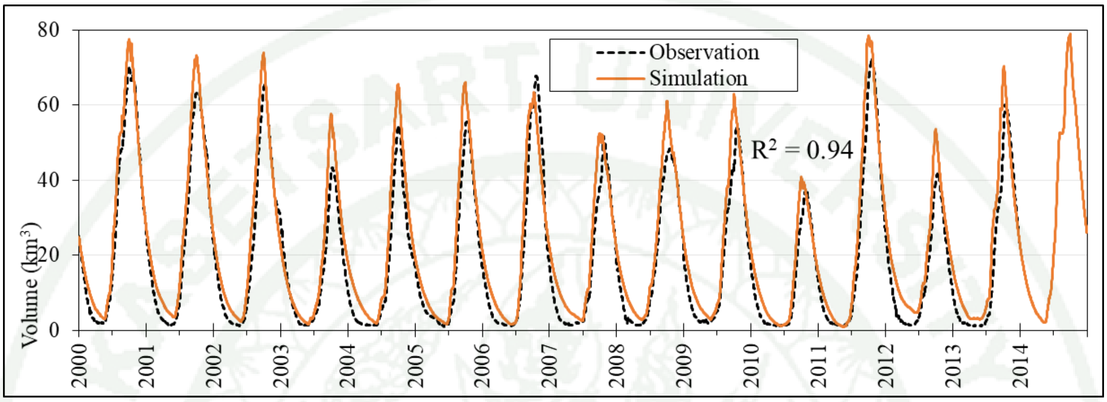

Figure 29 Observed vs. simulated lake volume

This problem should be occurred due to relationship between the water level of the Tonle Sap lake and the Mekong River. Bio direction changing of the Tonle Sap Lake, it might be affected to water level accuracy of the stations during the end of dry and wet periods. So, model provided not good simulation during these changing.

4. Water Balance Components of the Tonle Sap Lake

Based on the result in Figure 30 and Table 11, the water balance analysis showed that the mean annual inflow of water balance of the lake ranged from 46.19 km^3 to 89.62 km^3. The highest inflow occurred in 2011 during the worst flood season on the lower Mekong River. The estimated average inflow of the lake was 69.28 km^3 during this study period over fifteen years. The mean yearly outflow was estimated 69.25 km^3 over the study period. The estimated mean outflow varied from 49.21 km^3

to 86.55 km^3. The annual inflow of Mekong River to the Tonle Sap Lake was estimated from 32.43 km^3 to 53.43 km^3 during these study periods over fifteen years. The mean annual inflow was 43.14 km^3. It showed that the Mekong River is the highest influence on the lake. The annual inflow from the watershed varied from 12 km^3 to 36 km^3.

On monthly time series, the Mekong River has an effect on the Tonle Sap Lake during the raining season from May to October were 0.4 to 15.6 km^3 respectively. The high inflow from the Mekong River to the lake occurs during June and September, shown in Figure 31.

The storage changes of the Lake on the end of each year showed that it varied from 15.86 km^3 for the dry year to 32.50 km^3 for the wet year.

Table 11 Summarized water balance components of the Tonle Sap Lake

year	Rainfall of watershed	Inflow from watershed	Inflow from Mekong River		Total inflow	Total outflow	Storage on the 31st December
	(mm)	(km^3)	(km^3)		(km^3)	(km^3)	(km^3)
2000	1,974.04	34.73	51.62	59.74 (%)	86.42	-86.55	27.38
2001	1,773.31	25.20	51.59	67.14 (%)	76.84	-79.18	25.62
2002	1,539.04	20.39	53.43	72.34 (%)	73.86	-75.17	23.23
2003	1,582.09	20.45	38.32	65.15 (%)	58.82	-62.29	17.60
2004	1,651.81	19.90	47.95	70.62 (%)	67.90	-62.32	19.92
2005	1,619.74	16.09	53.15	76.35 (%)	69.60	-66.75	21.96
2006	1,915.78	34.55	36.70	49.57 (%)	74.04	-73.52	22.64
2007	1,768.91	27.17	33.42	54.34 (%)	61.49	-60.83	22.13
2008	1,879.68	21.63	40.21	64.25 (%)	62.59	-62.59	23.44
2009	1,875.59	28.53	37.11	56.49 (%)	65.69	-68.83	21.18
2010	1,388.36	11.83	34.30	74.27 (%)	46.19	-49.21	15.57
2011	1,974.54	35.19	51.45	57.40 (%)	89.62	-77.27	31.28
2012	1,694.34	18.08	33.58	64.94 (%)	51.71	-65.73	16.76
2013	1,952.08	36.17	32.43	44.42 (%)	73.01	-68.30	23.65
2014	1,771.13	29.43	51.91	63.71 (%)	81.48	-80.19	26.37
Mean	**1,757.36**	**25.29**	**43.14**	**62.72 (%)**	**69.28**	**-69.25**	**22.58**

(%) of inflow from the Mekong River compared with total inflow

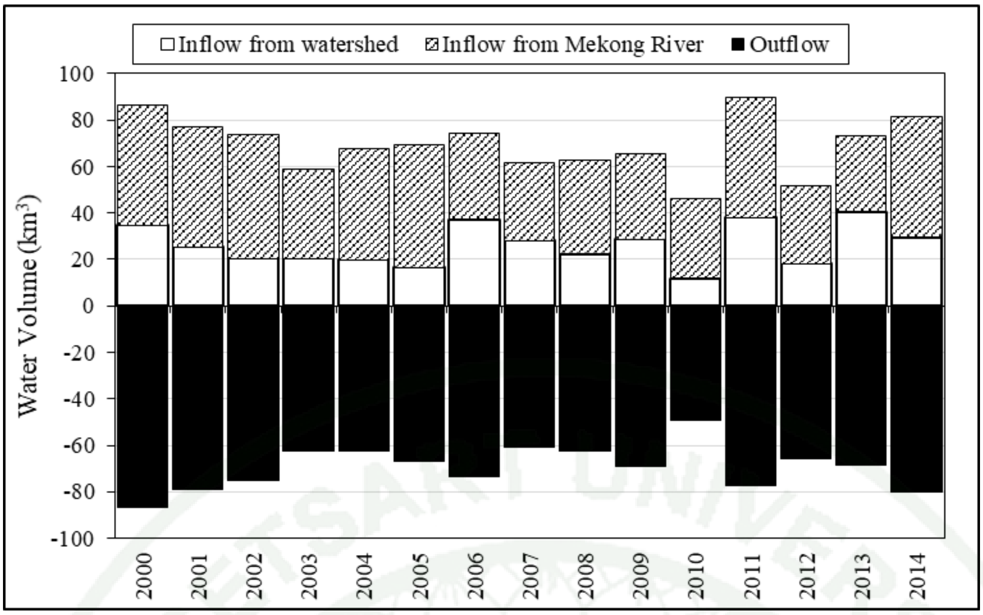

Figure 30 Yearly water balance components of the lake

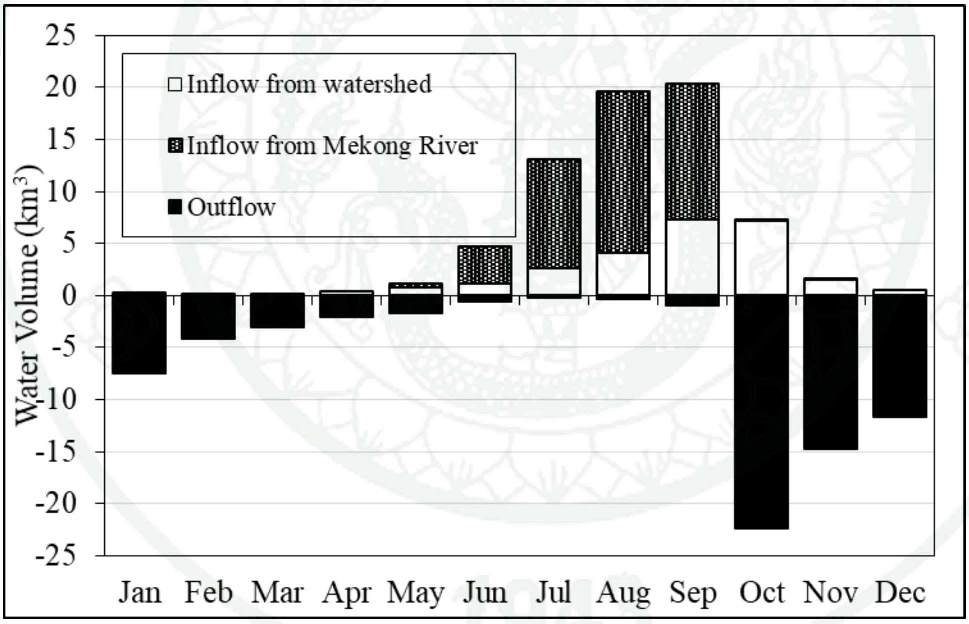

Figure 31 Monthly water balance components of the lake

Water balance analysis showed that the Mekong River is the main part of the Tonle Sap Lake. It retained more than half percent of the total inflow. And the lake's watershed was also important. It takes place more than thirty percent compared to total inflow.

5. Water Accounting Plus Sheets

The water accounting plus resource base and evapotranspiration sheets described below: resource based was divided into three main parts based on yearly, dry season and wet season. For the evapotranspiration sheet summarized into yearly during this study periods.

5.1 Resource based sheet

The components of resource based sheet is presented in Table 12. It was summarized into its frameworks. Annually, the water accounting plus resource base sheet is summarized in Figure 32. Surface inflow was 43.14 km^3. The gross precipitation was 153.56 km^3. Gross inflow was 196.70 and net inflow was equal to gross inflow. These are derived from rainfall of the Mekong River, catchment of the Tonle Sap Lake and the lakes itself. Additionally, the storage change was neglected on annually simulation. The net inflow was separated into four categories: Conserved Land Use 11.69 km^3 for forests, Utilized Land Use 72.87 km^3, Modified Land Use 36.72 km^3 for agricultural lands and Managed Water Use 6.23 km^3 for the water bodies in term of depletion "Landscape Evapotranspiration (ET) 127.70 km^3". The majority of water depleted was 57 % for ULU land use type. These are forests, plants, grasslands, bamboos forests, shrub lands, barren lands and wet lands. The water volume outflow was 96.24 km^3 which flew into the downstream of the Tonle Sap Lake. It was assumed to be committed flow 13.84 km^3 which is the amount of stored water in the lake and uncommitted flow 55.39 km^3 which is available outflow into the downstream.

In the dry season accounting, the water accounting plus resource base sheet is presented in Figure 33. Surface inflow was 0.1 km^3. The net inflow was 87.94 km^3 (gross inflow 21 km^3 plus storage change 66.73 km^3 and surface inflow). The depleted water was into four categories in term of ET: Conserved Land Use 4.01 km^3, Utilized Land use 23.35 km^3, Modified Land Use 12.65 km^3 and Managed Water Use 2.75 km^3. The water volume outflow was 42.98 km^3 which flew into the downstream of the Tonle Sap Lake. It was to be committed flow 8.60 km^3 and uncommitted flow 34.38 km^3.

In the wet season accounting, the water accounting plus resource base sheet is demonstrated in Figure 34. Surface inflow was 43.14 km^3. The net inflow was 116.95 km^3 (gross inflow 153.56 km^3 plus storage change -66.99 km^3 and surface inflow). The water depletion was 8.22, 50.93, 25.77 and 3.75 km^3 for Conserved Land Use, Utilized Land Use, Modified Land Use and Managed Water Use respectively. The water volume outflow was 28.29 km^3 which flew into the downstream of the Tonle Sap Lake. The committed and uncommitted flow were 5.66 km^3 and 22.63 km^3.

Table 12 Resource based sheet components

Components	Yearly	Nov-Apr	May-Oct
Rainfall (watershed)	143.563	19.778	131.838
Lake rainfall	9.970	1.220	8.965
Surface inflow	43.144	0.009	43.135
Storage change	0.000	66.730	-66.990
Outflow	69.248	42.980	28.286
Uncommitted	55.399	34.384	22.629
Committed	13.850	8.596	5.657

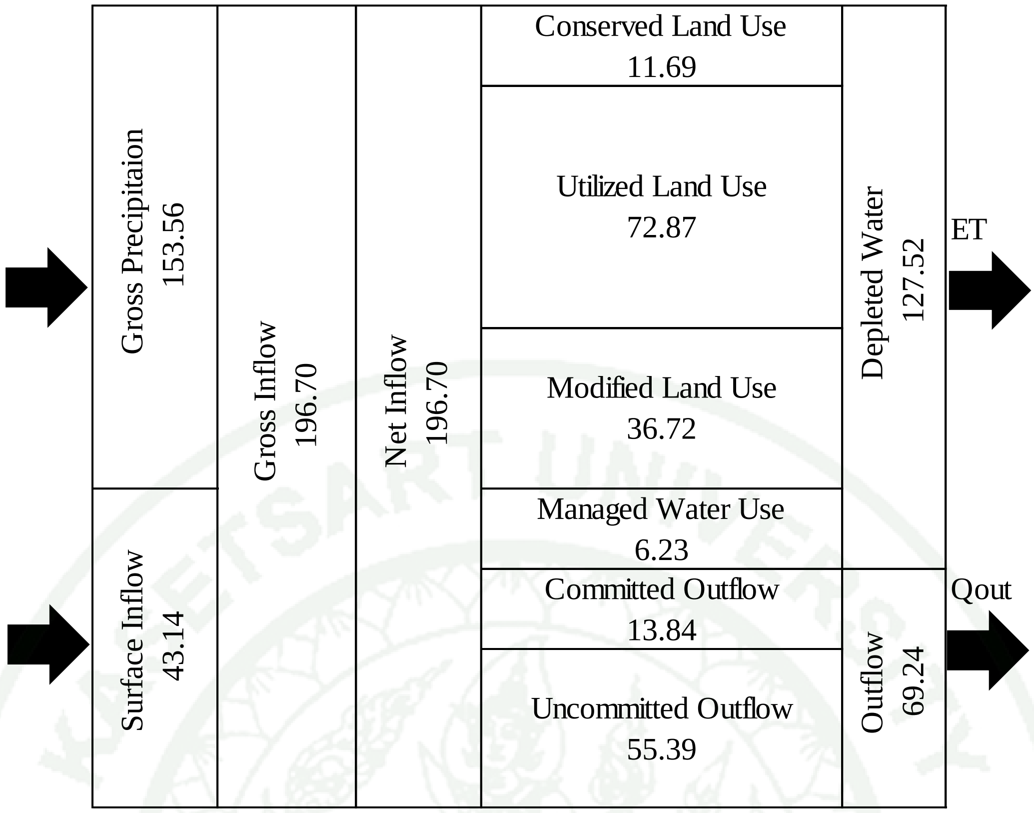

Figure 32 Annual resource based sheet components

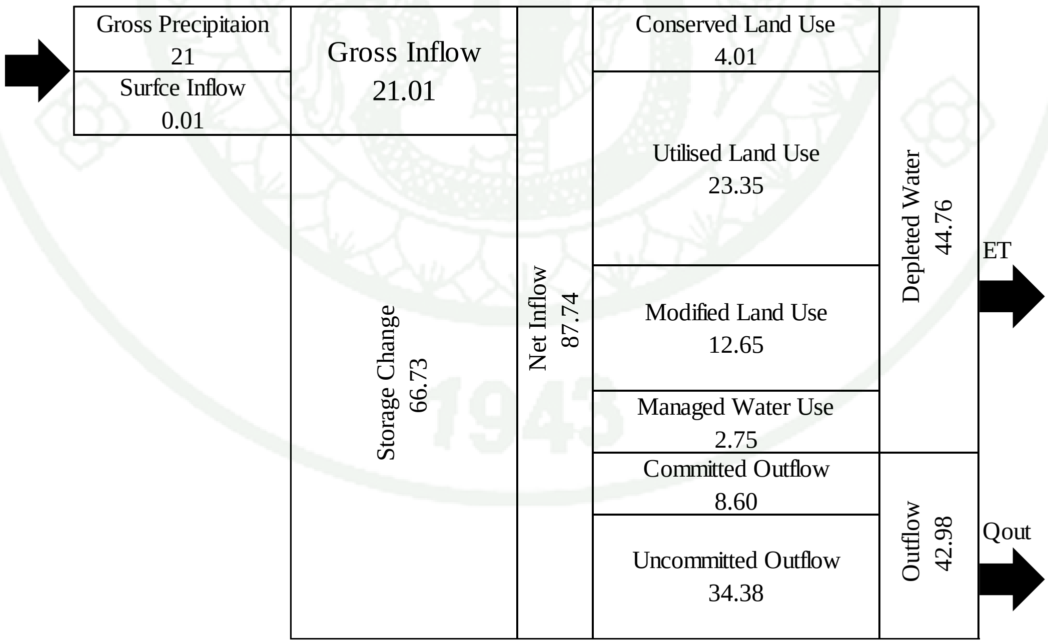

Figure 33 Seasonal (May to October) resource based sheet components

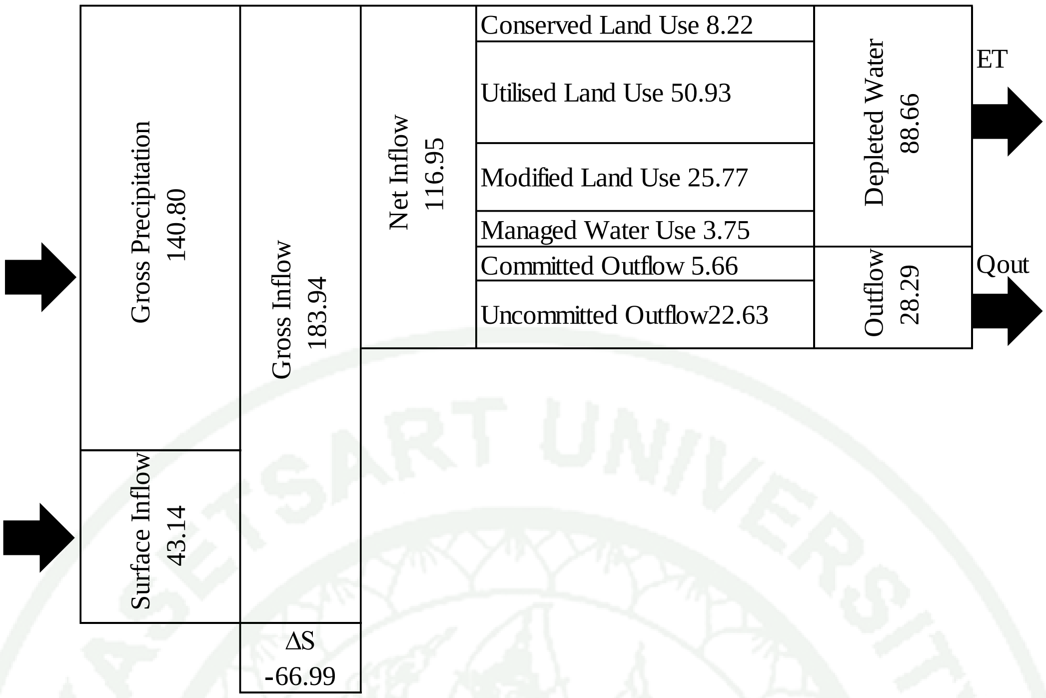

Figure 34 Seasonal (Nov-Apr) resource based sheet components

During the annual simulation, the lake retained high inflow from rainfall around 78 percent compared to net inflow. Inflow from the Mekong River also showed high one around 22 percent. The highest water depletion was more than half percent and, outflow was only 35 percent. For the seasonal based sheet showed that the highest depleted water occurred during wet season around 76 percent. Only 24 percent was released to downstream. Moreover, storage change of the lake was also an important role to the lake. It affected to the volume water on seasonal.

5.2 Evapotranspiration sheet

The water depletion in term of ET each land use class are presented in Table 13. The WA+ Evapotranspiration sheet illustrated in Figure 35. This sheet divided the total of depleted water 127.52 km^3 into CLU 11.69 km^3 (9%), ULU 72.88 km^3 (57%), MLU 36.72 km^3 (29%) and MWU 5.23 km^3 (5%). Evaporation and transpiration were depleted 40.25 km^3 (31.6%) and 87.28 km^3 (68.4%) respectively. All from E is non-beneficial and T is beneficial. Indicators is presented in Table 14.

Table 13 Components of evapotranspiration sheet

Time scale	Land use class	CLU	MLU	MWU	ULU	Total
Annual	E (km^3)	3.35	10.58	5.66	20.66	40.25
	T (km^3)	8.34	26.15	0.57	52.22	87.28
	ET (km^3)	11.69	36.72	1.16	72.88	122.46
Nov-Apr	E (km^3)	1.34	4.22	0.22	8.21	14.00
	T (km^3)	2.67	8.42	0.01	17.14	28.25
	ET (km^3)	4.01	12.65	0.23	25.35	42.24
May-Oct	E (km^3)	2.29	7.20	0.44	14.12	24.05
	T (km^3)	5.93	18.56	0.57	36.81	61.87
	ET (km^3)	8.22	25.77	1.01	50.93	85.92

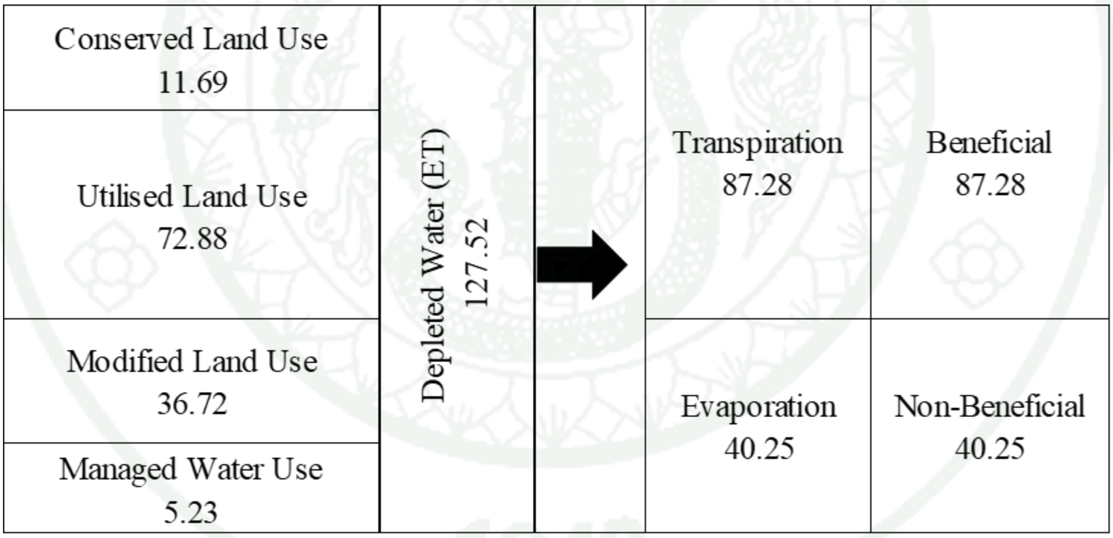

Figure 35 Annual evapotranspiration sheet components in km^3

The evapotranspiration sheet provided the water depletion in term of different categories. The highest water depletion was in Utilized Land Use classes. It take place more than half However, this landuse type, most of water depletion occurred from wetlands. Hence, no method has been described to conserve water. Modified Land Use also demonstrated a high one around 29 percent which happened to the agriculture land. To maintain this amount of water, It is to be attention on water use for agriculture by improving land productivity. These will be a help to decrease water consumption and increase production. The main sources for reducing water depletion is to reduce soil evaporation.

5.3 Indicators of WA+ sheets

The WA+ provided some indicators of each sheets (Table 14). In the Tonle Sap basin, the annual resource based sheet, exploitable water fraction was 0.35 which represented the portion of exploitable water compared to net inflow. It showed that a less water was flow out to downstream. The seasonal from May to October also demonstrated that the amount of water was less outflow (0.24). However, from November to April, it was 0.49. Around half of net inflow in the Tonle Sap Lake indicated as outflow.

For the evapotranspiration sheet, T fraction ratio was 0.68, meaning the majority of water depletion from forests. All of these depleted water was beneficial. Moreover, this ration showed that the less water depleted in the Tonle Sap Lake basin was through soil and water.

Table 14 Indicators of WA+ sheets

Time step	Indicators	Resource Based Sheet	Evapotranspiration Sheet
Annual	Exploitable Water Fraction	0.35	
	Tfraction		0.68
	Beneficial fraction		0.68
May-Oct	Exploitable Water Fraction	0.24	
Nov-Apr	Exploitable Water Fraction	0.49	

CONCLUSION AND RECOMMENDATION

Conclusion

In this study, the water balance in term of water accounting of the Tonle Sap and its sub-basins was considered as simulation using satellite derived data coupling the Google Earth Engine (GEE) from 2000 to 2014. It showed that satellite derived data can provide a good understanding on the water resource management. To sum up, the water accounting framework can provide the information on the water resource management of the Lake coupling the remote sensing concepts. It was achieved a good first step on earth observation data during the simulated periods on water balance analysis in term of the water accounting of the Tonle Sap Lake. Additionally, the focus of this study focused on the WA+ resource based sheet and evapotranspiration sheet. The components of the water balance discharge of the lake have the lake's catchment, inflow from the Mekong River into the Tonle Sap Lake via the Tonle Sap River and lake itself. The inflow from the catchment into the lake was estimated as the surface runoff from all sub-basins surrounding the lake. The analysis was conducted on annual from 2000 to 2014, dry season from November to April and wet season from May to October.

The results of the water balance analysis showed that the large amount of water from the Mekong River takes high place into the Tonle Sap Lake around 62 percent compared to total inflow into the lake, but the lake's catchment also plays as an important role 36 percent of annual flow, and 2 percent is retrieved from rainfall of the lake itself. Moreover, The Mekong River has high effected inflow into the lake during the raining season from June to September and less inflow during the beginning and the end of wet season.

For the water accounting plus, the result showed that the water outflow is highest during the dry season. The results suggest that the Tonle Sap Lake need to introduce bidirectional control structures in order to conserve water during the dry season. Control structures can maintain these amount of water to use for drought season. However, this solution will be affected on flow regime of the lake, as well as ecosystem.

The depleted water in term of ET from ULU land use type is higher than others, following by MLU. These are agriculture, wetlands, barren lands or wilderness and shrub lands. Therefore, to improve the situation in water depletion, it can be reforestations on wetlands, barren lands or wilderness. Moreover, it is to be attention on water use for agriculture by improving land productivity. These will be a help to decrease water consumption and increased production. The main sources for reducing water depletion is reduce soil evaporation.

Recommendation

In this study, the earth observation was provided the main input data sources for the model. However, these data require the ground observation for the calibration process. It could cause some uncertainty and errors on satellites data parameters.

LITERATURE CITED

ADB. 2005. **The Tonle Sap Basin Strategy.** Asian Development Bank, Manila, Philippines.

Ahmed, M., H. Navy, L. Vuthy and M. Tiongco. 1998. **Socioeconomic Assessment of Freshwater Capture Fisheries in Cambodia: Report on a Household Survey.** Mekong River Commission Secretariat, Phnom Penh, Cambodia.

Alcamo, J., M. Flörke and M. Märker. 2007. Future Long-Term Changes in Global Water Resources Driven by Socio-Economic and Climatic Changes. **Hydrological Sciences Journal**. 52(2): 247-275.

Andreu, J., J. Capilla and E. Sanchís. 1996. Aquatool, a Generalized Decision-Support System for Water-Resources Planning and Operational Management. **Journal of hydrology**. 177(3-4): 269-291.

Batchelor, C., J. Hoogeveen, J.-M. Faurès and L. Peiser. 2017. **Water Accounting and Auditing. A Sourcebook.** Food and Agriculture Organization of the United Nations (FAO), Rome.

Bonheur, N. 2001. Tonle Sap Ecosystem and Value. **Technical Coordination Unit for Tonle Sap, Ministry of Environment, Phnom Penh**.

Campbell, I., S. Say and J. Beardall. 2009. Tonle Sap Lake, the Heart of the Lower Mekong, p. 251-272. *In*, eds. **The Mekong.** Elsevier, UK.

Campbell, I.C., C. Poole, W. Giesen and J. Valbo-Jorgensen. 2006. Species Diversity and Ecology of Tonle Sap Great Lake, Cambodia. **Aquatic Sciences**. 68(3): 355-373.

Choudhury, B.J. and N.E. DiGirolamo. 1998. A Biophysical Process-Based Estimate of Global Land Surface Evaporation Using Satellite and Ancillary Data I. Model Description and Comparison with Observations. **Journal of Hydrology**. 205(3-4): 164-185.

Churkina, G., S.W. Running, A.L. Schloss and T.P.O.T.P.N.M. Intercomparison. 1999. Comparing Global Models of Terrestrial Net Primary Productivity (Npp): The Importance of Water Availability. **Global Change Biology**. 5(S1): 46-55.

Dong, J., X. Xiao, M.A. Menarguez, G. Zhang, Y. Qin, D. Thau, C. Biradar and B. Moore III. 2016. Mapping Paddy Rice Planting Area in Northeastern Asia with Landsat 8 Images, Phenology-Based Algorithm and Google Earth Engine.

Remote sensing of environment. 185(142-154).

Droogers, P., G. Simons, W.G.M. Bastiaanssen and J. Hoogeveen. 2010. **Water Accounting Plus (Wa+) in the Okavango River Basin.** FAO Land and Water Division, Africa.

Dunn, S. and R. Mackay. 1995. Spatial Variation in Evapotranspiration and the Influence of Land Use on Catchment Hydrology. **Journal of Hydrology**. 171(1-2): 49-73.

Eastham, J., F. Mpelasoka, M. Mainuddin, C. Ticehurst, P. Dyce, G. Hodgson, R. Ali and M. Kirby. 2008. **Mekong River Basin Water Resources Assessment: Impacts of Climate Change.** Water for a Healthy Country National Research Flagship, Australia.

Falkenmark, M. and J. Rockström. (2006) **The New Blue and Green Water Paradigm: Breaking New Ground for Water Resources Planning and Management**, American Society of Civil Engineers.

FAO. 1998. Etc – Dual Crop Coefficient (Kc = Kcb + Ke), p. 135. *In*, eds. **Fao Irrigation and Drainage Paper No. 56.** FAO, Rome. Italy.

Fujii, H., H. Garsdal, P. Ward, M. Ishii, K. Morishita and T. Boivin. 2003. Hydrological Roles of the Cambodian Floodplain of the Mekong River. **International Journal of River Basin Management**. 1(3): 253-266.

Funk, C., P. Peterson, M. Landsfeld, D. Pedreros, J. Verdin, S. Shukla, G. Husak, J. Rowland, L. Harrison and A. Hoell. 2015. The Climate Hazards Infrared Precipitation with Stations—a New Environmental Record for Monitoring Extremes. **Scientific data**. 2(150066).

Funk, C.C., P.J. Peterson, M.F. Landsfeld, D.H. Pedreros, J.P. Verdin, J.D. Rowland, B.E. Romero, G.J. Husak, J.C. Michaelsen and A.P. Verdin. 2014. A Quasi-Global Precipitation Time Series for Drought Monitoring. **US Geological Survey Data Series**. 832(4): 1-12.

Gleick, P.H. 2000. A Look at Twenty-First Century Water Resources Development. **Water international**. 25(1): 127-138.

Goh, E. 2017. China in the Mekong River Basin: The Regional Security Implications of Resource Development on the Lancang Jiang, p. 237-258. *In*, eds. **Non-Traditional Security in Asia.** Routledge, London.

Gorelick, N., M. Hancher, M. Dixon, S. Ilyushchenko, D. Thau and R. Moore. 2017.

Google Earth Engine: Planetary-Scale Geospatial Analysis for Everyone. **Remote Sensing of Environment**. 202(18-27).

Hsu, K.-l., X. Gao, S. Sorooshian and H.V. Gupta. 1997. Precipitation Estimation from Remotely Sensed Information Using Artificial Neural Networks. **Journal of Applied Meteorology**. 36(9): 1176-1190.

Huffman, G.J., D.T. Bolvin, E.J. Nelkin, D.B. Wolff, R.F. Adler, G. Gu, Y. Hong, K.P. Bowman and E.F. Stocker. 2007. The Trmm Multisatellite Precipitation Analysis (Tmpa): Quasi-Global, Multiyear, Combined-Sensor Precipitation Estimates at Fine Scales. **Journal of hydrometeorology**. 8(1): 38-55.

Joyce, R.J., J.E. Janowiak, P.A. Arkin and P. Xie. 2004. Cmorph: A Method That Produces Global Precipitation Estimates from Passive Microwave and Infrared Data at High Spatial and Temporal Resolution. **Journal of Hydrometeorology**. 5(3): 487-503.

Junk, W.J., M. Brown, I.C. Campbell, M. Finlayson, B. Gopal, L. Ramberg and B.G. Warner. 2006. The Comparative Biodiversity of Seven Globally Important Wetlands: A Synthesis. **Aquatic Sciences**. 68(3): 400-414.

Karimi, P. 2014. **Water Accounting Plus for Water Resources Reporting and River Basin Planning.** University of Mashhad, Iran.

Karimi, P., W. Bastiaanssen, D. Molden and M. Cheema. 2012a. Basin-Wide Water Accounting Using Remote Sensing Data: The Case of Transboundary Indus Basin. **Hydrology & Earth System Sciences Discussions**. 9(11).

Karimi, P., W.G. Bastiaanssen and D. Molden. 2013. Water Accounting Plus (Wa+)–a Water Accounting Procedure for Complex River Basins Based on Satellite Measurements. **Hydrology and Earth System Sciences**. 17(7): 2459-2472.

Karimi, P., D. Molden, W. Bastiaanssen and X. Cai. 2012b. Water Accounting to Assess Use and Productivity of Water: Evolution of a Concept and New Frontiers. **Water accounting: international approaches to policy and decision-making, edited by: Chalmers, K. and Godfrey, J**. 76-88.

Keller, A.A. and J. Keller. 1995. **Effective Efficiency: A Water Use Efficiency Concept for Allocating Freshwater Resources.** Center for Economic Policy Studies, Winrock International Arlington.

Kummu, M. 2003. The Natural Environment and Historical Water Management of Angkor, Cambodia, *In*. Washington DC.

Kummu, M., S. Tes, S. Yin, P. Adamson, J. Józsa, J. Koponen, J. Richey and J. Sarkkula. 2014. Water Balance Analysis for the Tonle Sap Lake–Floodplain System. **Hydrological Processes**. 28(4): 1722-1733.

Lévite, H., H. Sally and J. Cour. 2003. Testing Water Demand Management Scenarios in a Water-Stressed Basin in South Africa: Application of the Weap Model. **Physics and Chemistry of the Earth, Parts A/B/C**. 28(20-27): 779-786.

Lonfat, M., F.D. Marks Jr and S.S. Chen. 2004. Precipitation Distribution in Tropical Cyclones Using the Tropical Rainfall Measuring Mission (Trmm) Microwave Imager: A Global Perspective. **Monthly Weather Review**. 132(7): 1645-1660.

Mainuddin, M., J. Eastham and M. Kirby. 2010. **Water-Use Accounts in Cpwf Basins: Simple Water-Use Accounting of the Niger Basin.** CSIRO Land and Water, Canberra, Australia.

Maliehe, M. and D.M. Mulungu. 2017. Assessment of Water Availability for Competing Uses Using Swat and Weap in South Phuthiatsana Catchment, Lesotho. **Physics and Chemistry of the Earth, Parts A/B/C**. 100(305-316).

McCabe, M.F. and E.F. Wood. 2006. Scale Influences on the Remote Estimation of Evapotranspiration Using Multiple Satellite Sensors. **Remote Sensing of Environment**. 105(4): 271-285.

Mingzhou, Q. 1997. Research on Classification of Land Use and Factors of Affecting Landuse Classification. **Areal Research and Development**.

Molden, D. 1997. **Accounting for Water Use and Productivity.** International Water Management Institute Colombo, Sri Lanka.

Molden, D., H. Murray-Rust, R. Sakthivadivel and I. Makin. 2003. **A Water-Productivity Framework for Understanding and Action.** CABI Publishing in association with International Water Management Institute, UK.

Molden, D. and R. Sakthivadivel. 1999. Water Accounting to Assess Use and Productivity of Water. **International Journal of Water Resources Development**. 15(1-2): 55-71.

Molden, D.J., R. Sakthivadivel, C.J. Perry and C. De Fraiture. 1998. **Indicators for Comparing Performance of Irrigated Agricultural Systems.** International Water Management Institute, Colombo, Sri Lanka.

Monteith, J. 1988. Does Transpiration Limit the Growth of Vegetation or Vice Versa?

Journal of Hydrology. 100(1-3): 57-68.

MRC. 2002. **Fisheries in the Lower Mekong Basin: Status and Perspectives.** Mekong River Commission Phnom Penh, Cambodia.

Patel, N.N., E. Angiuli, P. Gamba, A. Gaughan, G. Lisini, F.R. Stevens, A.J. Tatem and G. Trianni. 2015. Multitemporal Settlement and Population Mapping from Landsat Using Google Earth Engine. **International Journal of Applied Earth Observation and Geoinformation**. 35(199-208).

Peter, D., S. Gijs, B. Wim and H. Jippe. 2010. Water Accounting Plus (Wa+) in the Okavango River Basin. **Indicators**. 6(3).

Phua, P. 2011. China's Collaboration with Indochina Countries in Hydropower Development in the Mekong Region: How Far Can It Go?, p. 95-124. *In*, eds. **China-Asean Sub-Regional Cooperation: Progress, Problems and Prospect.** World Scientific, China.

Pink, R.M. 2016. Laos: The Poorest Country in Asia, p. 119-138. *In*, eds. **Water Rights in Southeast Asia and India.** Palgrave Macmillan, New York.

Promkotra, S. 2014. Dynamics of Suspended Sediments Related to Fine Particles in Lower Mekong River. **Applied Mechanics and Materials**. 446(1528-1533).

Psomas, A., Y. Panagopoulos, D. Konsta and M. Mimikou. 2016. Designing Water Efficiency Measures in a Catchment in Greece Using Weap and Swat Models. **Procedia engineering**. 162(269-276).

Rainboth, W.J. 1996. Fao Species Identification Field Guide for Fishery Purpose. **Fish of the Cambodian Mekong, Rome**.

Running, S.W., Q. Mu, M. Zhao and A. Moreno. 2017. Modis Global Terrestrial Evapotranspiration (Et) Product (Nasa Mod16a2/A3) Nasa Earth Observing System Modis Land Algorithm. **NASA: Washington, DC, USA**.

Rutter, A., K. Kershaw, P. Robins and A. Morton. 1971. A Predictive Model of Rainfall Interception in Forests, 1. Derivation of the Model from Observations in a Plantation of Corsican Pine. **Agricultural Meteorology**. 9(367-384).

Schowengerdt, R.A. 2006. **Remote Sensing: Models and Methods for Image Processing.** Elsevier, Tucson, Arizona.

SEI. 2016. **Weap - Water Evaluation and Planning System: Tutorial - a Collection of Stand-Alone Modules to Aid in Learning the Weap Software.** Stockholm

Environment Institute (SEI), U.S. Center, Somervill, MA.

Setegn, S.G., R. Srinivasan, A.M. Melesse and B. Dargahi. 2010. Swat Model Application and Prediction Uncertainty Analysis in the Lake Tana Basin, Ethiopia. **Hydrological Processes**. 24(3): 357-367.

Shilpakar, R.L., W.G. Bastiaanssen and D.J. Molden. 2011. A Remote Sensing-Based Approach for Water Accounting in the East Rapti River Basin, Nepal. **Himalayan J. Sci**. 7(9).

Sivapalan, M., K. Takeuchi, S. Franks, V. Gupta, H. Karambiri, V. Lakshmi, X. Liang, J. McDonnell, E. Mendiondo and P. O'connell. 2003. Iahs Decade on Predictions in Ungauged Basins (Pub), 2003–2012: Shaping an Exciting Future for the Hydrological Sciences. **Hydrological sciences journal**. 48(6): 857-880.

Smakhtin, V. 2004. **Taking into Account Environmental Water Requirements in Global-Scale Water Resources Assessments.** International Water Management Institute, Colombo, Sri Lanka.

UN. 2007. **System of Environmental Economic Accounting for Water.** United Nation Statistics Division, Geneva.

Wassmann, R., N.X. Hien, C.T. Hoanh and T.P. Tuong. 2004. Sea Level Rise Affecting the Vietnamese Mekong Delta: Water Elevation in the Flood Season and Implications for Rice Production. **Climatic Change**. 66(1-2): 89-107.

Welcomme, R. 1985. River Fisheries, Food and Agriculture Organization Fisheries Technical Paper 262. **FAO, Rome**.

Xu, C.-Y. and V.P. Singh. 1998. A Review on Monthly Water Balance Models for Water Resources Investigations. **Water Resources Management**. 12(1): 20-50.

Zhang, L., G.R. Walker and W.R. Dawes. 2002. Water Balance Modelling: Concepts and Applications. **ACIAR Monograph Series**. 84(31-47).

APPENDICES

Appendix A

Publications

Paper No 1:

Mab, P., S. Ly, C. Chompuchan, and E. Kositsakulchai. 2019. Evaluation of Satellite Precipitation from Google Earth Engine in Tonle Sap Basin, Cambodia. THA 2019 International Conference on Water Management and Climate Change towards Asia's Water-Energy-Food Nexus and SDGs, 23-25 January 2019. Bangkok

PROCEEDINGS

THA 2019

INTERNATIONAL CONFERENCE ON

"Water Management and Climate Change towards Asia's Water-Energy-Food Nexus and SDGs"

Swissôtel Bangkok Ratchada
Bangkok, Thailand
23-25 January 2019

CONTENT (con't)

THA 2019 International Conference on
"Water Management and Climate Change towards Asia's Water-Energy-Food Nexus and SDGs"
23– 25 January 2019, Bangkok, Thailand.

Evaluation of Satellite Precipitation from Google Earth Engine in Tonle Sap Basin, Cambodia

Phanit Mab[1], Steven Ly[2], Chuphan Chompuchan[1], Ekasit Kositsakulchai[1,3,a,*]

Abstract Precipitation is important to life on Earth. It is a predominant process in the global hydrologic cycle and is an indispensable component of water balance analysis. However, in some area like the Tonle Sap basin in Cambodia, the information on precipitation is deficient and sometimes difficult to access. In this case, satellite remote sensing coupled with GIS techniques have been applied and considered as a powerful and effective tool in handing precipitation analysis tasks. Recently, the Google Earth Engine (GEE) platform provides satellite datasets and collection of the tool for analysis of data using JavaScript without downloading huge data from the Internet. In this study, we aimed to evaluate the application of GEE platform for retrieving and analyzing precipitation data of the Tropical Rainfall Measuring Mission (TRMM) in Tonle Sap basin (TLS). The methods included: (1) to collect the satellite precipitation data (3B43V7) by manual download and by retrieving them from GEE platform; (2) to analyze monthly precipitation over the study area by GIS analysis functions and by JavaScript on the GEE platform, data in 2010 was sampling as a case study; and (3) to compare results from both GIS and GEE with observation data from ground stations. The results showed the good correlations between the precipitations from manual download and those from a GEE platform, with R greater than 0.9. In short, the application of GEE platform is very effective; it provides a comprehensive tool for managing time-consuming tasks, like precipitation data collection and analysis, and results in reliable outputs.

Keywords *Satellite precipitation, Mekong River, Google Earth Engine*

[1]Research Laboratory for Intelligent system in Agro-hydrological Monitoring and Management (INAMM)
Faculty of Engineering
at Kamphaeng Sean, Kasetsart University,
Nakhon Pathom, 73140 Thailand.
[2]Department of Civil and Earth Resources Engineering, Kyoto University, Japan.
[3]Water Engineering and Management Program,
Asian Institute of Technology,
Pathumthani, 12120 Thailand.

[a]ekasit.k@ku.th (corresponding author)

Introduction

Precipitation is a critical variable in the global hydrologic cycle, and it influences our daily lives (drought, floods, agricultural, irrigation, outdoor activities, etc.)[1]. However, the accessibility of precipitation data in the Tonle Sap Lake region is one of limitations to conduct a comprehensive hydrological analysis.

In this case, the techniques of satellite remote sensing have been widely used and been considered as a powerful and effective tool in perceiving precipitation. However, a massive datasets have to be downloaded; satellite image processing with geographic information system (GIS) analysis function is the prerequisite before retrieval ofrainfall information.

Recently, the Google Earth Engine (GEE) leverages cloud computing services to provide analysis capabilities on over 40 years of Landsat data[2], and others satellites. As a remote sensing platform, its ability to analyze global data rapidly lends itself to being an useful tool on data visualization [3]. Additionally, dataset is processing of geospatial datasets an online for rapid visualization of complex spatial analyses using the Javascript Application Programming Interface (API). This API allows us to develop a code in order to get datasets of publicly available remotely sensed imagery and other data.

This study aimed to apply the GEE platform for automatically retrieving and analyzing precipitation data of the Tropical Rainfall Measuring Mission (TRMM) in Tonle Sap Lake basin (TLS), Cambodia. The methods included: (1) to collect the monthly precipitation data (3B43V7) by manually download and to retrieve from GEE platform; and (2) to compare a selected precipitation data of whole TLS basin in 2010, derived by GIS analysis functions and by JavaScript on a GEE platform, and (3) to compare both GIS and GEE with observation data from ground stations.

Material and Method

A. Study Area

The Tonle Sap Lakeis the largest permanent freshwater lake, locating in Cambodia at the Lower Mekong River basin [4]. During the dry season, the lake is about 120 km long and 35 km widewith an area of about 2500 km^2. A bathymetrical survey of the lake proper, conducted between 1997 and 1999, revealed a relatively flat bottom, with a maximum depth of about 3.3 m[5].During the flood period the Lakeexpands to 250 km long and 100 km wide with an area of about 17,500 km^2, and the depth reaches 8-10 m. The floodplain surrounding the lake extends 20-40 km and is dominated by seasonally inundated forest and rice field [5, 6]. The Tonle Sap basin, extends over 44% of Cambodia's total area 80,000 km^2. 32% of Cambodia's total populationdepend on this lake in living [7].

There arefiveprovinces bordering Tonle Sap Lake namely: Siem Reap, Battambang, Pusat, Kampong Cham, and Kampong Thom. Tonle Sap Basin consists of 11 sub-basins: namely (1) Stung Sreng, (2) Stung Chikreng, (3) Tonle Sap, (4) Stung Pursat, (5) Stung Dauntri, (6) Stung Boribo, (7) Stung Sangker, (8) Stung Monkong Borey, (9) Stung Staung, (10) Stung Sen, (11) Stung Chinit and (12) Stung Sieamreap (Fig. 1).

Tonle Sap basin climate influences from the tropical monsoon seasons. Dry season runs from December to April and rainy season comes when the winds shift into the southwestmonsoonfrom May to November. The monsoon returns south during August and October when the rainfall is usually heavier, with the highestrainfall in October.

B. Satellite Precipitation-TRMM 3B43V7

Many studies have been conducted on detecting diurnal cycles of precipitation over different parts of the world usingsatellite data, especially the Tropical Rainfall Measuring Mission (TRMM)[8].

Recently, data 3B43 is monthly executed to produce the precipitation rate field (3B43). These were combining the 3-hourly merged high-quality/IR estimates (3B42) with the monthly accumulated Global Precipitation Climatology Centre (GPCC) rain gauge analysis. Data are available from 1998 to presentat https://pmm.nasa.gov/data-access/downloads/trmm.

C. Precipitation Processing by GEE Platform

Google Earth Engine (GEE)platform facilitates a fast analysis by using Google's cloud-computing infrastructure(https://earthengine.google.org/).The pre-processed monthly data of Tropical Rainfall Measuring Mission data, or TRMM3B43V7, available through GEE was used to assess precipitation data across the study area. The spatial resolution of the above datasets are all equal to 0.25° × 0.25° with monthly gridded rainfall data [9, 10].

This process is using JavaScript coding in GEE platform screen. TRMM 3B43V7 datasets could be specified location of boundary of Tonle Sap basins in coding. At the end, the amount of precipitation data had retrieved each sub-basins in CSV which can open with MS Excel to interpret data in number.

D. Thiessen Polygon Method

The Thiessen polygon methodallows for areal weighting of rainfall from each gauge. A_i is polygon area, P_i is average precipitation and A is total area [11].

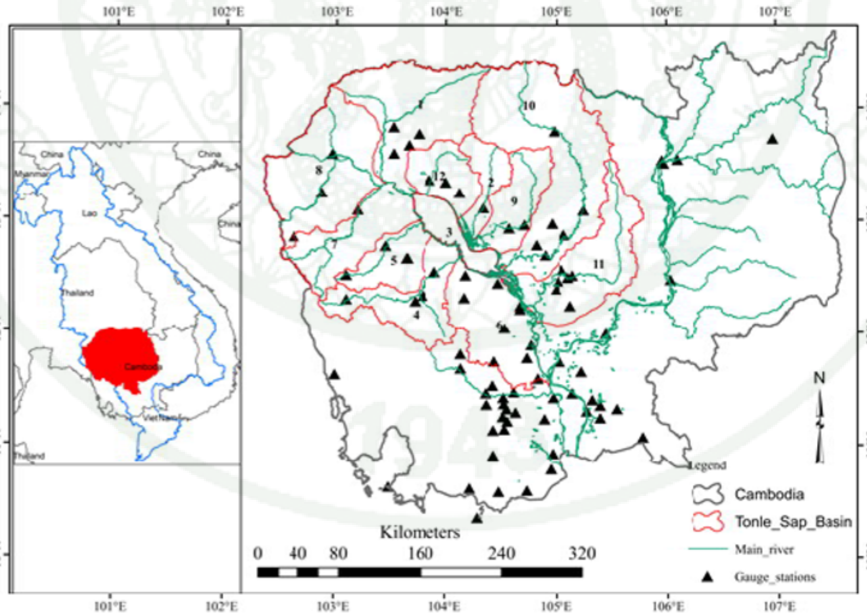

Fig. 1. Boundary of Tonle Sap Basin and location raingauge stations

E. Statistical Indicators

Correlation coefficient (r) is measured on a scale between -1 and +1 to determine the extent to which two sets of paired values are related in a linear fashion. The number closer to -1 and +1 are -1 is a perfect negative linear correlation, whereas the number closer to +1 is a perfect positive linear correlation, and 0 is no correlation.

$$r = \frac{\sum_{j=1}^{N}(X_j - \bar{X})(Y_j - \bar{Y})}{\sqrt{\sum_{j=1}^{N}(X_j - \bar{X})^2 \sum_{j=1}^{N}(Y_j - \bar{Y})^2}} \quad (2)$$

Root mean square error (RMSE) is the square root of the mean of the summation of squared differences between two sets of values where there are n number of paired values x and y. This statistic provides an absolute (neither positive nor negative) value of differences between two sets of values. A smaller value signifies less error.

$$RMSE = \sqrt{\frac{1}{N}\sum_{j-1}^{N}(x_j - y_j)^2} \quad (3)$$

F. Methodology

In this study, 94 rainfall stations from Mekong River Commission (MRC) and Cambodia's Ministry of WaterResources and Meteorology (MoWRAM) were selected which covered almost the entire of Tonle Sap basin.

To achieve the research objectives, data processing methods were divided into three main parts (Fig. 2), including manual data acquisition and GIS processing, GEE-based data processing and gauge observation using Thiessen Polygon method.

The first part is to download monthly precipitation in 2010 (TRMM 3B43v7) in raster format (HDF), and use GIS analysis functions to interpret data, change coordinate system to the same area. Using the function "Zonal statistic as table" in order to get the amount of precipitation with "shape file of boundary".

The second part is to develop the JavaScript code on the GEE platform (https://code.earthengine.google.com).The code included: importing the TRMM image dataset; specifying the boundary of study area by uploading shape file into GEE data script; extracting the mean monthly precipitation of the basin by writing code on script (see example in Fig. 3). After having execute the code, the precipitation data were retrieved on sub-basins automatically.

Lastly, the areal precipitation from gauge station were estimated by Thiessen Polygon method. Precipitation of basin was summarized using "Zonal statistic as table" with boundary of basin. The precipitation data retrieved from the first and second methods were finally compared with the observed data from gauge stations for the entire basin and each sub-basin. Statistical indicators, correlation coefficient (r) and RMSE, were estimated.

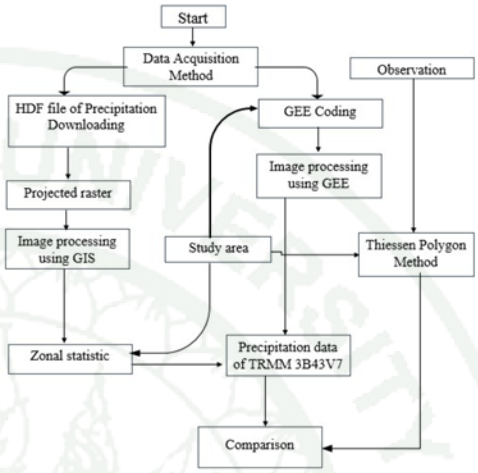

Fig. 2. Research framework

Results and discussions

A. Monthly Precipitaion Depth

Fig. 4 shows monthly precipitation of the Tonle Sap Basin in 2010, derived from 3 methods: GIS analysis of downloaded TRMM data (GIS), GEE processing (GEE) and observed rainfall with Thiessen Polygon estimation (OBS).

1) TRMM Precipitation from GIS vs. GEE Processings

The amount of precipitation from TRMM 3B43V7 using both GIS analysis of downloaded data (GIS) and Google Earth Engine processing (GEE) methods were well matched with almost identical rainfall depths from January to December on 2010. In dry season from November to April, rainfall varied from 8 to 70 mm, while in wet season from May to October, rainfall varied from 100 to 300 mm. The highest precipitation can be observed in October around 300 mm. GEE provided an almost similar the amount of rainfall compared to manually download rainfall. There are somewhat difference between 0.005 to 1.8 mm due to round-off errors during data processing.

2) Precipitation from GEE Processings vs. Observation

From Fig. 4, TRMM precipitation from GEE processing and basin rainfall estimation from gauge station (OBS) were well captured the amount of monthly rainfall. By comparing GEE rainfall with rain gauge data, we can observed an over-estimated rainfall by GEE mostly during dry period from January to June (4 to 20 mm), in October and in December. Rainfall by GEE were under-estimated during wet period from July to September 30 to 49 mm. However, these values were observed as less error between rainfall from GEE and observation. Fig. 5 showed the spatial data on the monthly average rainfall in millimeters from the GEE platform.

3) Precipitation from GIS Processing vs. Observation

Based on result shown in Fig.4, the differences of rainfall depths between GIS processing (GIS) and the gauged observation (OBS) are comparable to those between GEE and OBS. The identical months of over- or under-estimation were observed. The GIS rainfall were over-estimated from the lowest of 4 mm on December to the highest of 20 mm on June.

B. Statistical Indicators

Statistical indicators of the whole basin were shown in Table I, the amount of precipitations from manual download and those from a GEE platform provided an almost similar monthly rainfall depth with r greater than 0.99 whole basin. Finally, both methods GEE and GIS provided a good correlation with the gauge which showed the r value greater than 0.97 and the highest RMSE of basin about 16 mm.

Statistical indicators of each sub-basins were presented in Table II, the indicators demonstrated the good correlations of rainfall between GIS *vs.* GEE, GEE *vs.* observation, and GIS *vs.* observation. The correlation coefficient, r, are 0.99, 0.81 and 0.80 respectively.

Table I. Statistical Indicators of Basin

Method	*r*	*RMSE*
GIS vs. GEE	0.999	0.70
GEE vs. OBS	0.975	16.40
GIS vs. OBS	0.977	15.88

Table II. Statistical Indicator of each Sub-basins

Sub	GIS *vs.* GEE		GIS *vs.* OBS		GEE *vs.* OBS	
basin	*r*	*RMSE*	*r*	*RMSE*	*r*	*RMSE*
1	0.9898	1.20	0.8713	23.56	0.8818	23.97
2	0.9997	1.13	0.8719	27.21	0.8259	27.73
3	0.9998	1.73	0.9611	17.72	0.9347	17.94
4	0.9998	2.15	0.9723	24.81	0.9424	25.80
5	0.9905	1.39	0.8437	23.49	0.8824	23.62
6	0.9996	2.36	0.8089	20.73	0.8984	21.46
7	0.9991	2.36	0.9032	39.27	0.8010	38.77
8	0.9997	7.26	0.8864	29.70	0.8725	26.18
9	0.9997	0.86	0.9392	19.51	0.9697	19.82
10	0.9994	1.30	0.9393	19.99	0.9638	20.14
11	0.9997	1.00	0.8326	24.96	0.8757	24.64
12	0.9997	6.59	0.8872	28.41	0.8897	27.94

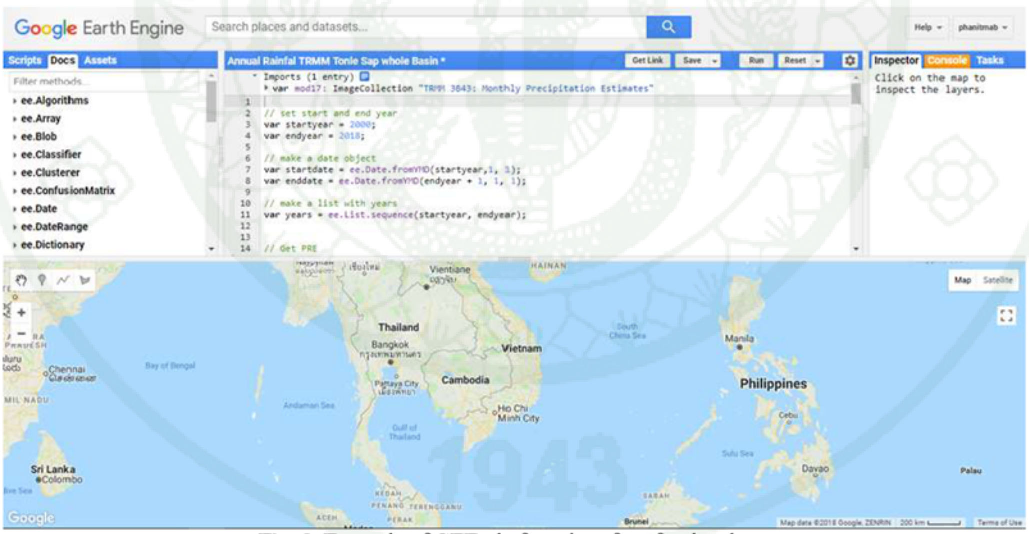

Fig. 3. Example of GEE platform interface for developer

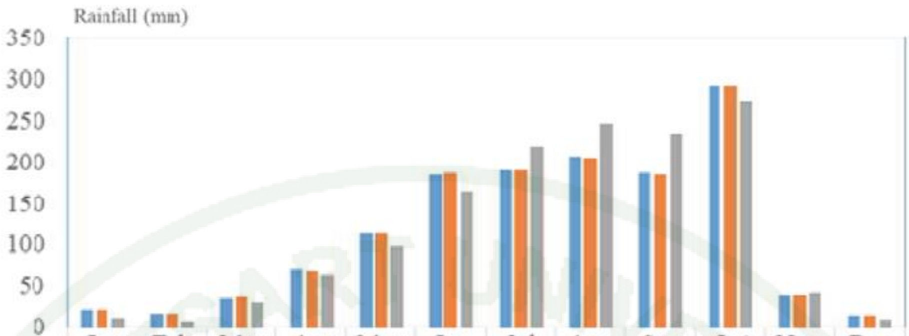

	Jan	Feb	Mar	Apr	May	Jun	Jul	Aug	Sep	Oct	Nov	Dec
GIS	20.5	15.8	33.8	68.6	112.6	185.0	189.5	205.6	186.3	291.2	37.5	12.8
GEE	20.9	15.8	35.3	67.7	112.3	186.5	188.6	203.8	185.0	291.6	38.2	13.0
Observe	11.0	7.0	28.7	61.6	97.2	164.2	217.2	246.3	234.9	273.6	42.7	8.1

GIS GEE Observe

Fig. 4. Montly rainfall in 2010 estimated by three methods: GIS analysis of downloaded data (GIS), GEE processing (GEE) and observed rainfall with Thiessen Polygon estimation (OBS)

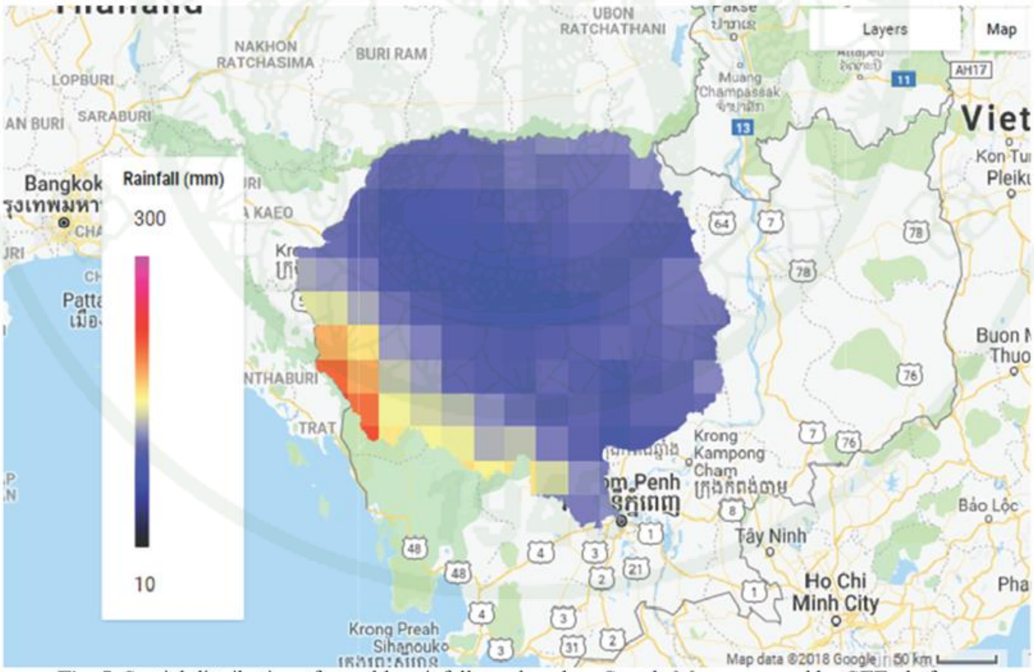

Fig. 5. Spatial distribution of monthly rainfall overlayed on Google Map processed by GEE platform

Conclusions

Both precipitations from manually download and those froma GEE platform provided an almost similar rainfall depth for each sub-basins and the entire basin. However, the amount of precipitation of each sub-basins had some error because of uncertainty and location of the gauges in basins. TRMM 3B43V7 dataset provided high correlation when compared with the gauge stations. In short, the GEE platform is an effective tool which provides a comprehensive for managing time-consuming tasks, namely precipitation data collection and analysis. It is a new concept of remote sensing platform on how to get satellite datasets easily and quickly with results in reliable outputs.

Acknowledgment

This paper was supported by the Kasetsart University Scholarships for ASEAN for Commemoration of the 60th Birthday Anniversary of Professor Dr. Her Royal Highness Princess Chulabhorn Mahidol. Moreover, the authors would also like to express their gratitude to the Google Earth Engine (GEE) developers for providing a registration during this research on retrieval datasets.

References

[1] G. Langella, A. Basile, A. Bonfante, and F. Terribile, "High-resolution space–time rainfall analysis using integrated ANN inference systems," Journal of hydrology, vol. 387, no. 3-4, pp. 328-342, 2010.

[2] J. Dong, X. Xiao, M. A. Menarguez, G. Zhang, Y. Qin, D. Thau, C. Biradar, and B. Moore III, "Mapping paddy rice planting area in northeastern Asia with Landsat 8 images, phenology-based algorithm and Google Earth Engine," Remote sensing of environment, vol. 185, pp. 142-154, 2016.

[3] N. N. Patel, E. Angiuli, P. Gamba, A. Gaughan, G. Lisini, F. R. Stevens, A. J. Tatem, and G. Trianni, "Multitemporal settlement and population mapping from Landsat using Google Earth Engine," International Journal of Applied Earth Observation and Geoinformation, vol. 35, pp. 199-208, 2015.

[4] I. Campbell, S. Say, and J. Beardall, "Tonle Sap Lake, the heart of the lower Mekong," in The Mekong: Elsevier, 2009, pp. 251-272.

[5] I. C. Campbell, C. Poole, W. Giesen, and J. Valbo-Jorgensen, "Species diversity and ecology of Tonle Sap Great Lake, Cambodia," Aquatic Sciences, vol. 68, no. 3, pp. 355-373, 2006.

[6] W. J. Junk, M. Brown, I. C. Campbell, M. Finlayson, B. Gopal, L. Ramberg, and B. G. Warner, "The comparative biodiversity of seven globally important wetlands: a synthesis," Aquatic Sciences, vol. 68, no. 3, pp. 400-414, 2006.

[7] ADB, "The Tonle Sap Basin Strategy," 2005, p. 9.

[8] M. S. K. Kiany, R. C. Balling Jr, R. S. Cerveny, and D. S. Krahenbuhl, "Diurnal variations in seasonal precipitation in Iran from TRMM measurements," Advances in Space Research, 2018.

[9] Z. Duan and W. Bastiaanssen, "First results from Version 7 TRMM 3B43 precipitation product in combination with a new downscaling–calibration procedure," Remote Sensing of Environment, vol. 131, pp. 1-13, 2013.

[10] G. J. Huffman, D. T. Bolvin, E. J. Nelkin, D. B. Wolff, R. F. Adler, G. Gu, Y. Hong, K. P. Bowman, and E. F. Stocker, "The TRMM multisatellite precipitation analysis (TMPA): Quasi-global, multiyear, combined-sensor precipitation estimates at fine scales," Journal of hydrometeorology, vol. 8, no. 1, pp. 38-55, 2007.

[11] P. B. Bedient, W. C. Huber, and B. E. Vieux, Hydrology and floodplain analysis. 2008.

Appendix B

JavaScript code developed with google earth engine platform

```
// set start and end year
var startyear = 2000;
var endyear = 2014;
// make a date object
var startdate = ee.Date.fromYMD(startyear,1, 1);
var enddate = ee.Date.fromYMD(endyear + 1, 1, 1);
// make a list with years
var years = ee.List.sequence(startyear, endyear);
// Get Rainfall Data
var Pre = mod17.select("precipitation")
var annualPre = ee.ImageCollection.fromImages(
years.map(function (year) {
var annual = Pre
filter(ee.Filter.calendarRange(year, year, 'year'))
 .sum()
.multiply(720);
return annual
.set('year', year)
.set('system:time_start', ee.Date.fromYMD(year, 1, 1));
}));
var title = {
  title: 'Annual Precipitation',
  hAxis: {title: 'Time'},
  vAxis: {title: 'Precipitation (mm)'},
};
var chart = ui.Chart.image.seriesByRegion({
  imageCollection: annualPre,
  regions: table,
  reducer: ee.Reducer.mean(),
  band: 'precipitation',
  scale: 2500,
  xProperty: 'system:time_start',
  seriesProperty: 'SITE'
}).setOptions(title)
  .setChartType('ColumnChart');
  print(chart);
```

Figure 36 JavaScript for Retrieving Yearly Precipitation from GEE Platform

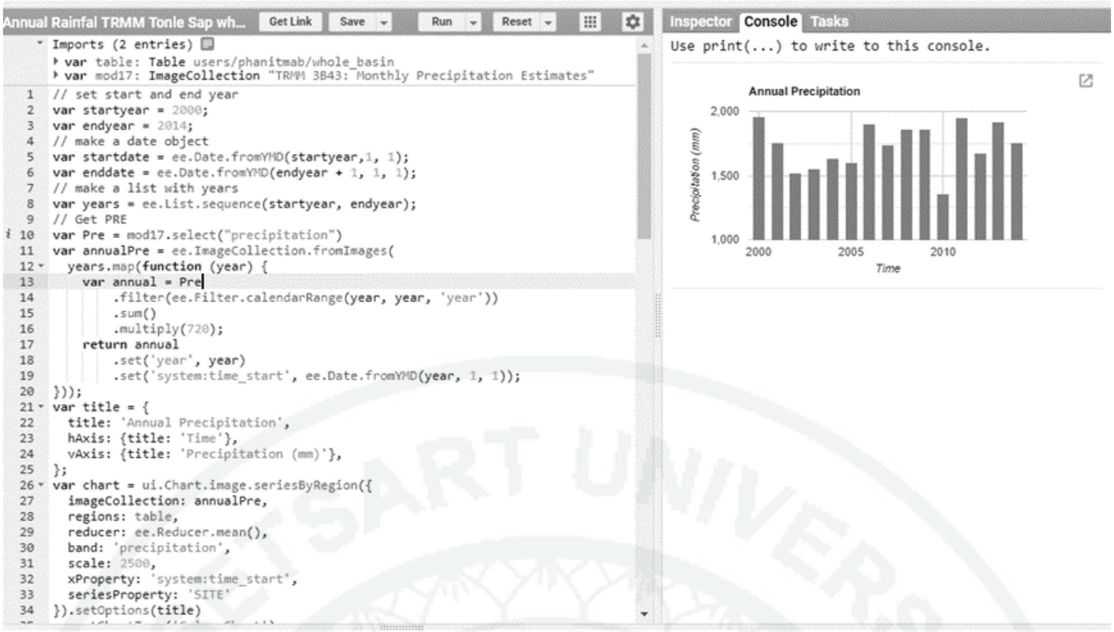

Figure 37 JavaScript on yearly rainfall data

```
// set start and end year
var startyear = 2000;
var endyear = 2014;
// make a date object
var startdate = ee.Date.fromYMD(startyear, 1, 1);
var enddate = ee.Date.fromYMD(endyear + 1, 1, 1);
// make a list with years
var years = ee.List.sequence(startyear, endyear);
// make a list with months
var months = ee.List.sequence(1, 12);
//Precipitation
var monthlyPrecip =  ee.ImageCollection.fromImages(
  years.map(function (y) {
return months.map(function(m) {
      var w = TRMM.filter(ee.Filter.calendarRange(y, y, 'year'))//change here
                    .filter(ee.Filter.calendarRange(m, m, 'month'))
                    .sum()
                   .multiply(720);//change here
                        return w.set('year', y)
              .set('month', m)
              .set('system:time_start', ee.Date.fromYMD(y, m, 1));

    });
  }).flatten()
);
var title = {
  title: 'Monthly precipitation',
  hAxis: {title: 'Time'},
  vAxis: {title: 'Precipitation (mm)'},
};
var chartMonthly = ui.Chart.image.seriesByRegion({
  imageCollection: monthlyPrecip,
  regions: table,
  reducer: ee.Reducer.mean(),
  band: 'precipitation',//change here
  scale: 2500,
  xProperty: 'system:time_start',
  seriesProperty: 'SITE'
}).setOptions(title)
  .setChartType('ColumnChart');
print(chartMonthly);
```

Figure 38 JavaScript for Retrieving Monthly Precipitation from GEE Platform

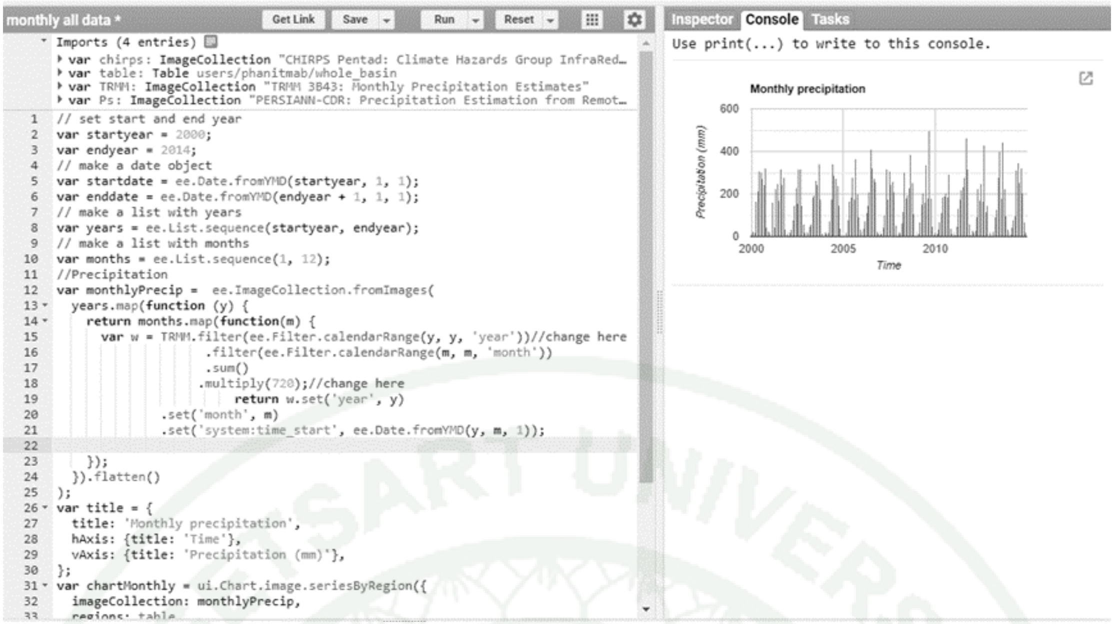

Figure 39 JavaScript on monthly rainfall data

3.

```
// set start and end year
var startyear = 2000;
var endyear = 2014;
// make a date object
var startdate = ee.Date.fromYMD(startyear,1, 1);
var enddate = ee.Date.fromYMD(endyear + 1, 1, 1);
// make a list with years
var years = ee.List.sequence(startyear, endyear);
// Get PET
var Pet = mod16.select("PET")
var annualPre = ee.ImageCollection.fromImages(
  years.map(function (year) {
    var annual = Pet
        .filter(ee.Filter.calendarRange(year, year, 'year'))
        .sum()
        .multiply(0.1);
    return annual
        .set('year', year)
        .set('system:time_start', ee.Date.fromYMD(year, 1, 1));
}));
var title = {
  title: 'Annual PET',
  hAxis: {title: 'Time'},
  vAxis: {title: 'PET (mm)'},
};

var chart = ui.Chart.image.seriesByRegion({
  imageCollection: annualPre,
  regions: table,
  reducer: ee.Reducer.mean(),
  band: 'PET',
  scale: 2500,
  xProperty: 'system:time_start',
  seriesProperty: 'SITE'
}).setOptions(title)
  .setChartType('ColumnChart');

  print(chart);
```

Figure 40 JavaScript for Retrieving Yearly PET from GEE Platform

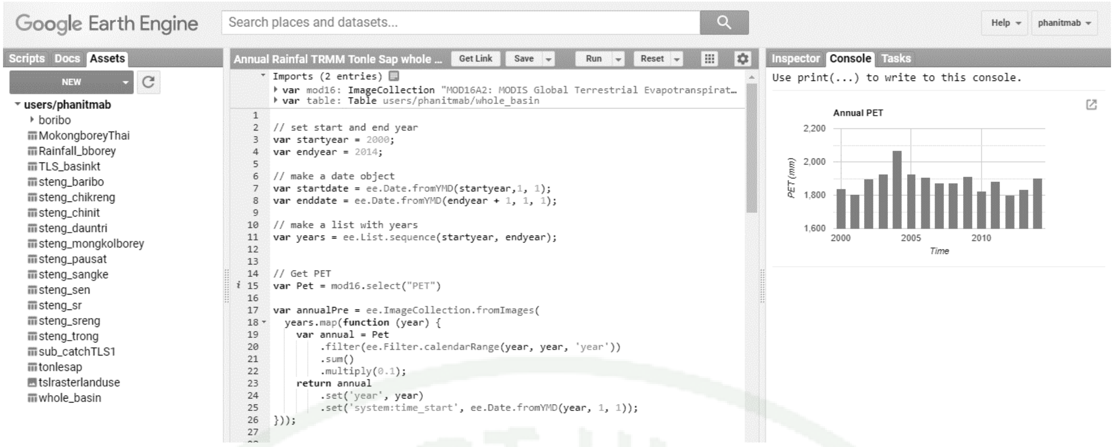

Figure 41 JavaScript on yearly PET data

```
// set start and end year
var startyear = 2000;
var endyear = 2014;
// make a date object
var startdate = ee.Date.fromYMD(startyear, 1, 1);
var enddate = ee.Date.fromYMD(endyear + 1, 1, 1);
// make a list with years
var years = ee.List.sequence(startyear, endyear);
// make a list with months
var months = ee.List.sequence(1, 12);
//PET
var monthlyPet =  ee.ImageCollection.fromImages(
  years.map(function (y) {
    return months.map(function(m) {
      var w = Mod16.filter(ee.Filter.calendarRange(y, y, 'year'))//change here
                    .filter(ee.Filter.calendarRange(m, m, 'month'))
                    .sum()
                   .multiply(0.1);//change here
                        return w.set('year', y)
              .set('month', m)
              .set('system:time_start', ee.Date.fromYMD(y, m, 1));

    });
  }).flatten()
);
var title = {
  title: 'Monthly PET',
  hAxis: {title: 'Time'},
  vAxis: {title: 'PET (mm)'},
};
var chartMonthly = ui.Chart.image.seriesByRegion({
  imageCollection: monthlyPet,
  regions: table,
  reducer: ee.Reducer.mean(),
  band: 'PET',//change here
  scale: 2500,
  xProperty: 'system:time_start',
  seriesProperty: 'SITE'
}).setOptions(title)
  .setChartType('ColumnChart');
print(chartMonthly);
```

Figure 42 JavaScript for Retrieving Monthly PET from GEE Platform

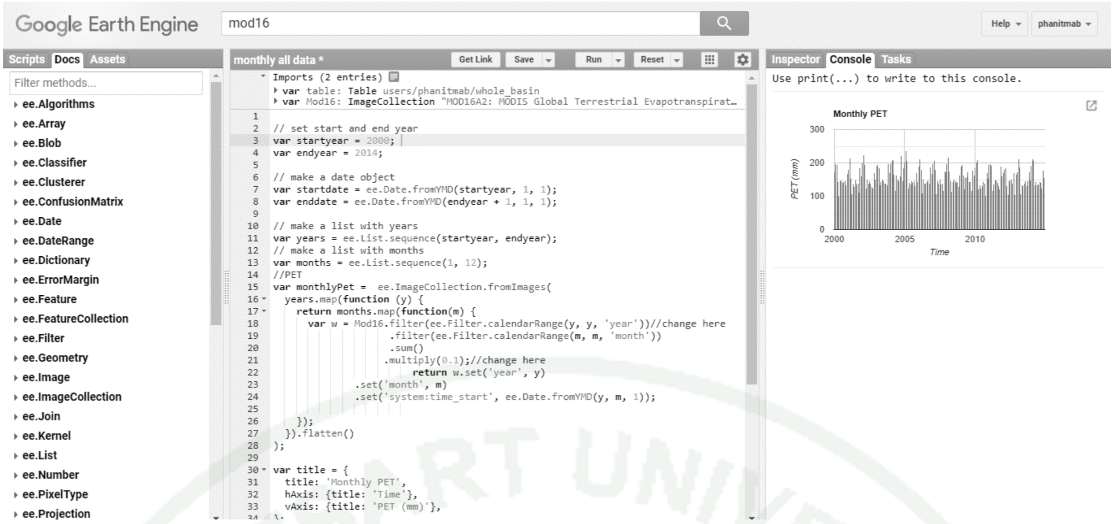

Figure 43 JavaScript on monthly PET data

Appendix C

Monthly rainfall data of sub-basins in millimeter from 2000 to 2014 (TRMM)

Table 15 Monthly rainfall data of ST1

Year	Jan	Feb	Mar	Apr	May	Jun	Jul	Aug	Sep	Oct	Nov	Dec	Annual
2000	17	7	38	140	158	246	225	193	210	383	109	115	1,841
2001	72	1	189	52	145	187	122	242	271	320	16	12	1,629
2002	0	1	28	43	95	191	120	237	312	246	136	38	1,447
2003	0	22	78	69	171	161	200	252	352	138	3	0	1,448
2004	4	3	12	62	139	259	209	209	249	246	62	0	1,455
2005	1	1	10	97	120	124	245	176	404	325	94	30	1,628
2006	14	15	71	100	137	203	261	401	302	269	27	27	1,826
2007	11	1	47	81	279	189	287	331	301	234	39	0	1,798
2008	28	3	67	137	275	207	183	245	381	315	133	6	1,980
2009	1	17	42	172	198	149	236	251	388	217	43	1	1,716
2010	29	2	90	58	65	272	153	172	196	311	71	24	1,444
2011	1	1	48	116	143	188	235	292	417	390	79	7	1,917
2012	30	20	26	103	211	186	254	135	358	121	180	1	1,625
2013	9	2	21	74	109	318	317	142	402	178	183	32	1,788
2014	2	6	28	76	94	281	362	190	342	203	92	46	1,722

Table 16 Monthly rainfall data of ST2

Year	Jan	Feb	Mar	Apr	May	Jun	Jul	Aug	Sep	Oct	Nov	Dec	Annual
2000	2	4	8	128	191	305	290	199	296	385	35	16	1,859
2001	2	0	127	35	218	241	142	316	278	340	31	17	1,747
2002	1	0	9	80	122	205	166	302	409	124	34	12	1,464
2003	0	1	41	40	181	221	253	217	413	166	19	3	1,555
2004	4	0	12	57	177	388	252	291	283	174	32	5	1,675
2005	0	2	14	53	168	138	252	136	374	233	89	38	1,497
2006	13	27	82	96	107	230	412	257	272	243	14	27	1,782
2007	9	13	24	75	315	192	313	230	228	170	34	1	1,605
2008	7	7	54	75	325	168	173	203	371	278	89	3	1,753
2009	14	11	54	109	175	170	347	158	569	178	45	2	1,833
2010	16	2	19	46	80	182	150	177	192	276	31	11	1,182
2011	8	3	19	114	156	199	203	313	414	371	76	12	1,888
2012	13	6	19	69	222	153	248	179	417	125	98	0	1,549
2013	25	2	17	74	164	265	324	154	457	235	63	50	1,830
2014	7	20	15	56	79	313	327	206	324	186	63	9	1,604

Table 17 Monthly rainfall data of ST3

Year	Jan	Feb	Mar	Apr	May	Jun	Jul	Aug	Sep	Oct	Nov	Dec	Annual
2000	11	22	19	200	236	332	328	276	232	287	76	40	2,061
2001	10	1	196	56	213	223	153	325	222	328	45	6	1,780
2002	0	0	15	55	118	270	151	294	290	233	63	32	1,520
2003	0	2	32	37	172	162	300	144	312	188	14	2	1,364
2004	4	1	14	83	229	333	334	268	257	147	36	0	1,705
2005	0	0	6	88	157	191	336	237	355	267	99	47	1,784
2006	0	16	55	115	132	213	330	377	285	223	15	13	1,774
2007	4	0	56	80	326	167	378	346	303	222	65	0	1,949
2008	3	32	60	135	287	206	202	286	296	231	125	7	1,870
2009	0	24	47	177	244	227	346	213	465	174	28	0	1,945
2010	24	0	27	70	90	225	193	199	197	226	43	14	1,310
2011	1	0	36	108	189	231	304	328	455	254	98	7	2,012
2012	31	7	19	97	217	238	305	162	392	133	150	1	1,752
2013	3	3	14	74	166	260	381	176	455	156	127	37	1,851
2014	1	0	41	99	142	358	455	222	311	216	46	44	1,935

Table 18 Monthly rainfall data of ST4

Year	Jan	Feb	Mar	Apr	May	Jun	Jul	Aug	Sep	Oct	Nov	Dec	Annual
2000	10	42	40	179	230	321	353	359	185	428	37	18	2,200
2001	17	3	226	44	279	246	202	388	208	240	27	4	1,885
2002	2	31	77	124	201	225	68	372	209	123	97	14	1,543
2003	0	1	39	46	167	196	238	226	350	197	12	1	1,473
2004	36	14	43	60	222	291	316	307	191	175	57	0	1,712
2005	0	3	28	102	205	248	368	113	382	193	128	15	1,786
2006	5	81	89	145	183	181	573	324	284	391	26	12	2,294
2007	7	37	46	132	337	139	303	147	310	321	109	0	1,887
2008	4	12	104	145	306	159	237	159	437	312	121	2	1,998
2009	3	18	99	182	246	85	425	76	579	242	82	2	2,040
2010	20	42	58	77	137	177	213	173	135	373	55	11	1,471
2011	1	19	90	184	156	204	249	170	600	407	72	7	2,158
2012	40	45	76	98	290	160	256	107	569	143	289	0	2,073
2013	16	2	52	126	68	296	590	118	471	247	122	20	2,128
2014	2	12	88	68	93	332	366	254	372	256	97	28	1,967

Table 19 Monthly rainfall data of ST5

Year	Jan	Feb	Mar	Apr	May	Jun	Jul	Aug	Sep	Oct	Nov	Dec	Annual
2000	16	20	29	170	187	284	222	274	232	281	15	7	1,736
2001	10	5	150	50	257	212	159	225	207	241	28	4	1,547
2002	3	48	43	96	178	168	178	255	270	130	24	23	1,415
2003	0	0	36	31	244	263	297	225	399	157	10	3	1,666
2004	38	56	22	97	140	330	279	245	202	95	8	0	1,512
2005	8	2	38	84	156	167	220	152	312	196	85	26	1,446
2006	3	43	94	95	185	190	390	285	289	241	14	3	1,831
2007	3	16	43	166	326	210	265	151	224	157	54	0	1,616
2008	3	12	59	83	340	186	203	222	360	280	105	4	1,857
2009	0	15	103	171	227	156	217	187	341	188	46	1	1,652
2010	17	27	44	76	170	154	197	238	173	353	16	8	1,471
2011	0	20	69	172	174	215	223	268	357	289	18	2	1,807
2012	31	29	36	90	203	135	246	155	474	108	126	2	1,635
2013	13	8	25	127	95	310	415	262	360	343	77	11	2,046
2014	0	5	81	73	95	217	214	307	309	205	55	5	1,567

Table 20 Monthly rainfall data of ST6

Year	Jan	Feb	Mar	Apr	May	Jun	Jul	Aug	Sep	Oct	Nov	Dec	Annual
2000	17	48	52	182	242	338	404	432	208	431	53	38	2,446
2001	50	4	233	57	301	286	217	425	260	271	24	9	2,138
2002	1	28	81	115	205	277	94	439	273	150	116	39	1,818
2003	0	53	72	81	181	118	285	236	257	243	43	1	1,571
2004	39	15	47	59	239	296	354	329	227	230	54	0	1,889
2005	1	5	42	119	210	271	420	151	424	208	131	30	2,012
2006	6	75	89	171	218	210	611	399	336	397	32	10	2,556
2007	14	41	49	159	346	170	363	213	373	344	81	0	2,154
2008	3	26	42	130	276	173	205	213	371	231	92	1	1,763
2009	3	25	104	210	270	117	453	135	640	247	68	11	2,282
2010	20	28	65	87	140	233	236	219	179	386	66	22	1,680
2011	2	22	93	190	177	243	301	217	658	430	76	9	2,417
2012	55	49	74	123	308	208	295	115	572	143	271	2	2,216
2013	25	2	56	116	99	343	604	153	481	229	144	18	2,272
2014	3	16	84	82	103	365	424	280	420	250	108	36	2,171

Table 21 Monthly rainfall data of ST7

Year	Jan	Feb	Mar	Apr	May	Jun	Jul	Aug	Sep	Oct	Nov	Dec	Annual
2000	15	38	35	165	238	353	369	371	228	391	32	16	2,250
2001	17	5	206	70	318	262	217	358	230	270	30	3	1,985
2002	3	29	66	102	242	255	140	366	245	139	61	29	1,678
2003	0	41	54	78	154	210	241	286	277	177	6	1	1,525
2004	60	17	35	79	234	352	385	322	193	159	30	0	1,867
2005	0	2	37	105	217	286	353	182	367	205	123	23	1,899
2006	5	75	92	127	241	239	577	362	309	399	46	4	2,476
2007	7	31	63	153	364	221	406	178	305	245	74	0	2,047
2008	10	10	118	170	326	189	256	199	470	298	120	3	2,169
2009	0	16	131	170	302	129	400	143	528	228	63	3	2,114
2010	21	38	57	89	202	208	264	254	147	392	44	14	1,729
2011	0	22	125	195	187	270	296	259	582	340	39	6	2,322
2012	51	54	67	100	277	182	303	152	542	152	234	1	2,114
2013	16	5	46	146	101	358	592	219	480	279	103	18	2,362
2014	0	16	83	69	109	353	345	323	407	247	77	13	2,043

Table 22 Monthly rainfall data of ST8

Year	Jan	Feb	Mar	Apr	May	Jun	Jul	Aug	Sep	Oct	Nov	Dec	Annual
2000	4	22	11	194	282	346	359	314	276	269	32	13	2,122
2001	2	2	140	42	226	303	217	412	274	293	48	11	1,970
2002	1	0	21	71	141	286	240	383	368	140	33	7	1,690
2003	0	48	83	79	207	134	361	262	326	253	29	1	1,783
2004	8	5	25	83	180	378	315	318	270	131	35	9	1,757
2005	0	0	12	63	181	202	279	259	379	164	77	42	1,659
2006	0	28	60	126	133	222	431	376	282	244	9	24	1,934
2007	1	8	48	80	357	156	351	346	251	219	49	0	1,866
2008	3	25	86	150	348	199	272	191	462	287	100	1	2,126
2009	2	13	63	142	205	198	461	259	592	171	38	1	2,143
2010	18	3	10	71	91	182	219	250	218	238	24	3	1,326
2011	1	4	27	116	206	239	243	357	532	287	61	4	2,078
2012	18	3	18	94	246	176	285	234	393	116	93	0	1,676
2013	1	1	23	79	196	226	398	197	515	195	69	48	1,948
2014	0	2	20	89	99	421	475	301	309	192	31	11	1,950

Table 23 Monthly rainfall data of ST9

Year	Jan	Feb	Mar	Apr	May	Jun	Jul	Aug	Sep	Oct	Nov	Dec	Annual
2000	3	5	9	119	174	275	270	180	284	414	27	11	1,770
2001	0	2	132	25	227	220	134	303	246	326	32	14	1,661
2002	2	8	11	73	117	187	136	290	323	113	25	7	1,293
2003	0	47	72	84	169	193	328	321	271	223	14	0	1,724
2004	6	0	8	64	160	389	239	282	278	137	26	0	1,589
2005	0	0	13	54	159	121	223	116	345	207	98	40	1,375
2006	8	35	82	81	97	207	387	207	229	220	20	24	1,596
2007	5	4	22	77	296	188	285	173	185	162	44	0	1,441
2008	1	17	55	92	367	182	213	315	395	223	91	2	1,954
2009	5	6	46	101	157	135	318	129	474	161	65	1	1,597
2010	15	3	11	39	94	137	127	142	167	309	30	11	1,088
2011	2	4	33	99	148	201	188	267	352	351	51	11	1,706
2012	10	4	21	62	196	141	187	169	425	121	104	1	1,441
2013	5	2	9	69	116	285	320	168	400	258	65	42	1,738
2014	2	7	19	52	74	244	267	226	278	209	60	5	1,443

Table 24 Monthly rainfall data of ST10

Year	Jan	Feb	Mar	Apr	May	Jun	Jul	Aug	Sep	Oct	Nov	Dec	Annual
2000	13	19	12	165	228	268	265	283	241	271	7	4	1,775
2001	2	5	117	31	207	260	167	284	220	262	47	8	1,609
2002	2	11	28	71	143	212	167	363	350	111	24	14	1,496
2003	0	5	60	46	249	243	279	304	431	139	16	3	1,775
2004	25	7	12	72	154	375	295	295	238	80	12	0	1,563
2005	1	0	24	73	156	130	271	171	338	150	84	30	1,428
2006	2	28	82	96	139	192	352	256	213	222	6	9	1,597
2007	2	6	32	105	313	149	258	232	221	166	31	0	1,515
2008	9	6	42	81	279	152	147	164	319	293	92	2	1,587
2009	0	11	81	126	157	147	294	176	435	131	51	0	1,611
2010	19	12	12	66	122	130	192	217	184	293	16	9	1,272
2011	0	12	24	99	206	199	210	272	334	319	14	1	1,691
2012	12	4	16	82	209	146	169	214	344	84	89	1	1,369
2013	1	3	11	76	132	243	317	209	415	236	51	37	1,731
2014	0	1	22	69	104	215	264	266	254	194	63	6	1,458

Table 25 Monthly rainfall data of ST11

Year	Jan	Feb	Mar	Apr	May	Jun	Jul	Aug	Sep	Oct	Nov	Dec	Annual
2000	3	6	8	142	187	316	286	214	296	352	41	23	1,874
2001	4	0	135	39	217	247	146	307	280	331	32	11	1,750
2002	0	0	14	74	121	233	161	293	396	144	38	9	1,482
2003	0	3	29	46	149	187	223	221	236	216	11	0	1,321
2004	2	1	9	60	156	364	247	280	281	178	43	12	1,632
2005	0	1	10	56	180	147	241	154	390	227	80	32	1,517
2006	1	14	88	98	112	235	420	326	265	230	7	29	1,824
2007	1	8	26	83	323	185	344	279	210	182	36	0	1,677
2008	2	3	43	97	297	156	156	220	397	243	88	3	1,703
2009	4	10	49	109	175	189	314	167	581	167	45	1	1,811
2010	19	0	10	54	80	194	169	187	201	267	38	3	1,224
2011	2	2	19	125	162	212	243	274	445	324	98	10	1,918
2012	13	5	14	72	195	172	313	163	402	113	99	0	1,562
2013	7	1	17	65	132	253	336	157	428	203	82	36	1,717
2014	2	10	16	67	86	302	377	230	295	235	29	6	1,655

Appendix D

Monthly potential evapotranspiration (PET) of sub-basins in millimeter (2000-2014)

Table 26 Monthly PET data of ST1

Year	Jan	Feb	Mar	Apr	May	Jun	Jul	Aug	Sep	Oct	Nov	Dec	Annual
2000	178	211	199	148	103	141	156	147	145	150	129	164	1,872
2001	182	225	165	116	137	130	152	140	144	109	181	166	1,847
2002	218	250	221	123	152	138	148	149	133	120	164	149	1,965
2003	196	216	198	131	139	149	146	148	138	122	194	177	1,954
2004	214	220	221	168	116	155	147	142	149	214	141	196	2,084
2005	211	251	231	134	137	134	144	145	138	119	166	137	1,949
2006	184	220	187	111	143	133	144	140	144	132	183	173	1,894
2007	204	221	189	106	140	134	147	140	139	109	172	169	1,870
2008	204	223	176	142	110	137	153	147	142	135	124	165	1,859
2009	191	199	160	108	146	152	164	142	147	117	178	169	1,875
2010	195	231	219	132	134	120	133	140	137	98	157	149	1,846
2011	197	199	191	125	131	152	154	146	130	118	180	160	1,883
2012	179	188	176	131	109	148	153	149	141	163	104	164	1,804
2013	171	221	186	102	128	126	134	151	132	138	165	143	1,796
2014	197	218	215	122	136	137	144	140	137	108	164	154	1,872

Table 27 Monthly PET data of ST2

Year	Jan	Feb	Mar	Apr	May	Jun	Jul	Aug	Sep	Oct	Nov	Dec	Annual
2000	178	198	199	147	108	159	155	149	150	152	141	174	1,910
2001	185	215	160	110	144	141	163	145	149	124	193	165	1,893
2002	198	229	191	123	155	146	155	145	139	133	181	158	1,953
2003	193	194	189	130	150	161	153	145	146	144	205	166	1,978
2004	193	200	210	167	123	171	160	153	170	233	150	177	2,107
2005	200	238	206	122	152	144	154	152	163	143	183	150	2,007
2006	196	211	179	109	163	146	146	150	162	150	198	169	1,979
2007	196	203	180	109	151	151	158	143	152	129	187	176	1,936
2008	189	194	164	124	165	168	180	151	150	125	186	169	1,965
2009	186	199	204	120	138	131	140	154	148	107	182	158	1,867
2010	191	201	196	112	143	155	155	148	140	128	199	163	1,929
2011	196	213	169	145	122	152	163	154	152	149	136	167	1,919
2012	174	182	183	136	108	152	158	155	146	177	106	173	1,850
2013	175	213	187	107	142	139	152	154	140	154	183	153	1,900
2014	193	214	212	135	149	136	140	153	150	136	192	161	1,971

Table 28 Monthly PET data of ST3

Year	Jan	Feb	Mar	Apr	May	Jun	Jul	Aug	Sep	Oct	Nov	Dec	Annual
2000	182	212	208	154	100	139	151	141	140	149	134	172	1,882
2001	194	228	169	119	135	125	146	135	136	122	190	166	1,864
2002	205	240	221	127	157	135	142	138	132	120	169	155	1,940
2003	193	216	205	141	142	146	140	139	133	130	196	169	1,951
2004	206	223	220	172	114	156	148	143	164	222	148	185	2,102
2005	203	243	241	145	135	136	142	133	135	130	169	143	1,955
2006	189	218	191	120	151	131	135	138	138	139	191	172	1,912
2007	197	216	194	110	132	121	140	138	135	114	172	172	1,840
2008	198	218	181	142	107	129	147	141	135	141	127	166	1,832
2009	189	222	218	123	126	117	127	136	130	99	166	157	1,811
2010	188	199	166	109	143	147	159	135	141	118	186	171	1,861
2011	190	213	205	129	126	147	149	141	127	126	188	164	1,906
2012	176	190	194	126	105	140	147	146	135	172	108	170	1,810
2013	177	224	181	98	120	121	130	141	125	144	173	147	1,781
2014	192	219	216	123	128	128	134	138	134	117	182	158	1,869

Table 29 Monthly PET data of ST4

Year	Jan	Feb	Mar	Apr	May	Jun	Jul	Aug	Sep	Oct	Nov	Dec	Annual
2000	172	188	190	143	104	144	148	143	143	142	129	161	1,808
2001	175	206	151	111	139	122	148	135	138	102	180	162	1,767
2002	205	218	190	120	152	142	149	143	125	122	162	149	1,877
2003	190	190	177	130	140	149	145	144	135	126	194	171	1,891
2004	192	198	207	160	114	154	139	137	145	217	142	186	1,991
2005	201	233	190	122	141	132	140	141	144	120	168	138	1,868
2006	185	207	178	109	144	136	136	141	144	133	185	167	1,866
2007	198	200	178	105	150	140	150	137	133	110	176	168	1,844
2008	198	218	167	144	113	143	148	145	140	134	123	161	1,833
2009	189	188	158	118	154	156	170	144	142	117	175	160	1,871
2010	182	202	200	126	140	126	131	141	141	96	161	147	1,792
2011	190	180	179	116	137	149	148	140	127	114	185	158	1,823
2012	164	169	171	135	104	146	146	147	137	163	101	162	1,744
2013	166	202	193	112	132	130	130	148	131	141	166	144	1,795
2014	190	199	199	136	142	135	138	141	139	116	167	152	1,856

Table 30 Monthly PET data of ST5

Year	Jan	Feb	Mar	Apr	May	Jun	Jul	Aug	Sep	Oct	Nov	Dec	Annual
2000	169	189	188	136	95	136	134	131	143	143	129	166	1,760
2001	175	209	135	96	131	123	140	134	130	98	178	158	1,707
2002	203	213	179	123	142	133	140	135	126	122	162	142	1,820
2003	187	184	168	133	139	146	142	135	131	130	195	174	1,864
2004	197	208	207	163	110	165	143	144	153	214	142	192	2,038
2005	216	237	184	118	134	126	140	129	141	125	161	139	1,850
2006	191	211	170	105	142	134	130	139	147	132	182	162	1,846
2007	209	208	170	105	146	136	146	129	129	115	172	171	1,836
2008	204	234	181	152	116	149	144	136	142	140	128	164	1,890
2009	203	200	165	133	159	154	178	148	141	111	169	157	1,920
2010	180	181	211	113	133	118	122	142	137	100	169	151	1,758
2011	208	188	187	110	138	138	139	139	129	113	187	163	1,839
2012	177	184	185	131	108	149	154	152	143	175	106	174	1,837
2013	176	200	192	115	130	130	133	142	131	146	165	149	1,809
2014	202	212	192	139	141	132	132	138	136	121	167	149	1,859

Table 31 Monthly PET data of ST6

Year	Jan	Feb	Mar	Apr	May	Jun	Jul	Aug	Sep	Oct	Nov	Dec	Annual
2000	175	191	192	151	108	148	155	150	147	146	129	161	1,854
2001	175	206	160	117	144	130	155	140	144	106	179	161	1,817
2002	197	216	199	123	159	147	155	150	133	123	166	152	1,920
2003	189	195	186	134	146	154	150	149	138	124	194	168	1,928
2004	191	197	210	169	119	158	145	141	147	216	139	181	2,013
2005	191	226	201	130	148	140	147	149	144	119	167	137	1,899
2006	183	207	183	113	147	140	143	145	146	133	185	165	1,890
2007	192	203	187	112	155	144	155	143	138	111	174	166	1,880
2008	189	208	171	149	115	147	154	151	143	139	122	159	1,848
2009	180	187	163	119	156	161	170	149	148	119	179	162	1,893
2010	180	210	204	136	148	132	139	144	145	98	160	150	1,844
2011	187	185	180	125	144	159	157	148	131	118	183	154	1,870
2012	166	167	185	129	97	143	141	151	130	163	96	158	1,726
2013	167	204	195	113	141	137	135	153	134	139	167	142	1,827
2014	183	195	202	135	148	143	146	145	142	113	167	153	1,872

Table 32 Monthly PET data of ST7

Year	Jan	Feb	Mar	Apr	May	Jun	Jul	Aug	Sep	Oct	Nov	Dec	Annual
2000	173	184	190	146	107	148	148	143	148	145	133	168	1,831
2001	176	202	148	109	144	128	151	137	137	102	185	165	1,784
2002	198	206	187	123	153	146	149	142	128	125	168	153	1,878
2003	190	186	175	136	142	151	148	143	136	129	197	169	1,904
2004	187	198	205	163	116	161	143	142	148	222	145	185	2,016
2005	197	221	184	124	142	133	142	138	147	124	172	144	1,866
2006	188	201	176	109	146	139	135	143	145	134	191	166	1,873
2007	194	195	176	109	154	144	152	136	132	113	179	171	1,855
2008	195	216	170	150	117	148	149	143	143	140	129	165	1,865
2009	189	184	160	126	158	157	175	147	143	117	178	161	1,896
2010	179	193	201	123	143	128	131	145	144	99	168	150	1,804
2011	191	177	180	119	144	148	147	141	128	115	193	163	1,845
2012	167	178	175	142	112	153	153	151	141	166	106	164	1,809
2013	172	197	194	114	133	133	133	145	131	144	169	150	1,815
2014	191	197	190	134	143	136	138	142	138	120	172	155	1,856

Table 33 Monthly PET data of ST8

Year	Jan	Feb	Mar	Apr	May	Jun	Jul	Aug	Sep	Oct	Nov	Dec	Annual
2000	176	202	198	146	100	152	151	141	142	151	138	170	1,865
2001	185	218	161	108	139	135	153	137	141	128	190	160	1,854
2002	195	234	197	125	150	139	148	136	132	127	178	156	1,918
2003	191	198	192	134	151	156	147	138	147	145	201	165	1,964
2004	196	208	210	165	120	172	160	154	177	228	149	176	2,115
2005	199	242	221	124	144	144	156	147	156	144	177	148	2,001
2006	191	210	181	112	160	144	147	149	153	146	193	167	1,953
2007	194	206	184	112	146	141	157	141	149	125	180	173	1,908
2008	193	212	174	143	118	144	159	149	143	150	133	163	1,881
2009	186	197	165	121	161	163	174	145	147	122	184	167	1,931
2010	186	204	208	118	133	130	137	149	143	112	181	157	1,859
2011	190	213	205	118	137	152	152	145	135	127	192	159	1,925
2012	163	167	176	135	103	147	144	152	134	164	100	164	1,748
2013	176	221	182	103	135	136	148	146	136	153	179	148	1,862
2014	186	216	218	135	147	135	137	145	146	132	192	160	1,949

Table 34 Monthly PET data of ST9

Year	Jan	Feb	Mar	Apr	May	Jun	Jul	Aug	Sep	Oct	Nov	Dec	Annual
2000	175	188	189	134	96	142	138	135	142	144	136	170	1,791
2001	180	209	150	99	129	119	141	132	137	111	185	161	1,753
2002	199	216	181	119	142	134	141	132	123	122	169	151	1,828
2003	190	189	180	126	135	147	138	131	135	133	200	168	1,873
2004	189	194	205	160	112	158	143	138	155	223	147	180	2,004
2005	200	230	189	114	139	126	138	135	148	130	172	144	1,866
2006	195	208	171	102	150	132	132	136	152	141	192	167	1,878
2007	195	195	170	100	139	137	144	128	136	116	179	175	1,817
2008	196	211	166	138	112	142	145	143	139	139	131	164	1,826
2009	194	191	161	121	156	152	167	139	137	117	178	166	1,879
2010	184	187	198	117	132	122	129	143	140	98	173	154	1,778
2011	191	190	189	103	135	141	140	136	130	118	192	162	1,826
2012	172	187	192	131	107	148	155	152	143	180	110	170	1,847
2013	175	204	187	108	136	127	135	142	130	148	173	150	1,814
2014	193	212	203	136	148	130	132	144	138	127	182	157	1,901

Table 35 Monthly PET data of ST10

Year	Jan	Feb	Mar	Apr	May	Jun	Jul	Aug	Sep	Oct	Nov	Dec	Annual
2000	171	189	191	139	99	150	141	134	143	147	131	169	1,803
2001	177	215	144	97	131	127	140	133	136	108	180	158	1,747
2002	198	213	182	127	143	136	144	137	127	124	169	145	1,845
2003	186	188	178	132	145	153	146	134	138	141	200	172	1,912
2004	196	200	208	168	117	173	154	149	167	223	148	185	2,087
2005	211	238	189	117	142	134	147	137	153	138	170	144	1,919
2006	195	214	172	107	153	142	138	142	155	139	188	164	1,908
2007	201	206	175	109	151	143	153	133	141	119	176	174	1,880
2008	200	222	180	151	118	151	154	146	147	147	131	162	1,908
2009	197	196	168	132	169	163	182	148	147	116	173	161	1,951
2010	183	186	212	117	136	126	133	150	141	109	178	154	1,824
2011	199	197	196	107	141	145	145	140	139	121	190	160	1,880
2012	169	176	178	133	100	142	145	148	139	169	99	167	1,765
2013	179	211	197	117	140	134	142	146	135	154	172	148	1,874
2014	197	225	211	146	154	134	138	143	142	130	177	151	1,950

Table 36 Monthly PET data of ST11

Year	Jan	Feb	Mar	Apr	May	Jun	Jul	Aug	Sep	Oct	Nov	Dec	Annual
2000	178	202	202	147	105	153	157	149	145	151	141	173	1,902
2001	188	217	161	110	141	136	159	143	146	125	193	164	1,884
2002	200	235	197	121	154	143	153	143	137	130	177	157	1,947
2003	194	197	192	129	150	158	148	143	143	141	204	167	1,965
2004	195	202	210	166	121	169	160	153	170	231	150	180	2,108
2005	198	239	216	122	144	143	154	153	157	139	178	148	1,989
2006	194	211	183	108	157	141	144	151	158	147	195	171	1,960
2007	196	206	184	109	145	142	156	144	151	124	183	176	1,916
2008	197	211	169	143	120	146	161	149	146	144	133	169	1,887
2009	189	195	164	120	158	161	175	144	149	124	188	171	1,937
2010	186	206	204	120	135	130	139	152	142	105	179	158	1,854
2011	190	204	199	115	139	155	155	148	138	126	197	164	1,929
2012	169	180	192	139	103	150	153	156	146	173	102	162	1,825
2013	173	216	183	102	135	135	149	152	136	151	182	153	1,866
2014	191	211	212	131	146	139	142	152	148	131	191	162	1,954

Appendix E

Rainfall stations 2010 in millimeter

Table 37 Characteristic of rainfall station group 1

No.	ID	Station Name	Latitude	Longitude
1	100303	Sihakniville	10.63	103.48
2	100401	Kompot	10.62	104.22
3	100403	Kirivong	10.60	104.73
4	100421	Koh Andet	10.79	104.95
5	110303	Koh Kong (Ville)	11.63	103.00
6	110403	Tonle Baty (Phnom Penh)	11.37	104.52
7	110404	Kompong Speu	11.43	104.52
8	110405	Kompong Tralach	11.90	104.77
9	110411	Phnom Penh (Ville)	11.60	104.83
10	110413	Phnom Srouch	11.37	104.37
11	110415	Oudong	11.78	104.73
12	110416	Sre Khlong	10.36	104.29
14	110425	Pochentong	11.33	104.55
16	110431	Baset	11.15	104.53
17	110433	Oral	11.68	104.13
18	110445	Trapeang Chor	11.81	104.13
19	110503	Svay Rieng	11.08	105.78
20	110512	Kamchay Mea	11.36	105.40
21	110514	Prey Veng	11.47	105.15
22	110520	Ba Phnom	11.25	105.40
23	120202	Pailin	12.86	102.62
24	120302	Pursat	12.55	103.90
25	120303	Moung Russey	12.78	103.45
26	120304	Dap Bat	12.34	103.79

Table 38 Characteristic of rainfall station group 2

No.	ID	Station name	Latitude	Longitude
27	120312	Kravanh	12.67	103.65
28	120313	Peam	12.29	103.72
30	120401	Kompong Chhnang	12.25	104.67
31	120402	Staung	12.94	104.57
32	120404	Kompong Thom	12.70	104.90
33	120406	Bamnak	12.32	104.17
34	120416	Rolear Pha'ear	12.22	104.67
35	120417	Ponley	12.45	104.47
36	120420	Tuk Phos	12.05	104.53
37	120425	Prey Prous	12.79	104.82
39	120503	Baray	12.40	105.00
40	120504	Kompong Cham	12.00	105.45
42	120516	Prasat Sombo	12.88	105.07
43	120423	Stung Chinit	12.52	105.15
44	110432	Kong Pisey	11.30	104.63
45	120517	Taing Kok	12.25	105.13
46	120603	Kratie	12.48	106.03
47	130202	Sisophon	13.60	102.97
48	130208	Bovel	13.25	102.87
49	130305	Battambang	13.10	103.20
50	130307	Kralanh	13.60	103.52
51	130321	Prasat Bakong	13.35	104.00
52	130326	Srey Snam	13.84	103.52

Table 39 Characteristic of rainfall station group 3

No.	ID	Station Name	Latitude	Longitude
54	130501	Stung Treng	13.52	105.97
55	130505	Sondan	13.10	105.25
56	130507	Thala Borivat	13.54	105.95
57	120518	Taing Krasaing	12.57	105.05
59	581102	Svay Donkeo	12.67	103.64
60	640103	Peam kley	11.47	104.36
61	100419	Angkor Borey	10.93	104.96
62	130302	Angkor Chum	13.68	103.66
63	130602	Ban Lung	13.73	106.96
64	100417	Chum Kiri	10.91	104.43
65	130404	Dam Dek	13.25	104.12
66	130405	Kampong Kdei	13.12	104.34
68	620101	KampongThmar	12.50	105.11
69	110522	Kampong Trabaek	11.14	104.43
70	110513	Kanchreach	11.41	105.33
71	130424	Kandal Chrass	12.97	104.71
72	140205	Krakor	12.52	104.18
73	110523	Mesang	11.33	105.55
74	110434	O Taroat	11.53	104.42
75	110524	Peam Ror	11.31	105.28
76	110525	Pear Raing	11.66	105.23
77	120422	Prasat Balaing_PH3	12.98	104.96
79	110436	Prey Dop	11.22	104.55
82	110430	SamakiMeanchey	12.47	105.02
83	110441	Samrong	11.24	104.89
84	110437	Sdock	11.26	104.51
85	130605	Sesan	13.55	106.09
87	130325	Siem Reap	13.37	103.85
89	100408	Takeo (Donkeo)	10.59	104.48
90	110409	Takhmao	11.43	104.97
91	120309	Talo	12.52	103.10
93	120427	Tpaung	11.75	104.43
94	130328	Varin	13.78	103.75

Table 40 Monthly rainfall on 2010 group 1

ID	Jan	Feb	Mar	Apr	May	Jun	Jul	Aug	Sep	Oct	Nov	Dec	Total
100303	46	1	3	56	250	204	439	303	174	472	131	30	2,108
100401	8	117	71	8	60	72	155	301	163	201	0	10	1,165
100403	7	0	17	118	71	102	223	97	153	167	69	0	1,023
100421	0	0	0	8	35	90	147	132	109	284	194	94	1,094
110303	78	142	163	151	323	705	603	675	277	566	129	1	3,814
110403	18	0	38	28	38	95	136	67	157	326	47	30	981
110404	26	22	149	41	192	81	127	147	147	237	52	0	1,220
110405	20	0	118	75	60	188	80	367	94	395	60	88	1,545
110411	25	0	47	100	97	172	246	279	166	444	106	31	1,712
110413	8	0	69	24	98	136	146	87	101	267	86	130	1,152
110415	41	0	77	7	0	196	118	279	164	375	66	50	1,372
110416	0	40	57	12	132	123	123	58	177	156	38	111	1,025
110425	0	0	36	56	27	254	79	195	343	372	78	0	1,439
110431	0	0	43	57	109	78	203	82	148	310	64	24	1,118
110433	32	86	43	155	131	90	165	152	190	323	64	34	1,465
110445	27	40	20	71	129	140	230	118	179	321	62	35	1,371
110503	24	0	12	98	127	239	299	285	209	450	113	0	1,855
110512	64	0	84	95	82	152	210	199	290	469	77	0	1,721
110514	53	0	122	100	94	150	214	234	256	545	91	28	1,887
110520	52	0	85	83	80	133	237	217	282	511	56	0	1,736
120202	14	3	57	131	340	207	385	211	338	227	8	4	1,923
120302	0	27	30	108	87	238	196	238	167	274	25	0	1,390
120303	8	13	96	89	31	121	206	124	194	232	102	15	1,229
120304	11	56	52	43	51	116	262	254	265	204	66	44	1,423

Table 41 Monthly rainfall on 2010 group 2

ID	Jan	Feb	Mar	Apr	May	Jun	Jul	Aug	Sep	Oct	Nov	Dec	Total
120312	0	0	46	6	85	180	290	222	398	334	212	30	1,803
120313	39	23	72	71	123	139	228	207	367	229	75	27	1,598
120401	26	22	149	41	192	81	127	147	147	237	52	0	1,220
120402	2	0	2	35	37	103	320	356	152	314	29	0	1,349
120404	24	0	1	28	177	222	260	213	124	289	39	1	1,377
120406	26	1	99	14	134	228	135	258	181	300	25	24	1,424
120416	12	0	15	30	111	120	98	136	202	284	116	0	1,124
120417	0	0	0	45	101	78	194	274	261	316	58	0	1,327
120420	38	0	47	101	130	253	179	226	211	470	187	0	1,840
120425	0	0	29	76	52	174	116	112	442	194	39	10	1,244
120503	29	0	27	20	105	126	96	263	122	263	182	0	1,232
120504	21	0	38	71	44	317	183	205	145	282	66	0	1,372
120516	15	0	0	58	127	105	258	164	162	582	47	0	1,517
120423	0	0	12	59	122	120	192	121	208	289	38	0	1,161
110432	21	0	59	39	72	194	152	130	184	259	67	5	1,181
120517	31	0	51	132	180	216	70	184	144	253	110	0	1,371
120603	6	0	0	48	89	182	216	283	231	391	49	0	1,495
130202	10	14	26	68	71	123	97	207	229	249	9	0	1,101
130208	0	0	0	51	73	106	235	235	279	26	0	0	1,006
130305	8	12	25	70	77	121	233	208	191	325	0	0	1,270
130307	12	10	4	42	94	139	130	391	151	255	43	13	1,284
130321	15	0	0	13	81	204	271	264	273	357	53	18	1,550
130326	0	0	38	0	106	268	158	202	242	215	16	10	1,255
130501	29	7	0	17	97	101	262	227	144	274	13	0	1,170
130505	13	0	0	165	133	197	272	225	172	362	72	0	1,611
130507	15	5	5	8	100	190	271	140	101	233	10	16	1,093

Table 42 Monthly rainfall on 2010 group 3

ID	Jan	Feb	Mar	Apr	May	Jun	Jul	Aug	Sep	Oct	Nov	Dec	Total
120518	24	0	0	123	126	160	229	323	242	309	42	6	1,584
581102	17	5	59	43	12	70	139	101	130	219	64	7	864
640103	0	0	59	19	24	128	82	145	113	116	96	46	829
100419	0	0	0	22	14	163	43	115	65	381	64	0	866
130302	13	1	10	96	114	157	271	196	248	278	25	0	1,408
130602	0	0	0	34	29	109	281	244	200	131	3	0	1,031
100417	0	0	43	57	107	77	200	81	146	306	63	24	1,102
130404	27	0	12	24	22	83	262	223	182	371	82	2	1,291
130405	2	0	2	111	181	61	138	350	297	222	9	0	1,372
620101	0	0	12	59	122	120	192	121	208	289	38	0	1,161
110522	47	0	56	58	92	171	264	220	276	511	73	0	1,768
110513	61	0	73	97	114	189	143	247	0	534	72	0	1,529
130424	8	0	0	0	30	104	175	192	112	435	21	0	1,077
140205	26	1	99	14	134	228	135	258	181	300	25	24	1,424
110523	63	0	59	86	97	160	199	226	299	498	53	0	1,739
110434	5	12	9	50	81	44	61	106	82	120	156	89	815
110524	47	0	98	74	84	133	130	206	268	511	67	0	1,618
110525	64	0	96	112	103	124	103	174	294	518	48	0	1,634
120422	13	0	0	72	51	168	182	255	159	56	0	0	956
110436	0	0	49	99	65	122	155	137	197	251	70	0	1,144
110430	26	0	115	75	94	193	126	287	171	372	166	120	1,745
110441	0	0	0	0	142	70	215	207	228	443	16	0	1,321
110437	0	13	0	20	31	75	78	91	119	252	112	19	810
130605	1	3	10	73	77	112	270	251	119	178	5	2	1,101
130325	15	0	0	13	81	204	271	264	273	263	45	9	1,438
100408	9	0	2	95	47	206	140	204	173	374	166	0	1,415
110409	13	0	53	136	71	235	82	102	180	742	80	23	1,718
120309	0	43	41	55	73	101	272	118	200	199	0	0	1,101
120427	11	4	57	77	59	245	117	263	248	322	58	72	1,534
130328	0	0	0	23	40	62	163	271	242	215	16	10	1,041

Appendix F

Gauge stations of sub-basins in m^3s^{-1}

Table 43 Monthly gauge station of ST1

Year	Jan	Feb	Mar	Apr	May	Jun	Jul	Aug	Sep	Oct	Nov	Dec	Annual
2000	3	2	2	3	4	8	31	27	11	50	12	3	13.0
2001	1	2	2	2	2	1	2	5	31	25	4	3	6.9
2002	2	2	1	2	2	3	3	7	28	20	7	20	8.1
2003	13	14	14	12	4	4	10	6	31	52	13	15	15.4
2004	13	3	4	5	4	12	12	26	48	47	7	10	16.0
2005	6	4	4	20	7	11	26	10	51	19	10	10	15.0
2006	13	9	7	8	17	21	23	31	59	62	42	18	25.9
2007	6	3	3	3	13	26	32	49	80	92	38	21	30.7
2008	12	7	3	6	25	29	23	42	49	44	79	31	29.1
2009	23	17	13	6	23	11	52	37	93	90	125	47	44.7
2010	44	29	15	15	46	49	16	61	87	118	49	38	47.3

Table 44 Monthly gauge station of ST2

Year	Jan	Feb	Mar	Apr	May	Jun	Jul	Aug	Sep	Oct	Nov	Dec	Annual
2000	4	3	4	5	7	2	13	11	33	75	5	2	13.7
2001	4	3	4	4	4	4	6	23	37	10	2	3	8.7
2002	3	5	5	5	4	4	7	106	29	6	1		15.8
2003	4	1	0	0	0	0	0	0	8	19	15	13	5.2
2004	7	2	1	0	1	4	0	3	8	11	4	4	3.7
2005	3	2	1	0	1	1	2	1	35	20	6	5	6.4
2006	4	1	0	1	0	1	2	6	44	59	9	6	11.2
2007	4	2	1	1	14	1	2	1	3	34	7	7	6.4
2008	6	3	1	0	1	1	0	1	70	8	34	5	10.8
2009	4	1	1	1	1	4	48	1	155	120	6	6	29.1
2010	3	5	3	1	1	1	1	2	1	148	4	3	14.3

Table 45 Monthly gauge station of ST3

Year	Jan	Feb	Mar	Apr	May	Jun	Jul	Aug	Sep	Oct	Nov	Dec	Annual
2000	34	18	11	18	33	132	210	211	234	231	117	46	107.9
2001	23	13	24	12	23	28	71	79	169	244	118	37	70.0
2002	18	11	6	6	7	37	32	68	172	172	60	22	50.9
2003	16	11	12	10	15	31	51	88	119	126	38	18	44.7
2004	11	8	5	4	8	59	33	152	131	101	30	17	46.6
2005	10	7	5	4	7	10	71	58	100	93	69	43	39.8
2006	17	3	3	5	10	5	82	158	228	234	53	27	68.7
2007	20	13	8	6	49	38	91	118	146	301	87	41	76.4
2008	27	26	14	17	34	36	25	49	76	98	77	35	42.9
2009	21	11	14	17	60	104	163	124	443	454	154	75	136.6
2010	54	38	13	7	4	12	16	47	56	115	45	19	35.6
2011	6	3	2	3	10	25	32	86	233	283	93	37	67.7

Table 46 Monthly gauge station of ST4

Year	Jan	Feb	Mar	Apr	May	Jun	Jul	Aug	Sep	Oct	Nov	Dec	Annual
2000	1	0	0	0	0	0	2	11	29	56	11	2	9.4
2001	1	1	1	1	1	0	1	1	18	71	24	1	9.8
2002	0	0	1	2	7	1	0	3	12	58	30	5	9.9
2003	1	1	1	1	1	1	1	7	1	80	20	1	9.6
2004	1	1	1	1	2	11	13	5	23	59	9	2	10.5
2005	1	0	1	1	5	11	17	7	28	83	22	5	15.0
2006	2	0	1	1	5	16	18	8	33	101	28	7	18.3

Table 47 Monthly gauge station of ST5

Year	Jan	Feb	Mar	Apr	May	Jun	Jul	Aug	Sep	Oct	Nov	Dec	Annual
2000	5	2	1	16	23	28	43	32	52	69	45	13	27.4
2001	4	1	7	3	8	19	33	28	30	48	51	14	20.5
2002	3	2	1	3	13	12	14	23	40	51	21	7	15.8
2003	2	1	2	3	6	4	9	54	21	70	40	8	18.4
2004	3	1	0	1	7	14	12	42	32	30	15	8	13.6

Table 48 Monthly gauge station of ST6

Year	Jan	Feb	Mar	Apr	May	Jun	Jul	Aug	Sep	Oct	Nov	Dec	Annual
2000	20	12	16	54	75	88	190	141	140	428	153	47	113.7
2001	24	11	22	16	20	43	69	81	94	282	63	20	62.1
2002	12	7	5	10	17	16	20	60	86	101	67	27	35.7
2003	11	5	14	19	27	15	109	92	112	420	37	17	73.2
2004	2	1	1	3	5	65	69	90	83	120	40	22	41.7
2005	4	1	0	6	7	13	43	114	95	184	112	76	54.5
2006	6	1	2	53	52	53	129	164	238	163	21	9	74.4
2007	5	2	3	6	145	166	234	118	300	157	84	11	102.5
2008	3	0	13	156	318	178	100	227	337	120	134	65	137.6
2009	5	2	3	51	101	84	94	71	153	193	103	33	74.4
2010	6	3	3	4	10	26	63	125	250	359	66	23	78.3
2011	8	2	6	12	41	63	45	131	172	282	50	14	68.7

Table 49 Monthly gauge station of ST7

Year	Jan	Feb	Mar	Apr	May	Jun	Jul	Aug	Sep	Oct	Nov	Dec	Annual
2000	15	12	8	20	109	34	549	191	1436	1555	62	28	334.9
2001	15	12	25	13	37	90	619	1366	62	118	94	20	205.8
2002	14	6	8	16	36	30	152	230	301	38	15	16	71.9
2003	5	2	6	4	10	19	122	214	141	134	36	10	58.4
2004	3	2	2	3	29	85	39	141	94	116	37	7	46.5
2005	1	1	1	2	2	11	90	252	150	142	81	23	63.0
2006	6	3	2	5	21	19	241	264	116	198	78	20	81.1
2007	5	2	3	3	51	27	152	106	44	110	99	27	52.5
2008	8	5	3	5	73	78	49	85	174	129	94	28	61.0
2009	8	4	7	7	30	87	160	126	142	166	79	21	69.8
2010	5	3	4	3	5	7	6	55	46	106	38	13	24.3

Table 50 Monthly gauge station of ST8

Year	Jan	Feb	Mar	Apr	May	Jun	Jul	Aug	Sep	Oct	Nov	Dec	Annual
2000	85	32	34	85	187	492	742	743	873	883	629	234	418.3
2001	85	33	20	13	23	114	553	702	814	809	582	201	328.9
2002	76	30	13	10	19	98	123	478	802	803	429	150	252.5
2003	58	22	10	12	12	56	64	159	582	377	116	65	127.8
2004	24	7	4	5	8	125	102	824	527	392	130	62	184.1
2005	21	6	2	1	7	17	340	227	613	476	189	95	166.1
2006	49	14	5	11	18	20	215	613	733	869	238	118	241.8
2007	89	50	7	0	210	51	169	1019	925	647	221	99	290.6
2008	55	21	11	12	375	127	101	608	703	678	334	105	260.9
2009	55	26	30	26	71	112	521	740	945	1139	260	91	334.7
2010	48	21	12	9	15	25	44	607	740	923	234	73	229.1
2011	33	12	10	9	28	106	133	388	957	1047	559	156	286.4

Table 51 Monthly gauge station of ST9

Year	Jan	Feb	Mar	Apr	May	Jun	Jul	Aug	Sep	Oct	Nov	Dec	Annual
2000	4	3	2	3	2	8	11	12	19	30	10	5	9.0
2001	3	2	2	1	2	2	5	7	6	22	8	4	5.4
2002	2	2	1	1	1	0	1	3	25	17	8	4	5.4
2003	2	2	1	1	1	2	2	3	2	3	3	1	2.0
2004	1	1	0	0	0	2	2	28	31	24	9	4	8.6
2005	2	1	1	1	2	3	4	8	17	21	9	4	6.2
2006	2	2	0	0	0	1	9	10	26	23	5	4	6.9
2007	3	1	1	1	7	0	2	4	9	17	3	2	4.3
2008	0	1	1	1	2	3	3	3	23	9	14	6	5.4
2009	3	2	1	1	3	4	5	3	21	35	9	4	7.5
2010	3	1	1	0	0	0	0	7	10	28	12	7	5.9

Table 52 Monthly gauge station of ST10

Year	Jan	Feb	Mar	Apr	May	Jun	Jul	Aug	Sep	Oct	Nov	Dec	Annual
2000	162	42	11	6	19	78	112	108	117	118	78	24	72.9
2001	6	2	1	2	4	1	22	68	104	113	107	23	37.9
2002	5	1	55	3	2	6	27	31	113	111	64	29	37.4
2003	1	0	0	0	0	0	1	1	41	167	35	2	20.7
2004	0	0	0	0	0	28	12	174	170	75	5	2	38.9
2005	1	0	0	0	0	1	19	27	93	117	59	0	26.4
2006	0	0	0	0	0	0	10	178	182	232	101	6	59.2
2007	0	0	0	0	16	0	1	47	112	149	53	0	31.7
2008	0	0	0	0	0	1	18	67	188	213	204	38	60.9
2009	0	0	0	0	0	1	14	52	118	236	53	2	39.7
2010	1	1	1	1	1	4	5	180	223	279	109	0	67.1

Table 53 Monthly gauge station of ST11

Year	Jan	Feb	Mar	Apr	May	Jun	Jul	Aug	Sep	Oct	Nov	Dec	Annual
2000	20	7	7	8	17	29	72	60	78	98	40	4	36.6
2001	3	4	4	6	8	3	4	35	87	84	23	4	22.1
2002	3	3	4	4	5	10	2	65	114	65	14	2	24.3
2003	0	0	0	0	0	2	18	16	115	38	3	0	16.1
2004	0	0	1	1	1	48	20	75	31	45	5	0	18.8
2005	0	0	0	0	0	0	94	12	135	64	10	1	26.4
2006	0	0	0	0	0	1	58	128	115	91	11	1	33.7
2007	0	0	0	0	9	2	18	68	57	92	24	19	24.1
2008	8	0	0	0	64	21	3	89	93	35	73	4	32.5
2009	0	0	0	0	10	14	108	18	178	125	12	2	39.0
2010	0	0	0	0	0	0	12	105	70	134	3	0	27.0
2011	0	0	0	0	0	1	1	25	132	104	37	7	25.6

Appendix G

Water level of Prek Kdam (PK), Phnom Penh Port (PP) and Kampong Loung (KL)

Table 54 Monthly water level (m a.s.l) in meter at Prek Kdam station

Year	Jan	Feb	Mar	Apr	May	Jun	Jul	Aug	Sep	Oct	Nov	Dec	Avg.
2000	4.1	2.6	1.6	1.2	2.3	4.5	7.4	8.7	9.9	9.8	8.1	5.9	5.5
2001	4.1	2.7	1.7	1.3	1.3	3.6	6.2	8.1	9.6	9.3	8.0	5.8	5.2
2002	4.0	2.5	1.6	1.2	1.3	3.3	6.0	8.0	9.4	9.2	7.3	5.4	4.9
2003	3.7	2.3	1.5	1.1	1.2	2.4	3.6	5.7	7.6	7.6	5.5	3.7	3.8
2004	2.2	1.3	1.1	1.0	1.1	2.9	4.0	7.2	8.7	8.1	5.6	3.8	3.9
2005	2.3	1.4	1.1	1.0	0.9	1.5	4.2	7.7	8.7	8.7	6.8	4.9	4.1
2006	3.2	1.9	1.2	1.0	1.0	1.7	4.5	7.4	8.3	8.8	7.0	4.7	4.2
2007	3.0	1.7	1.2	1.0	1.4	1.8	3.7	6.1	7.3	8.4	7.3	5.1	4.0
2008	3.2	2.0	1.3	1.1	1.7	3.4	4.9	7.3	8.0	8.2	7.2	5.4	4.5
2009	3.5	2.1	1.3	1.2	1.6	2.9	4.9	7.2	7.8	8.6	6.8	4.5	4.4
2010	2.8	1.7	1.1	0.9	1.0	1.2	2.0	4.8	6.6	7.2	6.1	4.2	3.3
2011	2.5	1.5	1.2	1.1	1.3	2.6	5.3	7.8	9.1	10.1	8.6	6.0	4.8
2012	4.0	2.5	1.5	1.1	1.2	2.5	4.1	5.9	7.3	7.2	5.3	3.7	3.9
2013	2.1	1.4	1.2	1.0	1.2	1.8	3.7	6.8	7.8	9.1	7.6	5.5	4.1

Table 55 Monthly water level (m a.s.l) in meter at Phnom Penh station

Year	Jan	Feb	Mar	Apr	May	Jun	Jul	Aug	Sep	Oct	Nov	Dec	Avg.
2000	3.4	2.2	1.5	1.2	2.3	4.7	7.6	8.7	9.8	9.3	7.3	5.0	5.2
2001	3.4	2.2	1.5	1.2	1.3	3.7	6.4	8.2	9.5	8.9	7.2	4.8	4.9
2002	3.2	2.2	1.4	1.1	1.2	3.4	6.3	8.2	9.3	8.8	6.6	4.6	4.7
2003	3.0	1.9	1.3	1.0	1.0	2.3	3.4	5.9	7.8	7.2	4.7	3.0	3.5
2004	1.9	1.3	0.9	0.7	1.0	2.9	4.0	7.5	8.7	7.5	4.7	3.2	3.7
2005	2.1	1.4	1.0	1.0	0.8	1.5	4.3	8.1	8.8	8.4	6.0	4.1	4.0
2006	2.7	1.7	1.2	0.9	1.0	1.7	4.7	7.6	8.2	8.6	6.2	3.8	4.0
2007	2.7	1.7	1.2	0.9	1.0	1.7	4.7	7.6	8.2	8.6	6.2	3.8	4.0
2008	2.6	1.6	1.2	1.0	1.7	3.6	5.1	7.5	8.0	8.0	6.9	4.7	4.3
2009	2.9	1.8	1.2	1.0	1.6	2.9	5.0	7.3	7.9	8.5	6.2	3.9	4.2
2010	2.7	1.9	1.4	0.9	0.9	1.2	2.0	5.0	6.8	7.2	5.6	3.6	3.3
2011	2.4	1.5	1.2	1.1	1.2	2.7	5.5	8.1	9.1	9.7	7.7	4.8	4.6
2012	3.1	2.1	1.5	1.1	1.3	2.4	4.1	6.1	7.4	6.7	4.4	3.0	3.6
2013	1.9	1.3	1.0	0.9	1.1	1.8	3.7	7.1	7.9	8.7	6.5	4.4	3.9

Table 56 Monthly water level (m a.s.l) in meter at Kampong Loung station

Year	Jan	Feb	Mar	Apr	May	Jun	Jul	Aug	Sep	Oct	Nov	Dec	Avg.
2000	4.9	3.2	1.9	1.2	1.4	3.1	5.7	7.9	9.2	9.5	8.5	6.8	5.3
2001	4.9	3.3	2.0	1.3	0.9	2.0	4.6	6.9	8.8	9.1	8.2	6.5	4.9
2002	4.7	3.1	1.8	1.1	0.8	1.7	4.0	6.4	8.6	9.0	7.6	6.6	4.6
2003	5.3	3.8	2.5	1.2	0.8	1.3	2.4	4.2	6.3	7.5	6.3	4.5	3.8
2004	2.8	1.6	1.0	0.8	0.7	1.4	3.0	5.3	7.8	8.0	6.3	5.1	3.6
2005	3.9	2.8	2.1	1.7	0.9	0.8	2.3	5.1	7.7	8.5	7.3	5.5	4.1
2006	3.9	2.5	1.4	1.0	0.8	0.8	2.4	5.6	8.3	9.3	8.5	5.8	4.2
2007	3.8	2.2	1.3	0.9	1.0	1.3	2.4	4.4	6.6	7.8	7.5	6.0	3.8
2008	4.0	2.1	1.5	0.8	1.0	2.1	3.9	5.9	7.5	8.0	7.6	6.3	4.2
2009	4.1	2.6	1.6	1.4	1.3	1.9	3.3	5.9	7.2	8.3	7.4	5.6	4.2
2010	3.8	2.3	1.3	0.9	0.7	0.6	0.9	2.9	5.5	6.7	6.5	5.0	3.1
2011	3.2	1.9	1.2	0.8	0.8	1.4	3.4	6.0	8.3	9.7	8.9	6.9	4.4
2012	5.0	3.2	1.8	1.0	0.8	1.3	2.8	4.5	6.5	7.3	6.1	4.5	3.7
2013	2.7	1.5	1.0	0.7	0.6	0.9	2.2	5.2	7.0	8.8	8.0	6.3	3.7

Table 57 Summarized water level data availability

Station	River Name	Province Name	Location		Data Availability
			Lat, N	Long, E	Monthly
Prek Kdam	Tonle Sap	Kandal	11°48'36"	104°48'45"	2000-2013
Phnom Penh Port	Tonle Sap	Phnom Penh	11º34'06"	104º55'06"	2000-2013
Kampong Loung	Great Lake	Pursat	12°34'22"	104°12'49"	2000-2013

Appendix H

Observed vs. simulated streamflow ST1 to ST11

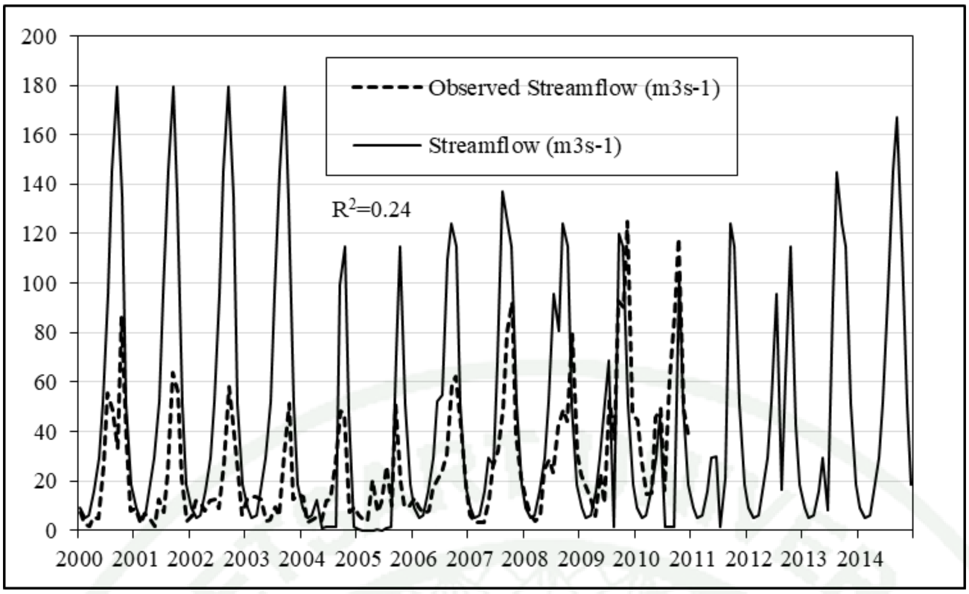

Figure 44 Observed vs. simulated streamflow of ST1

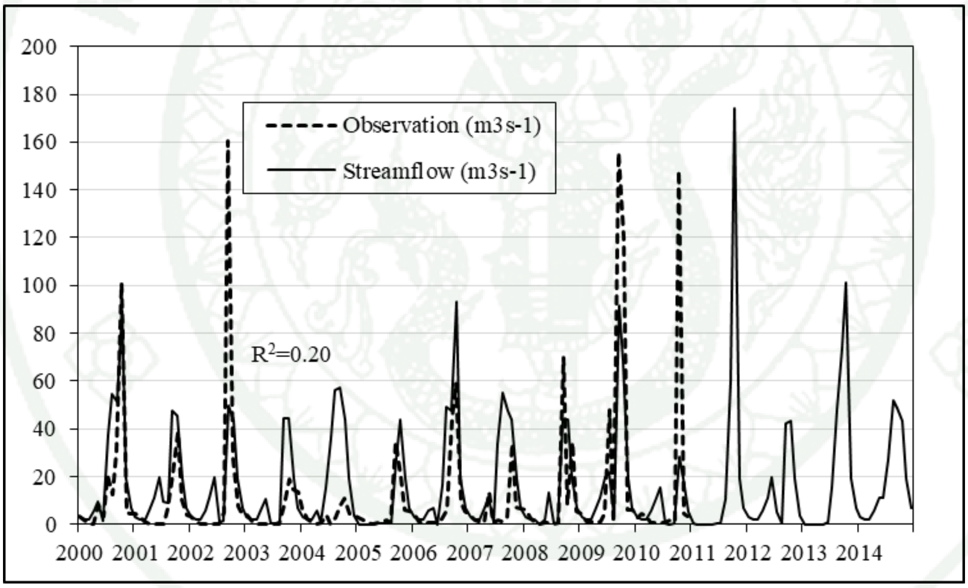

Figure 45 Observed vs. simulated streamflow of ST2

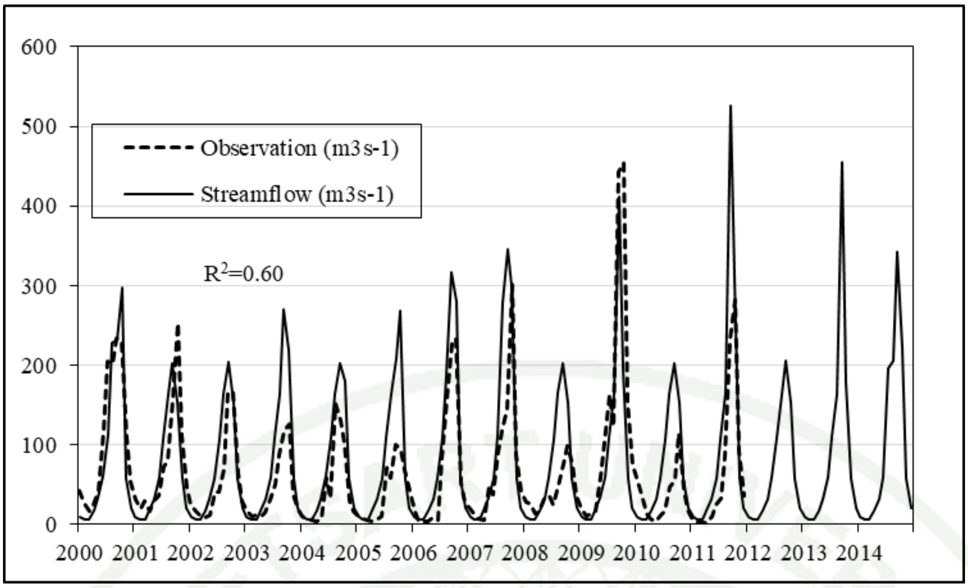

Figure 46 Observed vs. simulated streamflow of ST3

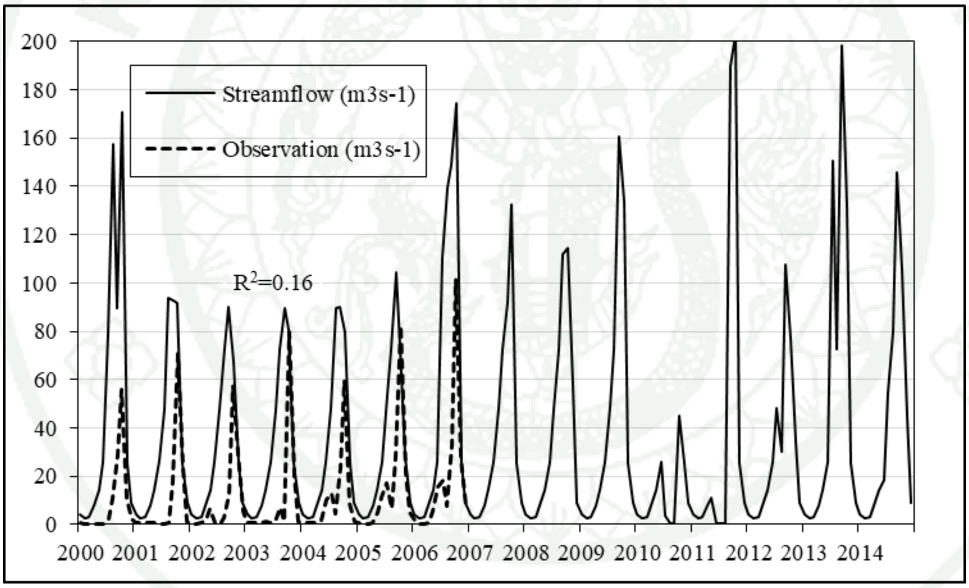

Figure 47 Observed vs. simulated streamflow of ST4

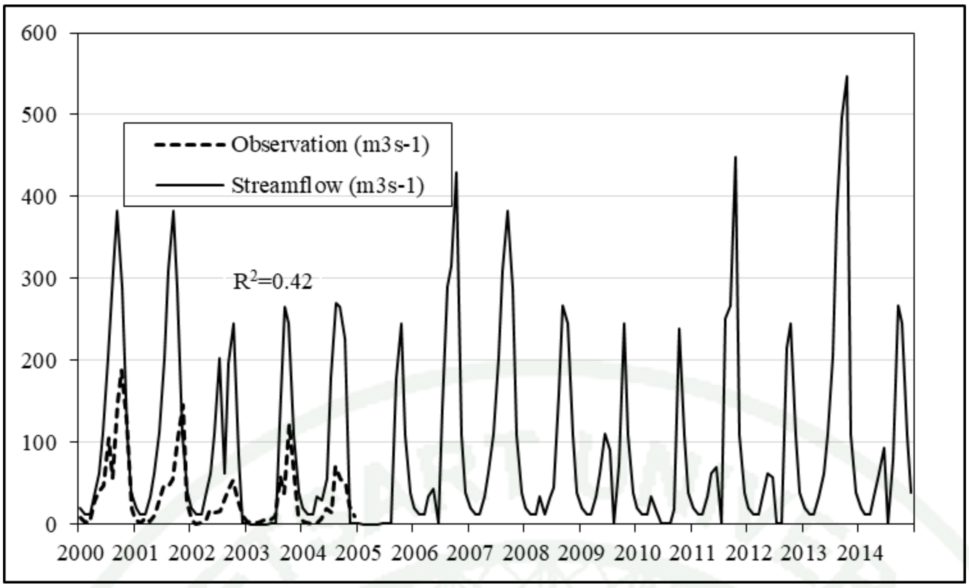

Figure 48 Observed vs. simulated streamflow of ST5

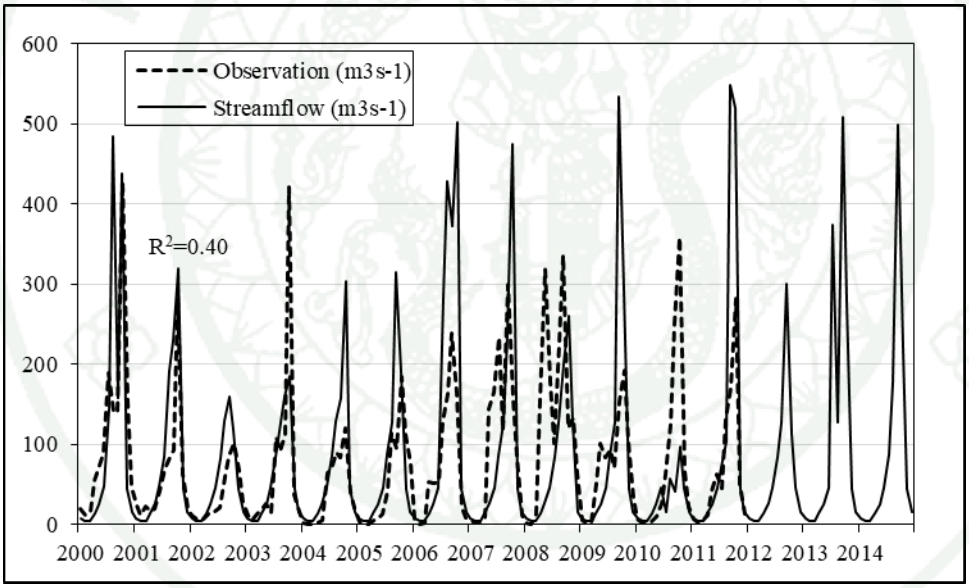

Figure 49 Observed vs. simulated streamflow of ST6

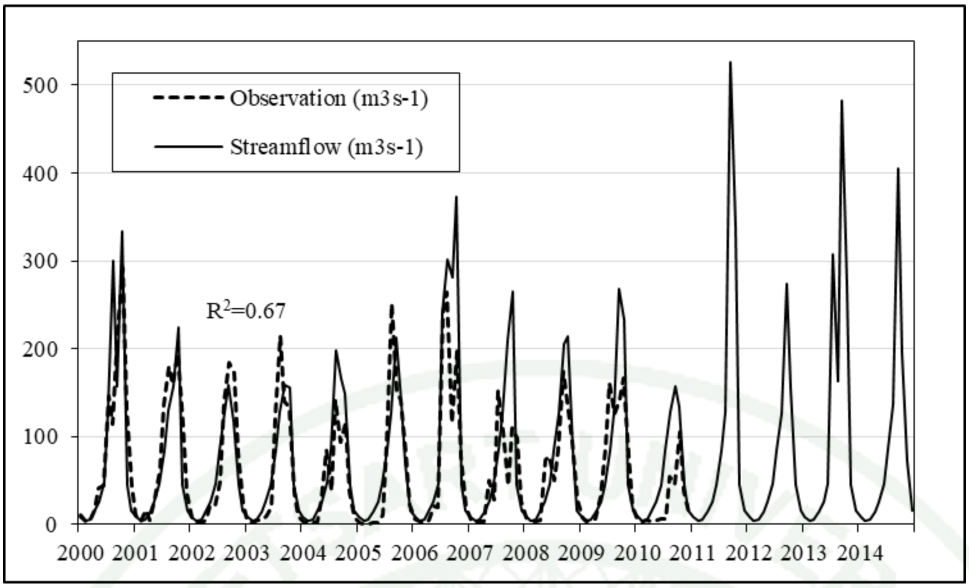

Figure 50 Observed vs. simulated streamflow of ST7

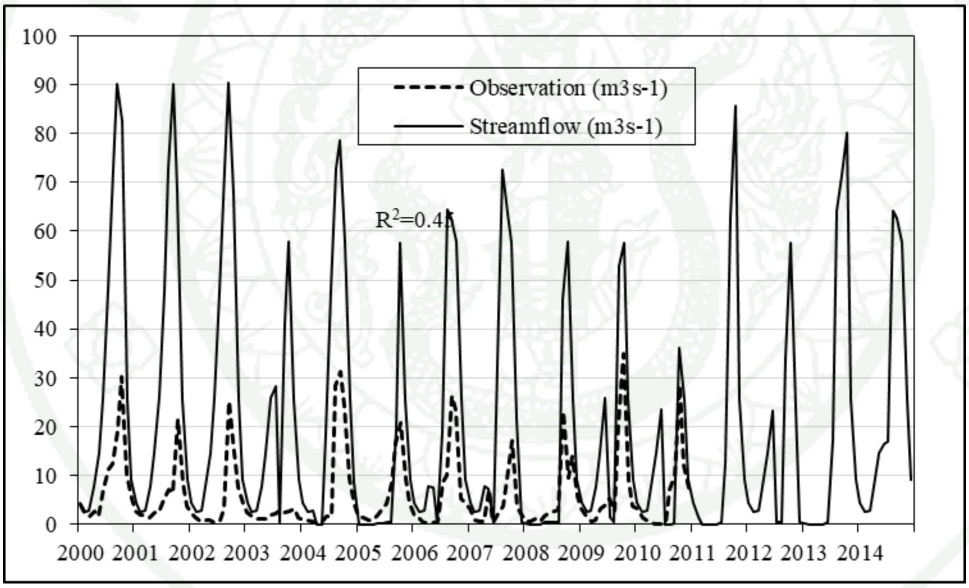

Figure 51 Observed vs. simulated streamflow of ST9

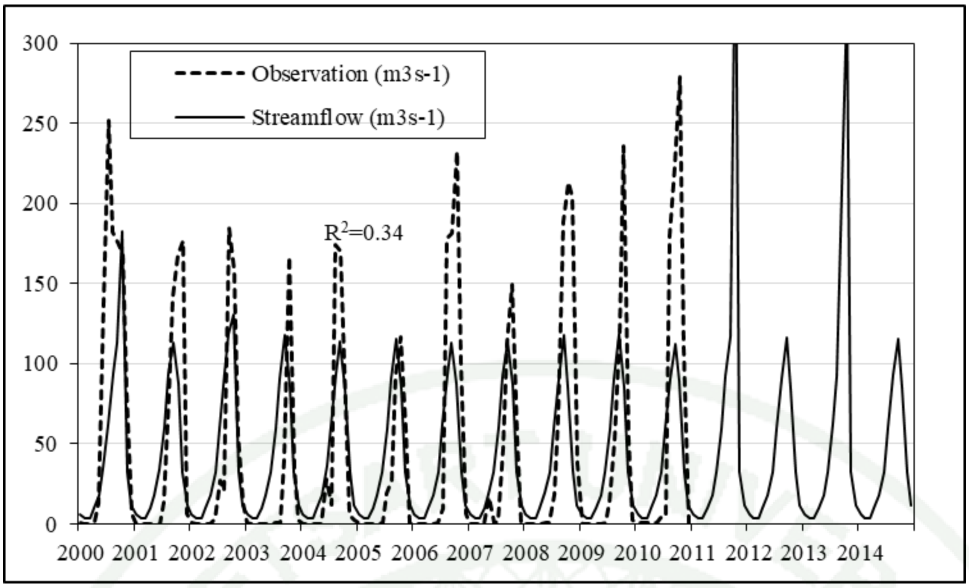

Figure 52 Observed vs. simulated streamflow of ST10

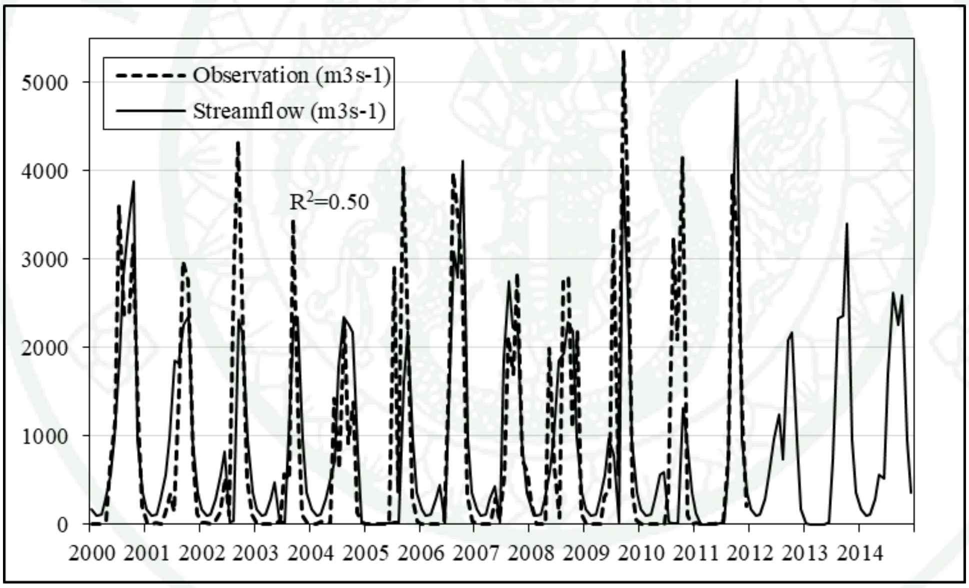

Figure 53 Observed vs. simulated streamflow of ST11

CURRICULUM VITAE

NAME	Mr. Phanit Mab
DATE OF BIRTH	05 June 1993
BIRTH PLACE	The Kingdom of Cambodia
SCHOLARSHIP	The Kasetsart University Scholarships for ASEAN for Commemoration of the 60th Birthday Anniversary of Professor Dr. Her Royal Highness Princess Chulabhorn Mahidol